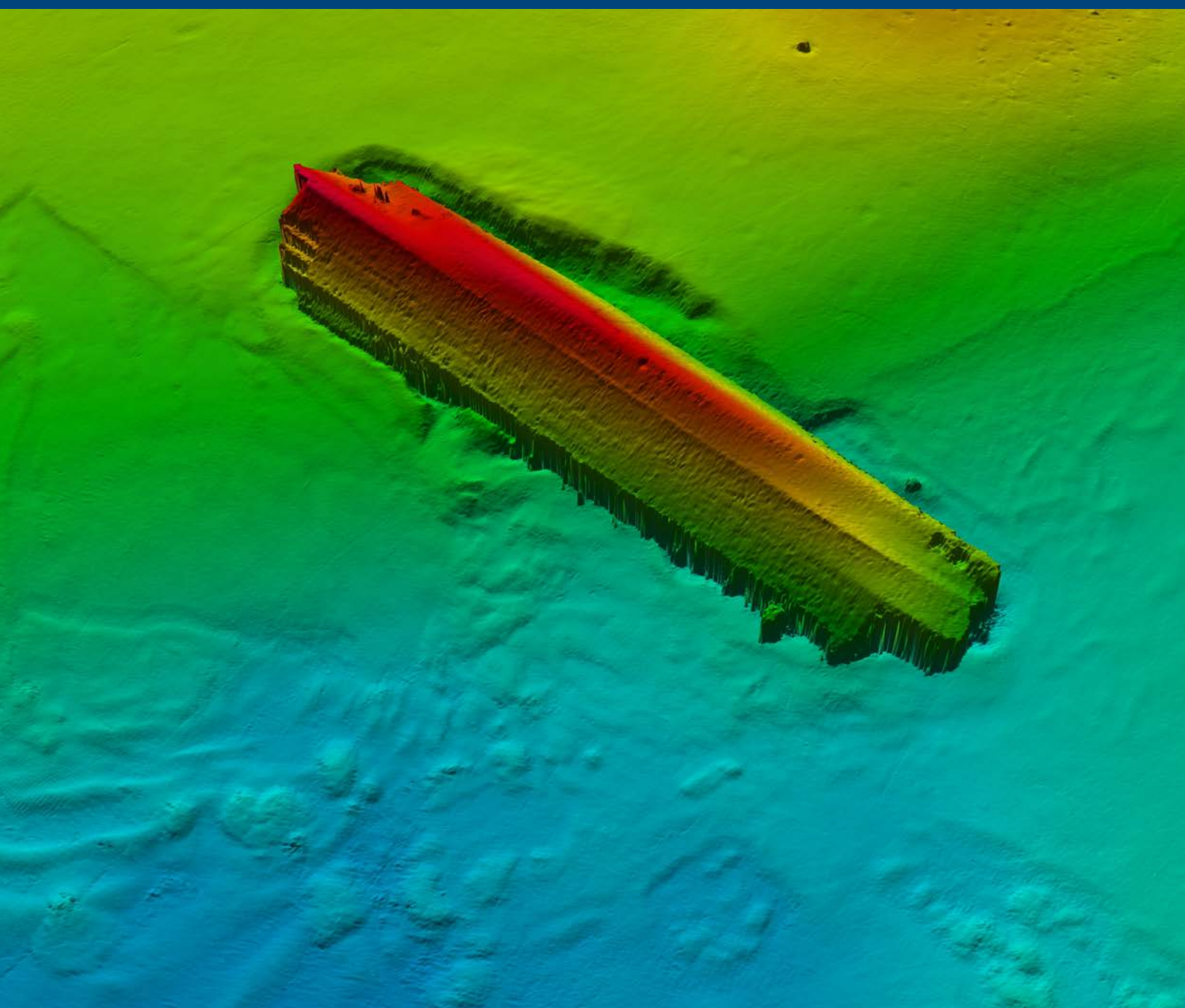


## *EL21-Estonia*

Report of the MS *Estonia* shipwreck site survey with RV *Electra*

Martin Jakobsson, Christian Stranne, Rickard Fornander, Matt O'Regan, Anton Wagner  
and the *EL21-Estonia* Shipboard Party

Stockholm 2021





Meddelanden  
från  
Stockholms universitets institution  
för  
geologiska vetenskaper

No 383

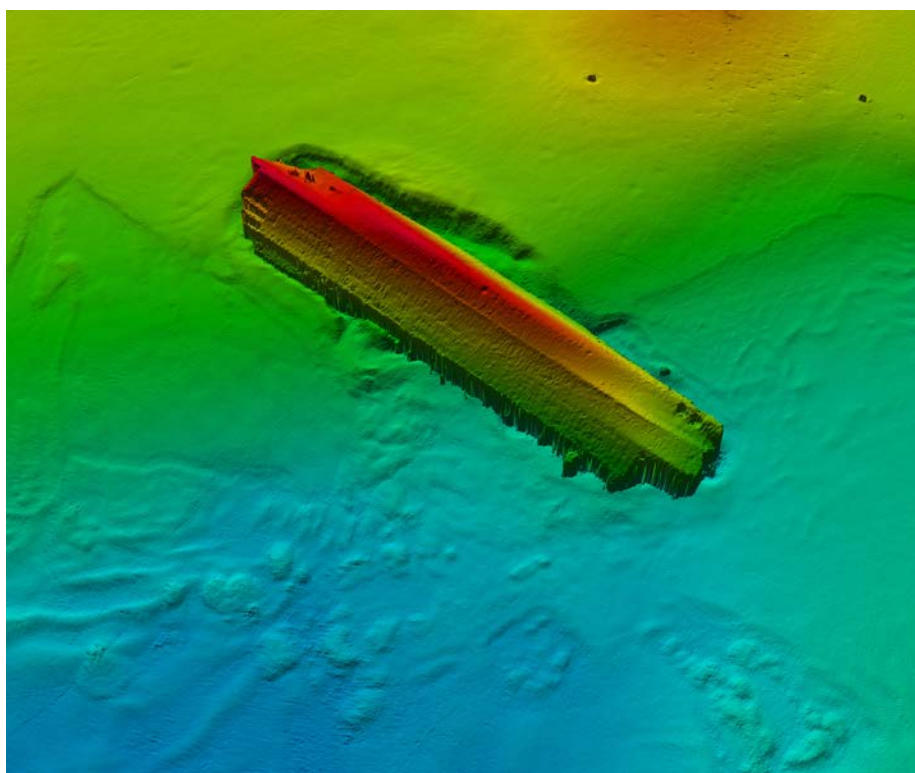
---

***EL21-Estonia***

Report of the MS *Estonia* shipwreck site survey with RV *Electra*

July 8th–15th, 2021

Martin Jakobsson, Christian Stranne, Rickard Fornander, Matt O'Regan  
Anton Wagner and the *EL21-Estonia* Ship Board Party



## Contents

<b>Introduction</b>	7
<b>Background</b>	10
<b>Expedition Participants and operational schedule</b>	11
<b><i>EL21-Estonia</i> survey planning</b>	12
<b>Methods</b>	15
<b><i>RV Electra</i>: Equipment overview</b>	15
<b>Seafloor and water column mapping with acoustic methods</b>	16
Position, heading and attitude	16
Multibeam echo-sounder	16
Sub-bottom profiling	18
Side-scan sonar	18
Midwater sonar	18
Acoustic Doppler Current Profiler (ADCP)	18
Water properties (sound speed, temperature, salinity)	18
Acoustic synchronization unit	19
<b>Sediment sampling, bottom inspection and mooring</b>	19
Piston/gravity corer	19
Grab sampler	21
Naming of stations	21
Bottom filming	22
Moored ADCP	22
<b>Post-processing and interpretation routines</b>	22
Multibeam bathymetry	22
Multibeam backscatter	24
Sub-bottom profiles	24
Side-scan imagery	24
Sediment thickness model	25
Midwater sonar	26
ADCP (Acoustic Doppler Current Profiler)	26
CTD (Conductivity Temperature Depth)	26
Multi sensor core logging (MSCL)	26
Fall Cone	28
LOI (Loss on Ignition)	28
Grain Size	29
Moored ADCP	29
<b>Results and interpretation</b>	30
<b>Seafloor and water column mapping with acoustic methods</b>	30
Multibeam bathymetry	30
Multibeam backscatter	38
Sub-bottom profiling	42
Side-scan sonar	48

Mid-water sonar	54
ADCP	55
<b>Water properties (sound speed, temperature, salinity)</b>	57
<b>Sediment sampling, bottom inspection, and mooring</b>	61
Piston coring	61
Grab samples	65
Bottom inspection	65
Moored ADCP	71
<b>Measurement of MS Estonia</b>	80
Measured listing based on the flat bottom	82
Measured listing based on the port side	83
Measured trim	83
<b>Sediment thickness compilation</b>	90
Input data and uncertainties	90
Distribution of sediments	91
<b>Conclusions</b>	93
Seafloor geology	93
Exposed bedrock and sediment thickness	93
MS <i>Estonia</i> 's listing and trim	93
Oceanographic conditions	93
<b>References</b>	95

(Separate PDFs)

**Appendix 1: Expedition daily notes**

**Appendix 2: Multibeam bathymetry and backscatter**

**Appendix 3: Sub-bottom profiling**

**Appendix 4: Side-scan sonar**

**Appendix 5: Mid-water sonar and ADCP**

**Appendix 6: CTD**

**Appendix 7: Sediment coring**

**Appendix 8: Sediment thickness**

#### *Acknowledgements*

*We thank the captains and crews of RV Electra and EVA-316 for great team work during the survey operations, and the Baltic Sea Centre at Stockholm University for their practical and efficient administrative support to the project. The Swedish Accident Investigation Authority and the Estonian Safety Investigation Bureau provided key background information and feedback throughout the project, which is gratefully acknowledged. The Swedish Geological Survey and Swedish Geotechnical Institute are thanked for providing helpful input. The Swedish Maritime Administration swiftly provided a side-scan sonar, when our broke down. Alasdair Skelton is thanked for advice about the possible composition of the outcropping bedrock. We would also like to thank the Swedish and Estonian survivors that patiently still are awaiting our presentations of the results, although our report cannot solve the trauma of why and exactly what happened when MS Estonia sunk.*

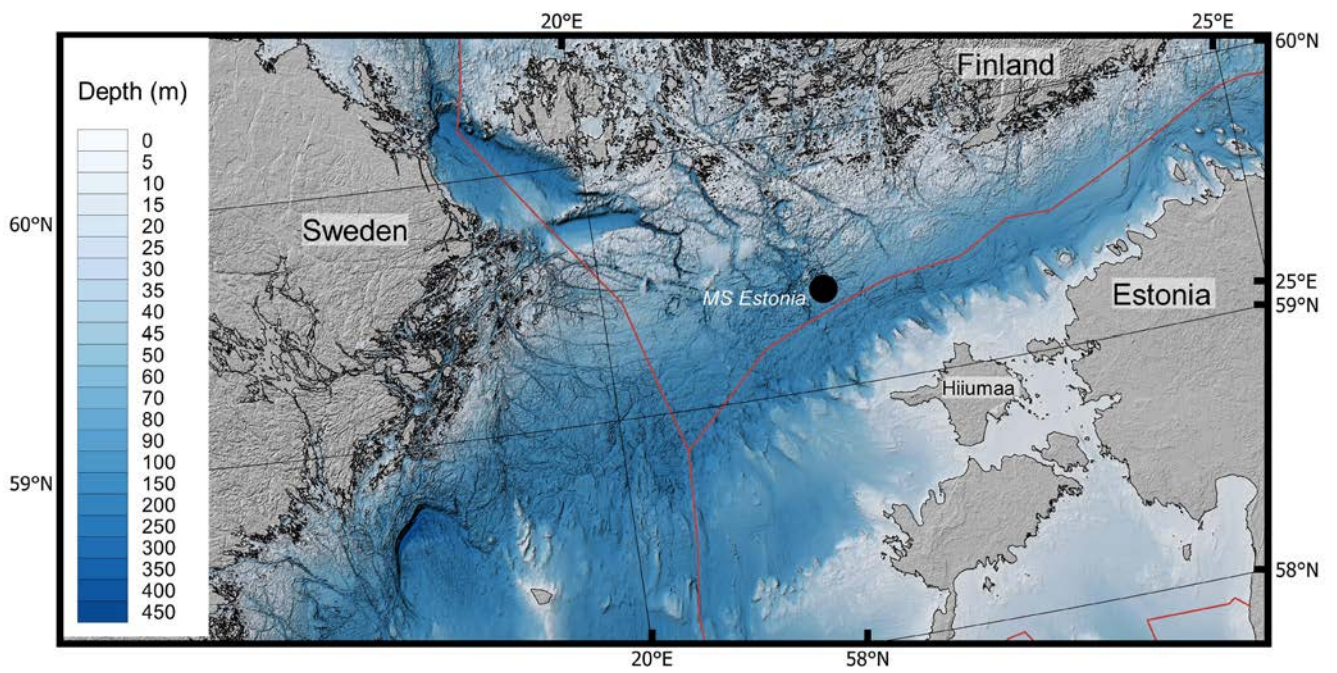


Figure I1. Bathymetric map of the central Baltic Sea showing the location of the shipwreck of MS Estonia. The bathymetry is from EMODnet (EMODnet Bathymetry Consortium, 2018).

## Introduction

MS *Estonia* sunk September 28, 1994, in heavy weather in the Baltic Sea at about 53 km northwest of the Estonian island Hiiumaa (Fig. I1). Between the 8th and 15th of July, 2021, Stockholm University carried out a survey of the MS *Estonia* wreck site with research vessel RV *Electra* (Photos I1 and I2). The survey was requested by the Swedish Accident Investigation Authority (SHK) and Estonian Safety Investigation Bureau (OJK). The requested tasks consisted of mapping MS *Estonia*'s present position on the seafloor as well as the seafloor topography (bathymetry) and geology of the wreck site for the purpose of establishing a base dataset to be used for further assessments of the accident as well for the preparation of additional investigations including, e.g., photogrammetry.

Planning of the expedition, including deciding the specific type of surveys, was done during a series of meetings in the spring of 2021. These meetings were chaired by the OJK and included participants from relevant governmental agencies and research institutions from Estonia, Finland and Sweden.

This report describes the applied acoustic mapping and sampling methods during the *EL21-Estonia* expedition and presents the results in the form of maps, graphs and computer 3D-visualizations. All raw (unprocessed) data have been shared with SHK and OJK continuously during the survey. Examples of processed data are shown and described in the *Results and interpretation* section, while appendices include higher resolution maps and tables. Geological interpretations based on the acquired data are included in this report. Some snapshots from the films of MS *Estonia*'s hull acquired with a Remotely Operated Vehicle (ROV) by the Estonian commercial diving company Tuukritööde OÜ are shown to support geological interpretations. The ROV results are presented in a separate report compiled by Tuukritööde OÜ (2021).

In summary, an area around the wreck of MS *Estonia* of approximately 2500×1800 m was surveyed using RV *Electra*'s installed multibeam bathymetric echosounder, sub-bottom profiler and midwater split-beam echo sounder as well as with a towed side-scan sonar. In addition, seismic reflection profiles were acquired by the Geological Survey of *Estonia* from RV *Electra* using their towed boomer system. Three sediment cores were retrieved with a 6 m long piston corer and bottom surface samples were taken with a grab sampler. Stations where salinity, water temperature and oxygen concentration profiles were acquired with a CTD (Conductivity, Temperature, Depth) instrument. Current measurements with an Acoustic Doppler Current Profiler (ADCP) installed in RV *Electra* were performed along the survey lines of the mid-water echosounder. An ADCP was also installed on a bottom mooring approximately 300 m northeast of the shipwreck during the duration of the survey to get additional current information.

RV *Electra* was supported by the Estonian icebreaker *EVA-316* from which high-resolution acoustic imaging of MS *Estonia* was conducted using a Mesotech scanning sonar placed at specific locations on the seafloor around and on the shipwreck. The scanning sonar results are presented in a separate report by Abbott (2021). Daily expedition notes are presented in Appendix 1.



*Photo 11. Aerial photo of the three vessels involved in the survey of the MS Estonia shipwreck. Top: The Subsurveyor VLT-089 used for the ROV (Remote Operated Vehicle) operations; Center: The 58 m long Estonian icebreaker EVA-316 used as a supply vessel and as a platform for acoustic imaging of MS Estonia by Abbott Acoustics using a Mesotech scanning sonar; Bottom: Stockholm University's 24 m long Research Vessel (RV) Electra that carried out geophysical mapping, geological coring and oceanographic station work. Photo: Madis Veltman, Postimees*



Photo 12. Stockholm University's Research Vessel (RV) *Electra*. Photo: OJK open archive



Photo 13. The Estonian icebreaker EVA-316. Photo Martin Jakobsson

## Background

Here we present a very brief synopsis of previous investigations of the seafloor geology carried out in the vicinity of MS *Estonia*. The idea is to give a general overview of the information that was available prior to our investigations and, thus, numerous details have been left out. The shipwreck of MS *Estonia* is resting on a sloping seafloor at water depths between about 75 and 85 m inside the Exclusive Economic Zone (EEZ) of Finland (Fig. I1). Following the tragic accident in September 28, 1994, the companies Rockwater A/S, Stavanger and Smit Tak from Rotterdam were contracted by the Swedish Maritime Administration to carry initial investigations for the purpose of providing information that would assist the decisions of further actions, including whether or not the shipwreck was going to be salvaged or covered at its location. Their first surveys were carried out between 1st and 4th December and included inspections of the shipwreck by divers and ROV (Remote Operated Vehicle) as well as some initial geological investigations of a 4 km<sup>2</sup> large area around MS *Estonia* (Rockwater A/S and Smit Tak, 1994). An extended investigation was made by Rockwater A/S in May 1995, which included geotechnical studies of the seabed at the shipwreck site. A decision was taken to cover MS *Estonia* at its location rather than salvage the shipwreck. A summary of the available geotechnical information from previous surveys of the shipwreck site has been published by Rudebeck and Kennedy (2021).

Based on their initial echo sounding surveys, Rockwater A/S compiled a detailed bathymetric contour map of a 500×500 m large area with the shipwreck in the centre. Their echo sounding survey lines were completed at a denser spacing within an inner box of 150×200 m. Sediment surface sampling, coring and Cone Penetration Test probing with pore water pressure measurements (CPTu) were included in the Rockwater A/S investigation. They mapped soft clays in the area south of MS *Estonia* where gas in the sediments partly had blanked the sub-bottom echo sounding profiles. The CPTu probing around the shipwreck encountered firmer sand and gravel within a sub-bottom depth of 20 m, apart from in an area in the south east where the probing was aborted before reaching harder substrates. The firmer geological layer was encountered at shallower sub-bottom depths of about 2.5 m north of MS *Estonia*. A geological map at the scale of 1:5000 including interpreted sediment thicknesses was compiled in 1995 by the Naval Research Institute in Helsinki, Finland (Fig. I2) (Nuorteva, 1995). This map shows that the shipwreck of MS *Estonia* is situated at the border between post glacial clay and glacial clay. Postglacial clay is generally very soft and the more recent deposited clay commonly has high organic content implying biogenic production of gas, which fits well with available descriptions. The geological map shows areas with till and bedrock at the seafloor, including directly north of the shipwreck (Fig. I2). An additional map at the scale of 1:10000 covering a wider area around the shipwreck was also published in 1995 by the Naval Research Institute in Helsinki, Finland.

The work of covering MS *Estonia* started in March 1996 by placing heavy rock material along strings on the seafloor, following the depth contours, and laying out geotextiles south of MS *Estonia*. The function of the so-called forced penetrations strings was to stabilize mapped soft clays south of the shipwreck by penetrating through them until more stable geological layers were encountered. The geotextiles were also laid out to stabilize the seabed. Sand was subsequently dumped over the stabilized area in June 1996. During this work, the daily echo soundings of the seafloor on July 21, 1996, revealed seafloor deformations. It became clear that submarine slides had occurred in the soft clays. After attempts of further stabilizing the seabed by dumping additional material, the work of covering MS *Estonia* was aborted at the end of July 1996. A seismic reflection survey was carried out by Netherlands Institute of Applied Geoscience TNO in 1997 for the purpose of gathering additional information about the sub-bottom geology for continued work on covering MS *Estonia* (Mesdag, 1997).

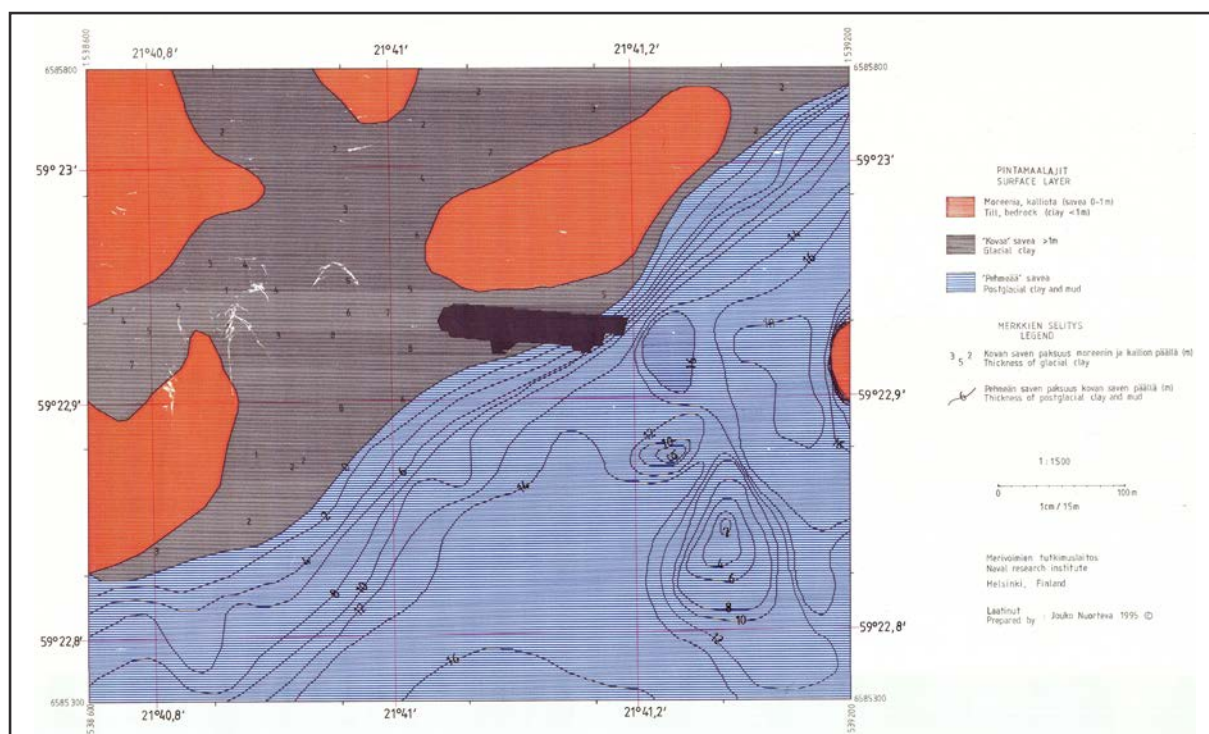


Figure I2. Geological map compiled 1995 by the Naval Research Institute, Helsinki, Finland.

## Expedition Participants and operational schedule

The team of expedition *EL21-Estonia* onboard RV *Electra* is listed in Table I1 along with shore-based personnel involved in the post-processing of the data. Operations onboard were carried out 24h implying working in shifts. The scientific staff consisted of four persons throughout the expedition. They operated all survey equipment during 12h shifts, while the crew applied a 6h watchkeeping schedule.

Table I1. Participants in expedition EL21-Estonia.

Name	Main Role	Organization
<b>Scientific crew</b>		
Björn Eriksson	Survey technician (Scientific staff)	Dept. of Geological Sciences, Stockholm University
Rickard Fornander	Survey technician (Scientific staff)	Ricfor AB
Martin Jakobsson	Chief scientist	Dept. of Geological Sciences, Stockholm University
Christian Stranne	Scientist	Dept. of Geological Sciences, Stockholm University
Steen Suuroja	Scientist (operated the boomer system during one day)	Geological Survey of Estonia
<b>Crew</b>		
Albin Knochenhauer	Skipper	Swedish Maritime Administration
Eva Lindell	Technician	Baltic Sea Centre, Stockholm University
Mattias Murphy	Skipper/Technician	Baltic Sea Centre, Stockholm University
Thomas Strömsnäs	Captain	Baltic Sea Centre, Stockholm University
Carl-Magnus Wiltén	Skipper/Technician	Baltic Sea Centre, Stockholm University
<b>Shore based</b>		
Matt O'Regan	Scientist	Dept. of Geological Sciences, Stockholm University
Anton Wagner	Technician	Dept. of Geological Sciences, Stockholm University

## EL21-Estonia survey planning

Planning of the expedition involved time allocation of each of the various geophysical survey methods and the geological coring considering a suite of parameters. For example, the optimal ship speed accounting for the trade-off between data resolution and survey time, data coverage of each applied mapping method, and the fact that running some of the sonar systems simultaneously requires time synchronization between the echo sounders, which lowers their ping rate and thus reduces the along track resolution. Due to the last-mentioned parameter, it was decided to run the multibeam, sub-bottom profiler and midwater echosounder separately as they do disturb each other acoustically without time synchronization. This approach generated the highest possible resolution that could be achieved.

A first overview survey with the multibeam echosounder was planned with 100% overlapping swaths and a swath angle of  $50^{\circ} \times 50^{\circ}$  (Fig. I3). The EM2040 multibeam, described below in methods, is capable of  $70^{\circ} \times 70^{\circ}$ . By decreasing the swath width to  $50^{\circ} \times 50^{\circ}$ , the across-track resolution of the acquired bathymetry is increased. However, the survey will take longer to complete as it will require closer survey lines to keep 100% overlap of the swaths, implying that the seafloor is

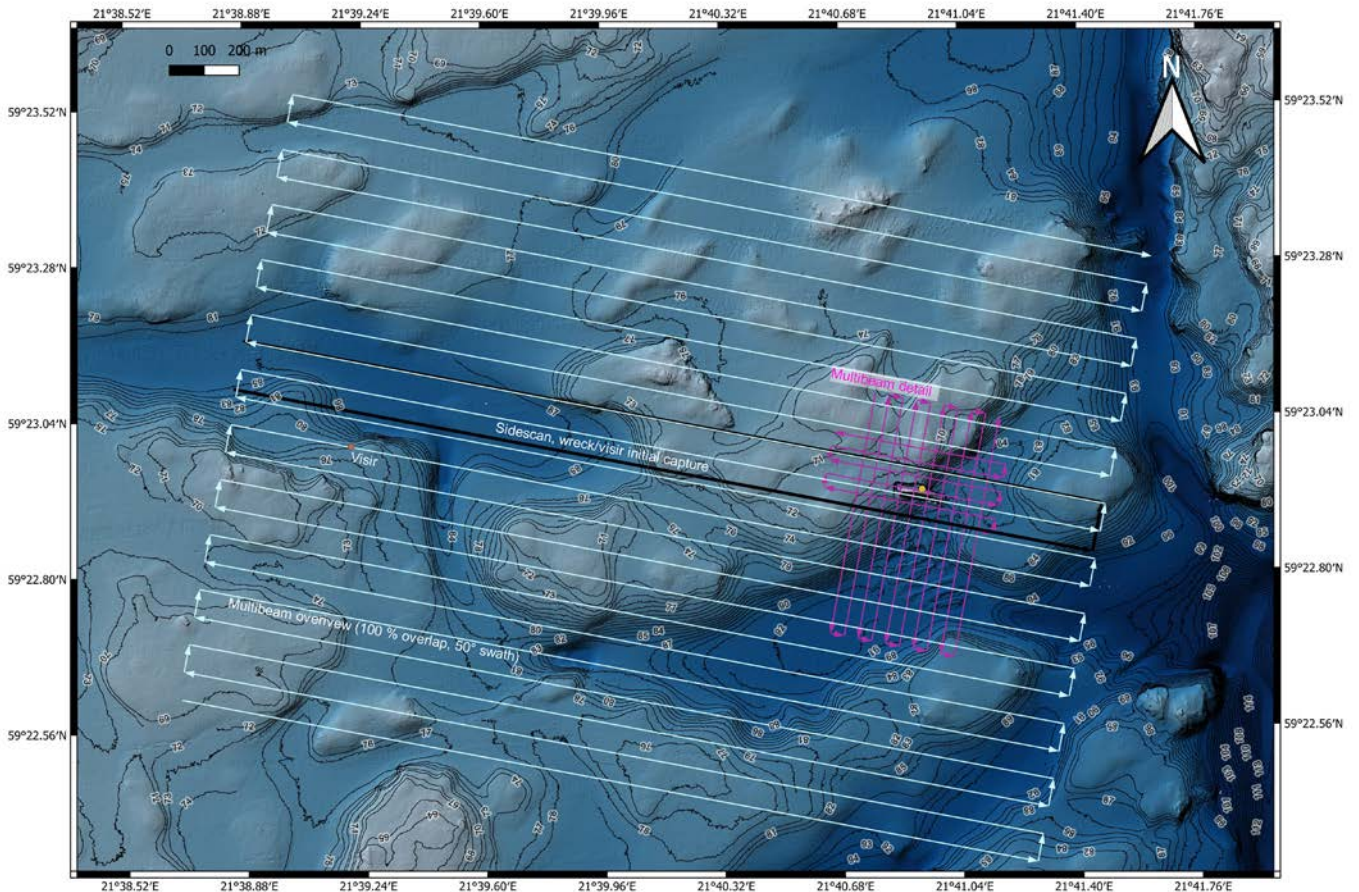


Figure I3. Planned multibeam overview (light blue lines) and detailed (purple) surveys. The location of MS Estonia is indicated by a yellow dot and also seen in the Finnish multibeam bathymetry from 2006, which was provided by the Finnish Transport and Communication Agency for planning purposes. Two planned side-scan survey lines are shown in black. These two lines were planned as an absolute minimum to cover the shipwreck and the location where the bow visir was recovered. The second side-scan line is difficult to see as it is covered by the multibeam track.

mapped twice by the multibeam. The chosen parameters resulted in approximately 80m between the survey lines considering the water depths in the survey area, which was provided by the Finnish Transport and Communication Agency (TRAFICOM) multibeam survey from 2006 (Fig. I3). The purpose of our first multibeam overview survey was to create a new up-to-date bathymetric map of the area that would help placing all other data to be acquired in a high-resolution spatial context. In addition, backscatter information was going to be collected along with the bathymetry. Backscatter is a measure of the amount of acoustic signal echoed back from the seafloor and it provides geologic information on the bottom type. A detailed multibeam survey focusing on the shipwreck was also planned, with a higher degree of overlapping swaths and further decreased swath width to maximize the resolution (Figs. I3 and I4).

Sub-bottom profiles were planned along every second multibeam survey line implying a line-distance of 160m. In addition, the survey plan included cross lines spaced at the same distance of 160m (Fig. I5). A regular grid of sub-bottom profiles facilitates the interpretation of the sub-bottom geology due to the abundance of crossing profiles. Midwater split beam sonar profiles were planned to be acquired together with ADCP data along the sub-bottom profile survey lines, but at a separate occasion. Table I2 shows all the planned surveys and estimated time.

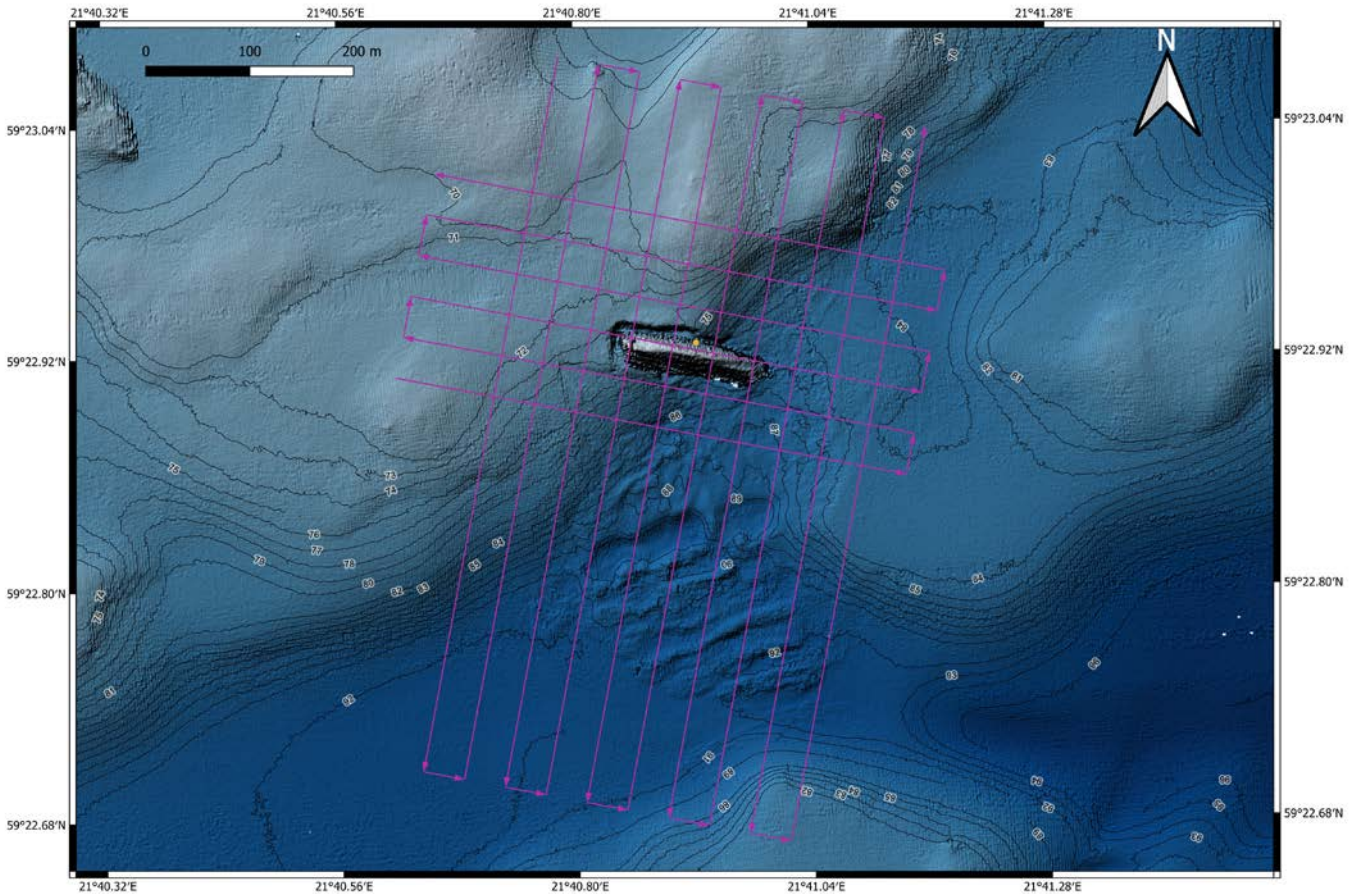


Figure I4. The planned detailed multibeam survey.

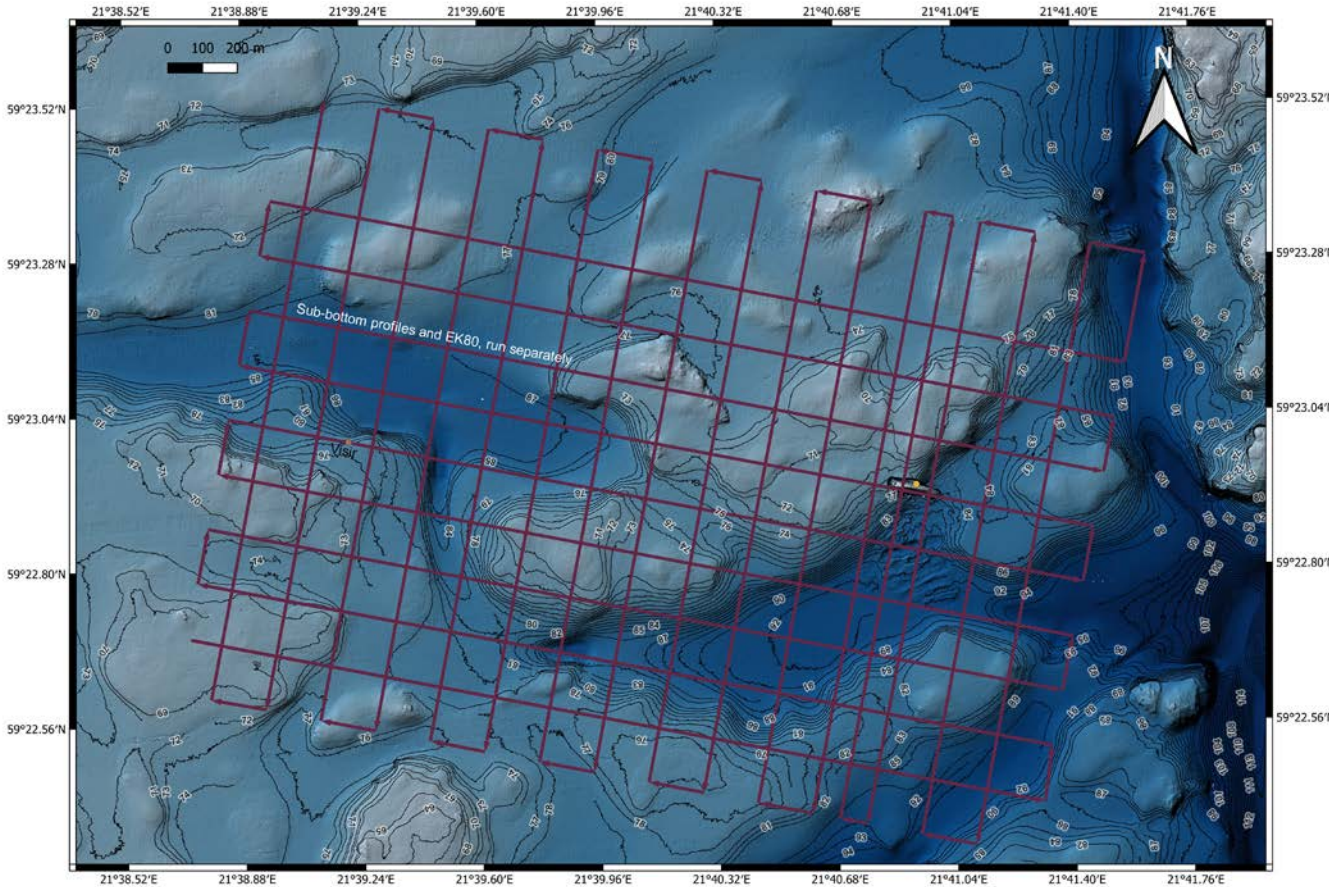


Figure 15. Planned sub-bottom profiles. The midwater split beam sonar was planned to be used separately together with the ADCP along the same survey lines.

Table 12. Overview of the planned activities and a rough time allocation including enough slack to permit for some down-time due to bad weather. One “Day” is a full 24 h.

Activity	Day
Multibeam overview, 100% overlap, swath angle (2x50°)	Day 1
Multibeam detail	Day 1
6 CTDs in survey area, 3 at start and 3 at end	Day 1
Sub-bottom profiling, every second multibeam + cross lines (line spacing 160 m)	Day 2
Midwater profiling (EK80), focused grid around wreck. ADCP (600 kHz) to be run simultaneously	Day 2
CTD profile, grid with stations	Day 2
Side-scan, min 2 passes of wreck site (several more will likely be required to optimize angle)	Day 3
Side-scan, cover full multibeam area 50% overlap, range 133 m, 50% overlap	Day 3
Bottom scanning, M3 from lowered frames (From EVA-316)	Day 4
Bottom scanning, M3 from lowered frames (From EVA-316)	Day 5
Bottom scanning, M3 from lowered frames (From EVA-316)	Day 6
Coring	Day 7
Coring	Day 8

## Methods

All maps in the *Methods* and *Result and Interpretation* sections of this report are in Universal Transverse Mercator (UTM) projection zone 34. Listed geographic coordinates of sample locations and observations are with reference to WGS 84.

### RV *Electra*: Equipment overview

RV *Electra* has a multibeam echo-sounder, sub-bottom profiler, midwater sonar, and an ADCP permanently installed in the hull. The transmitting and receiving acoustic transducer arrays of these systems are mounted in a purpose-designed keel (Fig. M1). Operations of these acoustic mapping systems are done from a dedicated control room (Photo M1).

The 24.3m long and 7.2m wide vessel has a 31 m<sup>2</sup> large lab. The aft section of this lab has a dedicated area from which the CTD and other devices can be launched through an opening in the side of the vessel. Coring and other sampling are mainly carried out from the aft deck using dedicated winches and core launching arrangements. The research vessel has dynamic positioning permitting station keeping. Table M1 provides a summary of the installed acoustic mapping equipment, motion sensor/navigation system, and geological sampling devices used during expedition *EL21-Estonia*. The individual systems listed in Table M1 are further described below.

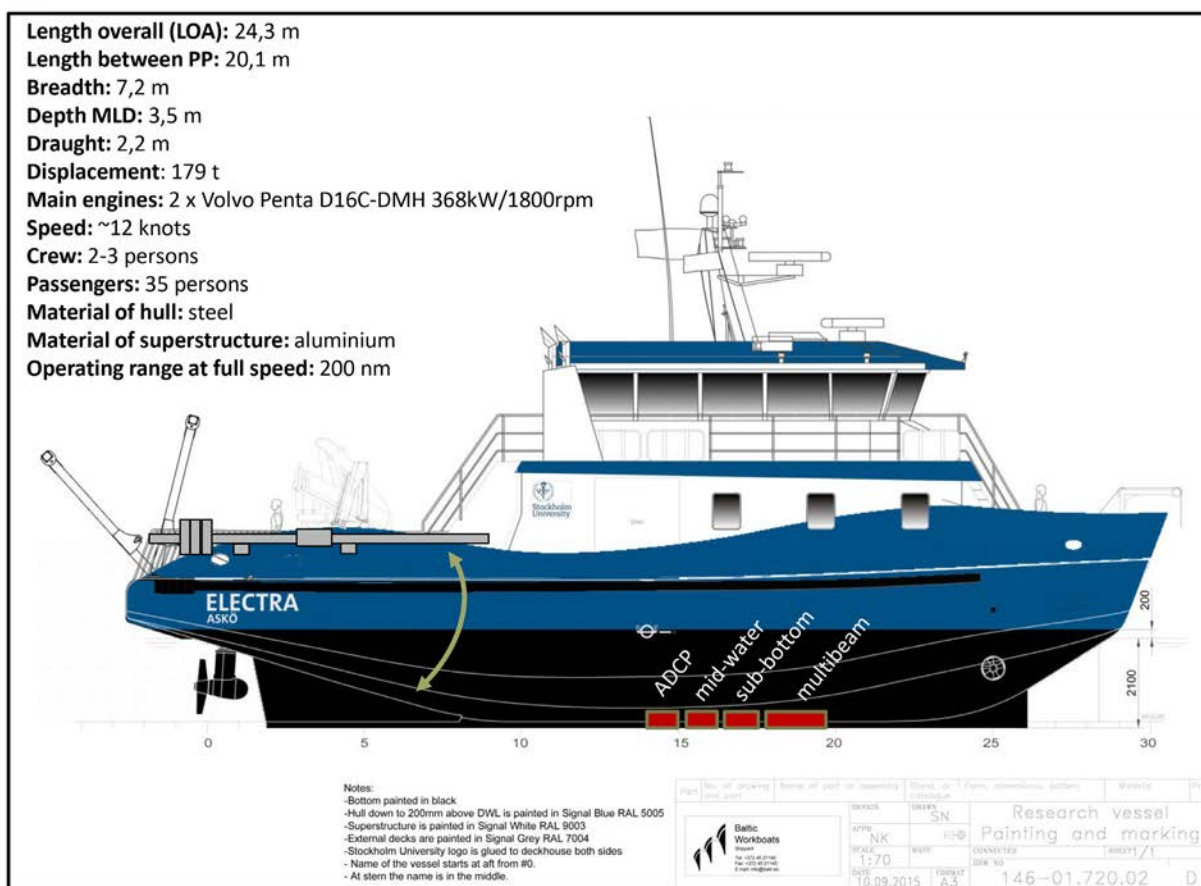


Figure M1. Specification of RV *Electra*. The transducers installed in the purpose-designed keel are shown as red boxes, not drawn to scale but they are installed in relationship to one another as shown in the drawing

Table M1. Technical specifications of RV *Electra*'s acoustic mapping equipment and motion sensor/navigation system as well as other devices used during the EL21-Estonia expedition.

<b>Multibeam:</b> Kongsberg EM2040, 0.4°×0.7°, 200–400 kHz (max depth 600 m)
<b>RTK GPS:</b> Kongsberg/Seatex Seapath 330+ (Position accuracy xy ±1 cm + 1 ppm RMS, z ±2 cm + 1 ppm RMS, heading accuracy 0.05°)
<b>Motion sensor:</b> Kongsberg/Seatex MRU5+ (heave/pitch/roll)
<b>Sub-bottom profiler:</b> Kongsberg Topas PS40, 24ch, parametric (35–45 kHz/1–10 kHz)
<b>Midwater split-beam sonar:</b> Kongsberg EK80, 70 kHz/200 kHz
<b>Side-scan:</b> Klein 5000 V2, 455 kHz
<b>Acoustic Doppler Current Profiler (ADCP):</b> Teledyne Workhorse Mariner, 600 kHz
<b>SVP (Sound velocity/pressure):</b> Valeport (mounted in the hull)
<b>SVS (Sound velocity sensor):</b> Valeport MiniSVS
<b>CTD:</b> Seabird 911+, including conductivity, temperature, pressure, dissolved oxygen, turbidity, fluorescence (Chlorophyll A) and PAR sensors
<b>GoPro Camera</b> mounted on CTD and in a water proof casing with two separate light sources
<b>Piston corer</b> , 6 m long loaded with 473 kg led weights
<b>Grab sampler</b>

## Seafloor and water column mapping with acoustic methods

### Position, heading and attitude

All mapping systems receive attitude, heading and positions from a Kongsberg Seapath 330+ system including a MRU5+ motion and reference unit and two GPS/GLONASS antennas mounted in the mast of RV *Electra*. The system is dual frequency (L1/L2 band) and capable of utilizing RTK corrections, which were received through the internet during the expedition using the Open Source Lefebure NTRIP Client (<http://lefebure.com/software/ntripclient>). Corrections were first taken from an Estonian provider, however later changed to be acquired from the National Land Survey of Finland positioning service as it provided a more stable solution at our survey location. Corrections were received using the RTCM 3 protocol. When steady corrections were received, the Seapath 330+ system generally reported accuracies in the cm range. The raw RTCM data were stored for addition postprocessing.

### Multibeam echo-sounder

RV *Electra* has a hull-mounted Kongsberg EM2040 0.4°×0.7°, 200–400kHz, multibeam echo-sounder. The transmit transducer array is (L×W) 727×142 mm and mounted along-ship while the receiving transducer array is 407×142 mm and mounted across-ship. These yields transmit and receive beam widths of 0.4° and 0.7° respectively. Maximum useable swath width across track is 70°×70°, implying that the multibeam is able to create a swath reaching 70° away from nadir towards each side. The multibeam is operated using Kongsberg's Seafloor Operation System (SIS), version 4.3.2 (Build 31, DBVersion 30.0). Both bathymetry and water column data were acquired during the expedition. The overview survey of the larger area was carried out according to plan using a 50°×50° swath width in 400kHz mode. For the detailed surveys of the shipwreck, the swath width was varied in order to generate the maximum amount of sounding on all parts of the hull: A narrow swath width of 25°×25° was used for most parts of the shipwreck, while we opened the swath to its maximum of 70°×70° during some lines to reach the parts of the wreck resting on the seafloor from a slant. The multibeam system was set to high-density equiangular mode for the shipwreck survey and to high-density equidistant mode for the overview survey.



Photo M1. RV Electra's survey room from where all acoustic mapping systems are controlled. (a) Computer screens are mounted on the aft wall in the control room and connected to a display matrix system permitting switching between all computers controlling sonars, Seapath navigation/attitude system and CTD. The display matrix system is also extended to the bridge, permitting control and display of the sonars systems on the bridge. (b,c) All units belonging to the sonar systems, Seapath navigation, and CTD are mounted in specifically designed racks located in a cooled enclosed part of the survey room. (Photos: Martin Jakobsson, reused from previous RV Electra cruise reports).

### Sub-bottom profiling

RV *Electra* has a Kongsberg Topas PS40, 24 channel, sub-bottom profiler installed. The transmit and receive transducers are located aft of the multibeam. The transmit transducer is (L×W) 830×540mm and the receive is 340×180mm. Topas PS40 is a parametric echosounder that produces low frequency (secondary) acoustic pulses in the range of 1–10kHz by non-linear interaction between two high frequency (primary) pulses in the range 35–45kHz. The PS40 is capable of generating a source level of >204 db for a 6kHz pulse. Sub-bottom penetration may exceed 50m in soft sediments. During the *EL21-Estonia* expedition a 4–10kHz 1ms long chirp pulse was used. The system was set to apply a maximum ping rate.

### Side-scan sonar

A Klein 5000 V2 with an operating frequency of 455kHz was provided by the Swedish Maritime Administration (SMA) just prior to the *EL21-Estonia* expedition as technical issues with Stockholm University's Klein 3000 were encountered during the pre-expedition equipment trials. The Klein 5000 V2 has a swath sonar option, which not was in operation on the provided tow fish.

RV *Electra* does not have a sonar winch that was setup to handle the Klein 5000 V2. For this reason, we had to tow the 70kg and 194cm long tow fish using the main coring winch and a separate sonar cable (Photos M6).

### Midwater sonar

A Simrad EK80 wide-band sonar system is installed in RV *Electra*. Broadband acoustic water column data were collected with two split-beam transducers: A Simrad ES70C transducer and a Simrad ES200-7C transducer, both with a 7° circular beam. All system parameters (i.e. transmit power, signal mode, pulse length) were kept constant during acquisition. The system was operated continuously with the two transducers pinging simultaneously in broadband mode with frequency ranges of 45–90kHz and 160–260kHz respectively. For the ES70C transducer, the transmit power was set to 750W and the pulse length was set to 4ms, and for the ES200-7C transducer the transmit power was set to 150W and the pulse length was set to 8ms. The two transducers are placed aft of the Topas transmitting and receiving units. The EK80 is operated using Kongsberg's dedicated software, version 1.8.3.

### Acoustic Doppler Current Profiler (ADCP)

An ADCP is a hydroacoustic instrument that measures horizontal and vertical ocean current components in the water column. A Teledyne RDI Acoustic Doppler Current Profiler (ADCP) is installed with a 600kHz transducer mounted furthest aft of all systems. The model is Workhorse Mariner, with a max range specified by the manufacturer to 50m. The ADCP was operated at a ping rate of 3.3Hz, in parallel with the midwater EK80 operations, with 2m depth bins ranging from about 6.5 to 85.5m depth.

### Water properties (sound speed, temperature, salinity)

A Seabird 911+ CTD (Conductivity, Temperature, Depth) sampling system is included in RV *Electra*'s standard scientific equipment. This CTD is equipped with 12 Niskin bottles (each 5 liter). In addition to conductivity, temperature and pressure (depth) sensors, there are sensors installed to acquire dissolved oxygen, turbidity, CDOM (Color Dissolved Inorganic Matter), and ChlA (Chlorophyll A) data. Data was logged with the dedicated Seabird software Seasave version 7.26.7.121.

A Valeport MiniSVS is installed in a dedicated pipe running through the hull with its opening end near the multibeam echo-sounder transducers to continuously record sound speed. A Valeport MiniSVP (Sound velocity, pressure) sound velocity profiler is also included in the multibeam equipment to record sound speed profiles at discrete stations.

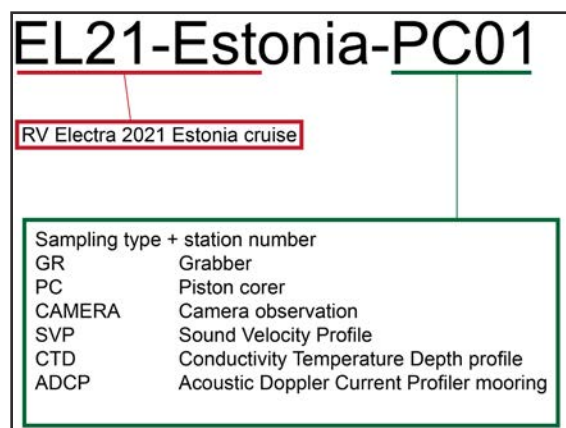
### Acoustic synchronization unit

The EM2040 multibeam, Topas sub-bottom profiler and EK80 split beam midwater sonar can all be synchronized through the installed Kongsberg K-Sync unit. This implies that these three acoustic systems can be operated simultaneously without acoustic interference, which otherwise may result in severely degraded data quality. In particular, the Topas sub-bottom profiler greatly disturbs the EK80 and to some extent also the EM2040. However, running all systems synchronized through K-Sync will not permit that any of the systems use a mode where more than one ping is sent into the water at the time. Therefore, the K-Sync unit was not used during the *EL21-Estonia* expedition and the EM2040, Topas, and EK80 surveys were instead carried out separately to maximize the quality. The EK80 was operated together with the ADCP as they do not disturb each other.

### Sediment sampling, bottom inspection and mooring

#### Piston/gravity corer

RV *Electra* is equipped with a large diameter piston corer and a tailored core-handling system on the starboard side (Fig. M1; Photos M2a–c). The corer can also be used in gravity core mode without the piston. Led weights of either 68 or 45kg are used on the core head. The core head can be loaded with a maximum weight of 563kg. The sediment that goes into the corer are captured in PVC liners with lengths of 6m and outer/inner diameter of 110/98.5mm. The trigger weight of the piston corer is comprised of a small 1 m long gravity corer that uses transparent polycarbonate liners with outer/inner diameter of 88/80mm. The standard piston core release arm is designed so that the led weights on the trigger weight should amount to 1/10 of the lead weights on the main core head. The core barrels come in 3m long sections and maximum of two barrels can be used on RV *Electra* implying up to 6m long cores. During *EL21-Electra* expedition, the corer was rigged in piston core mode with two 3m long barrels and the core head loaded with 473kg (Photo M2b).



The cores were cut into 1.5m long sections and stored in a portable refrigerator placed on the aft deck (Photo M2a) The naming convention of retrieved cores and all other stations is shown in Figure M2.

An InterOcean hydraulic winch (model 10031-20HLW), equipped with 600m of 11.43mm diameter wire (Rochester A302799), is used to launch the corer through the A-frame (Photo M2c). Max working load of the wire is 1818kg and its breaking strength is 7273kg.

Figure M2: Station naming convention.

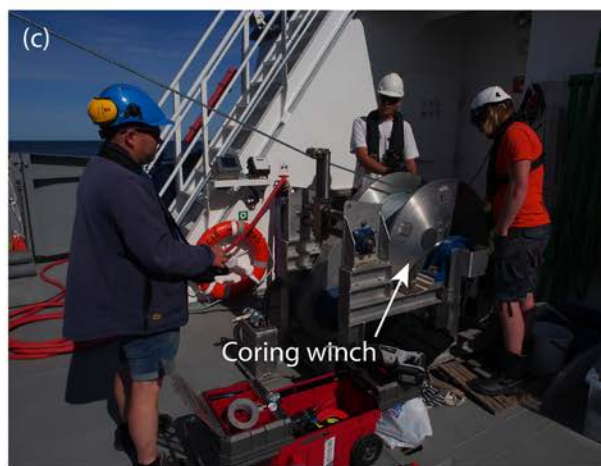
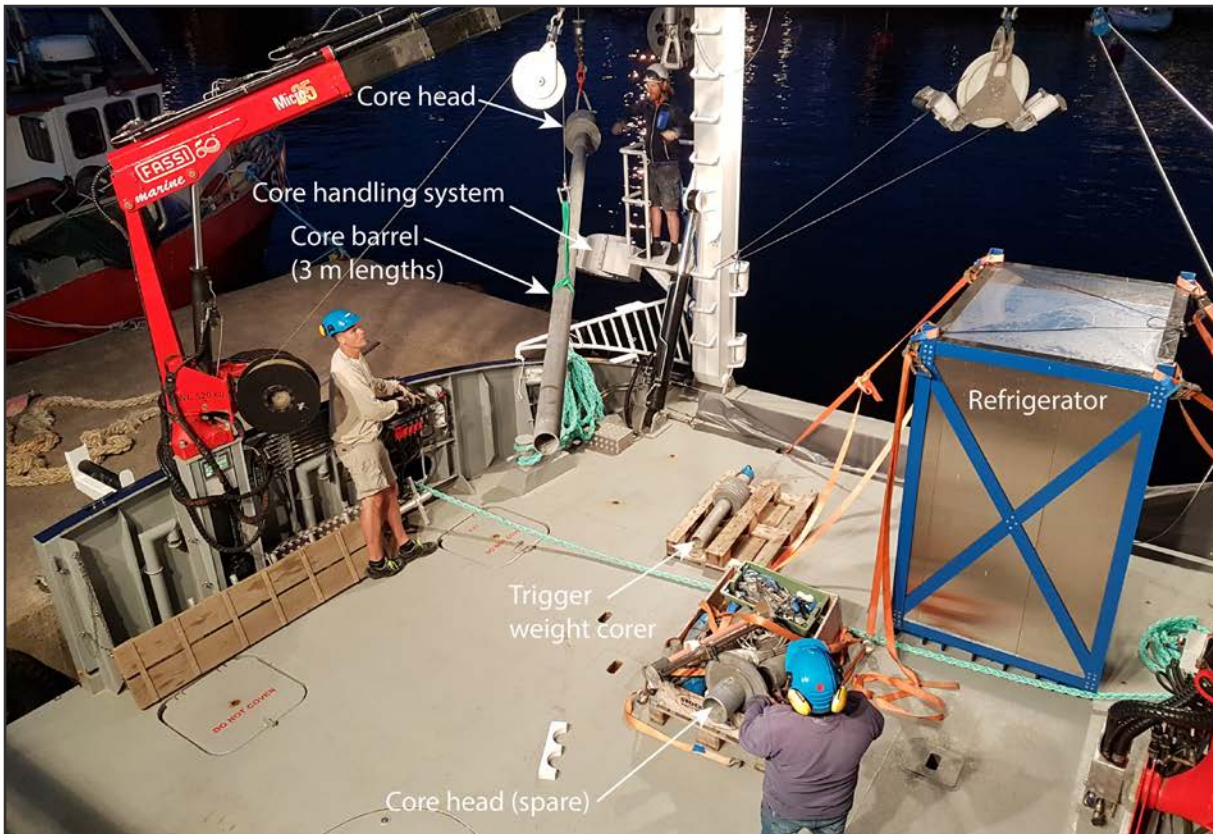


Photo M2. The coring system on RV Electra. (a) The corer has a launching system on the starboard side. A portable refrigerator for core storage is placed on the aft deck. (b) Core head loaded with 473 kg led weights. (c) Coring winch (InterOcean model 10031-20HLW hydraulic) equipped with 600 m of 11.43 mm diameter cable (Rochester A302799). (d) Corer in handling system. Photos: Martin Jakobsson (a and c are reused from previous cruise reports). Photos: Martin Jakobsson

## Grab sampler

The grab sampler that was used is referred to as of Van Veen type (Photo M3), named after Johan van Veen (Dutch Engineer) who invented this device in 1933. It takes disturbed surface sediment samples by closing two jaws when the sampler hits the seafloor. The jaws scoop up surface sediments.

## Naming of stations

Sampling and measurement stations were named following a convention where the cruise name precedes an abbreviation of the specific device used, in turn followed by a serial number. The retrieved sediment cores and grab samples were also named using this scheme. Table M2 lists the abbreviations and illustrates how the convention works. The short names of the stations are used on the maps in this report.

Table M2. Naming convention of sample and measurement stations.

Expedition	Device and abbreviation	Full name of station 01	Short name
EL21-Estonia	Conductivity Temperature Depth (CTD)	EL21-Estonia-CTD01	CTD01
EL21-Estonia	Sound Velocity Profiler (SVP)	EL21-Estonia-SVP01	SVP01
EL21-Estonia	Piston corer (PC)	EL21-Estonia-PC01	PC01
EL21-Estonia	Grab sampler (GR)	EL21-Estonia-GR01	GR01
EL21-Estonia	GoPro camera (CAMERA)	EL21-Estonia-CAMERA01	CAMERA01
EL21-Estonia	Acoustic Doppler Current Profiler mooring (ADCP)	EL21-Estonia-ADCP01	ADCP01

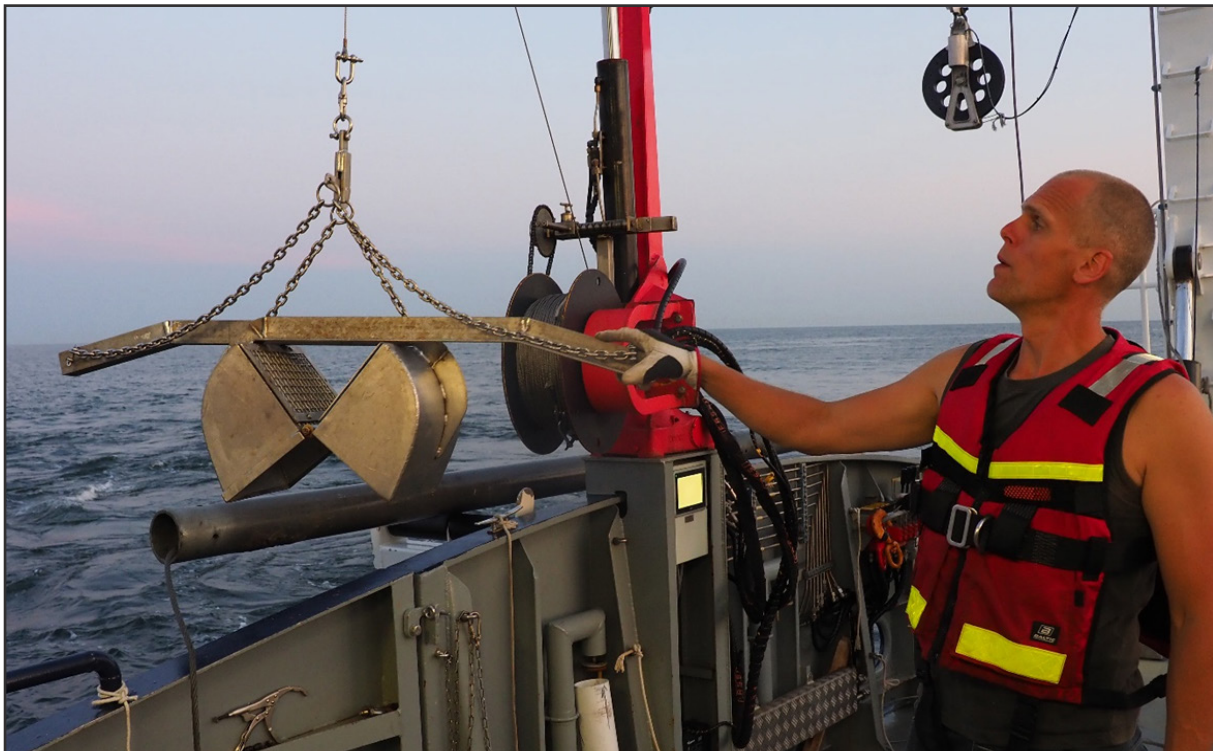


Photo M3. The Van Veen grab sampler used to take disturbed surface sediment samples for quick bottom characterization. Photo: Martin Jakobsson



Photo M4. GoPro Hero 7+ camera and light placed in water proof housings and mounted on the frame of the CTD carousel. Bottom inspections were carried out either along with CTD-casts or separately by lowering the carousel to the seafloor. Photo: Martin Jakobsson

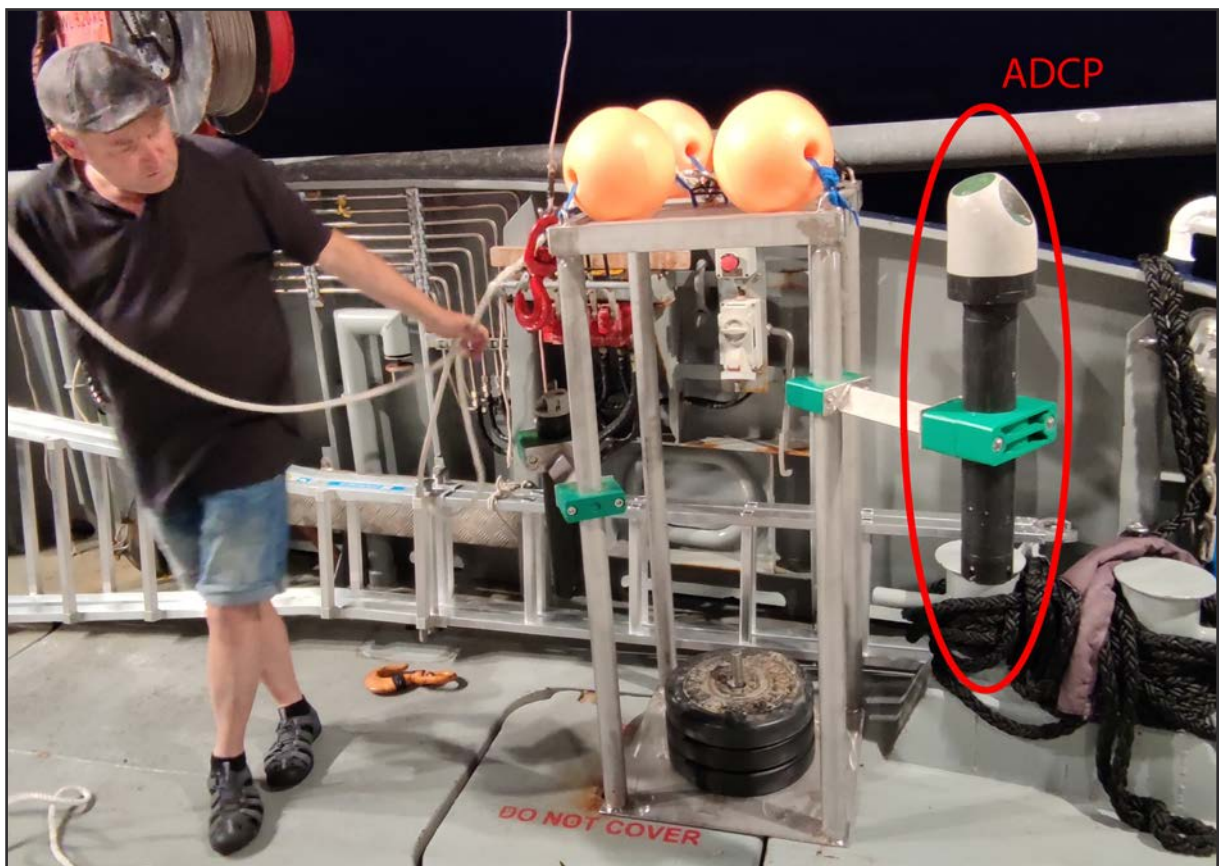


Photo M5. Frame of the moored ADCP (encircled in red). Photo: Christian Stranne

## Bottom filming

Bottom inspections were carried out using a GoPro camera, either along with CTD casts or separately. The setup consisted of a GoPro Hero 7+ camera in an underwater housing (US Company Group B; model ScoutPro H3) water proof to a depth of 2750m and an underwater light in a housing water proof to 1250m (US Company Group B; model Nautilux underwater video light and housing GPH-1250). The GoPro camera was mounted on the CTD carousel together with the underwater light (Photo M4).

## Moored ADCP

On July 9 at 18.30, a mooring was deployed with a bottom-mounted upward looking ADCP. The ADCP (Nortek Aquadopp profiler 400kHz) collected data continuously during the survey until the recovery at 07.30 on July 14 after completion of all other survey and sampling activities. The setup is shown in Photo M5. The bottom depth at the mooring site was 82m and the mooring position 53°23.010'N / 21°41.260'E. The profile interval was set to 10 minutes. Each profile was an average over 10 bursts (one each minute) with each burst consisting of 2 pings. Data was recorded in 34 two-meter bins, covering a depth range between approximately 15 and 80m.

## Post-processing and interpretation routines

### Multibeam bathymetry

The multibeam bathymetry data were postprocessed using the QPS Qimera software (Version 2.4.1) in three main steps: 1) sound velocity correction, 2) vertical datum adjustment using the RTK GPS heights to reference depths to the vertical datum RH2000 using the SWEN17\_RH2000 geoid separation model, and 3) removal of outliers.

The software TerraPos by Terratec was used with raw data from the Seapath 320+ to get the maximum out of the RTK corrections. However, due to issues with the saved raw files from the motion sensor, this only worked for the detailed survey over the MS *Estonia* shipwreck.



For the detailed survey, RV *Electra*'s trajectory was created by postprocessing the raw navigation files in TerraPos, and subsequently smoothed. Since the multibeam data were collected during a relatively short period of time, the smoothed curve resulted in a constant value of 19.40m above the GRS80 ellipsoid. The separation value between RH2000 and GRS80 is 18.97m (acquired from the SWEN17\_RH2000 geoid model), and RV *Electra*'s Center of Gravity (CoG) is thus  $19.40 - 18.97 = 0.43$  meters above the RH2000 model. By adding a waterline value of  $-0.47$  (waterline is lower than CoG) the water level is found to be 0.04 m below RH2000 during the time of the survey. Thus, for the overview survey where the SWEN17\_RH2000 not could be used direct due to issues with the saved raw data, a static offset of 4 centimetres was applied in Qimera, implying that all depths are referenced to RH2000.

Photo M6. Side-scan sonar towed in the main coring winch wire and with separate signal cable. Photo: Martin Jakobsson

In the third step, the multibeam data undergoes iterative analysis and corrective measures to ensure that all identified outliers are flagged as rejected. This includes both manual editing and the use of statistical automated algorithms such as the CUBE filtering (Calder and Mayer, 2003) followed by manual verification of the filtered area to ensure that not too many depth data points are flagged as outliers by CUBE. In all instances the ‘rejected’ data is merely flagged as disabled, with no data actually deleted.

The detailed survey July 12 when the weather was calm and RV *Electra* could be run at a slow speed was finally gridded with a cell-size resolution of 0.25×0.25m, while the overview survey was gridded at 1.5×1.5m. Analyses of the high resolution 0.25×0.25m grid should consider that the theoretical foot print of a 0.4° beam at 80m water depth has a diameter of 56cm, implying a certain degree of oversampling and that objects smaller than 56cm can likely not be detected.

### Multibeam backscatter

Multibeam backscatter was postprocessed using QPS FMGT (Version 7.9.6). A mosaic was created for the entire area at a resolution of 0.25×0.25m, while the detailed survey over the wreck permitted higher resolution, down to 0.15×0.15m. Statistics of backscatter values were compiled at blocks of 2×2 and 4×4m. An Angle Range Analysis (ARA) was performed over the entire area.

### Sub-bottom profiles

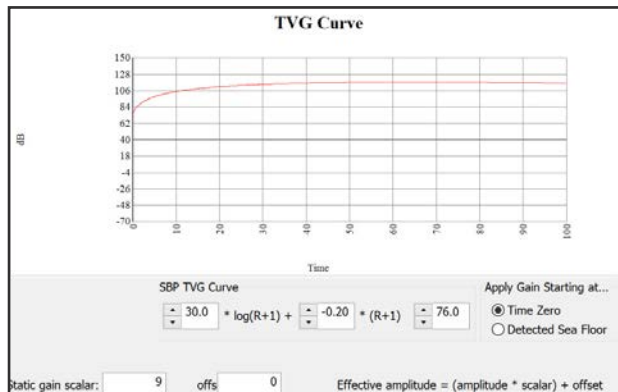


Figure M3. The Time Varied Gain (TVG) function applied in SonarWiz on the sub-bottom profiles as they are shown in this report.

The Topas PS40 sub-bottom profiling data were logged in Kongsberg’s raw-format (.raw) and converted using the Topas acquisition software into SEG-Y-format in order to be readable in standard post-processing software. The SEG-Y-files were imported into the post-processing and interpretation software SonarWiz (Version 7.07.07). While different types of gains were applied in SonarWiz during the interpretation process, the Topas sub-bottom profiles in this report are shown with an applied Time Varied Gain (TVG) beginning at time zero, along the function shown in Figure M3, together with a stacking of two traces. Following the gain setting, the sea-

floor was digitized in each profile. This permitted a subsequent vertical datum adjustment of all profiles so that the digitized seafloor aligns with multibeam bathymetry.

### Side-scan imagery

SonarWiz (Version 7.07.07) was used to postprocess the side-scan sonar data with the goal of producing a high-quality mosaic, which together with all other geophysical mapping data facilitates the interpretation the seafloor geology as well as identification of objects of potential interest on the seafloor. Klein’s acquisition software SonarPro used during the survey is able to store the acquired data both in their own SDF-format and the widely used XTF-format. It turned out that SonarWiz had an issue with importing the SDF-files due to a software bug (SonarWiz personal communication). For this reason, the XTF files were used. The postprocessing consisted of gain settings and bottom tracking in order to perform a slant range correction. Side-scan im-

agery without underwater positioning of the tow fish may suffer from a great deal of absolute positional uncertainty since positions provided from the ship's system must also account for the cable layback and tow fish depth. Prominent features in the multibeam bathymetry (mainly rock outcrops) that also could be identified in the side-scan images were used to verify the positioning. In some occasions, the side-scan records were moved horizontally a few meters to align perfectly with the multibeam bathymetry.

### Sediment thickness model

The acoustic basement (AB) is here defined as the deepest coherent reflection observed in the sub-bottom profiles (Fig. M4). The AB was digitized in all profiles and interpreted to generally correspond to a bedrock or till surface. This interpretation implies that the thickness of overlying softer sediments could be estimated (Fig. M4). The conversion from two-way-travel time recorded by the sub-bottom profiler to depth in meters was made in SonarWiz using a sound velocity of  $1600\text{ ms}^{-1}$ . Absolute depths of the interpreted AB reflector as well as calculated sediment thicknesses along all sub-bottom profiles were exported from SonarWiz as xyz points into ASCII flat files.

Grids representing the AB and sediment thickness in the area were created in QGIS (QGIS Development Team, 2018) using the Grass plugin *v.surf.rst* (Version 7.8.5), which applies an interpolation between points using a spline in tension algorithm (Mitasova et al., 2005). A high tension of 150 was applied to avoid over- and under-shooting of the surface. The gridding was supported by the digitized outcrops of bedrock interpreted from the side-scan images and multibeam backscatter data (Fig. M5). In addition, constraining points were inferred where bedrock was observed in the ROV investigations made by Estonian Tuukritööde OÜ commercial diving company (see results). It should be noted that the ROV was not fitted with an underwater positioning system implying that there is a rather large uncertainty with respect to the exact positions where bedrock is observed along the northern side of MS *Estonia*'s hull. However, the AB surface and sediment thicknesses grids were compiled at a grid-cell size of  $10\times 10\text{ m}$  and must be considered to provide generalized models associated with uncertainties. The largest uncertainties are likely from the interpretations of the AB in the sub-bottom profiles and the fact that the sub-bottom

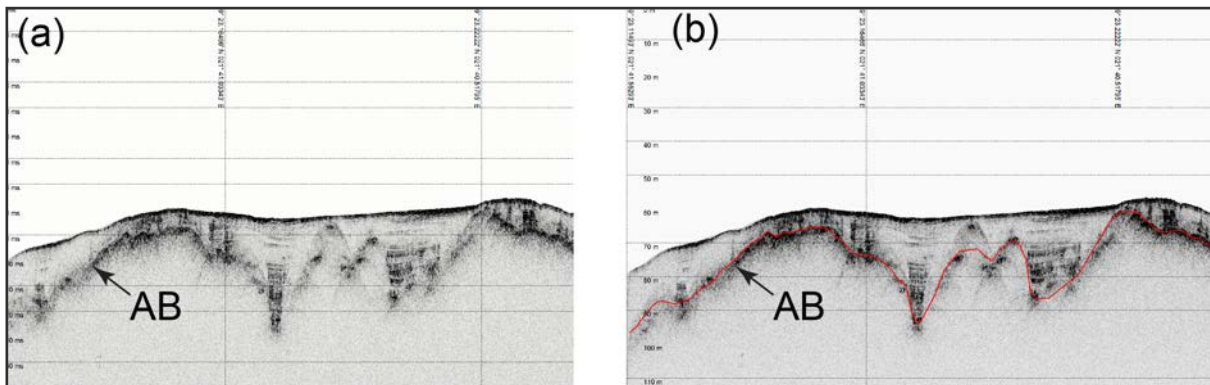


Figure M4. Sub-bottom profile illustrating the concept of identifying the Acoustic Basement (AB), here defined as the deepest coherent observed reflector. (a) Profile without interpretation. (b) Profile with interpretation of the AB inferred with a red line. Softer sediments, which are penetrable with the used 4–10 kHz 1 ms long chirp pulse, are assumed to generally make up the stratigraphy above AB. The typical signature of stratified (likely varved glacial clay) is seen in this profile above the AB.

profiles are spaced apart with approximately 150m, implying a great deal of interpolation between the points using the spline in tension function. It should also be noted that the shipwreck distorts the sub-bottom profiles crossing it, which made it impossible to pin-point the AB below the shipwreck.

### Midwater sonar

All EK80 data were processed in MATLAB 2021b using a series of internal scripts provided by Kongsberg Maritime (L. Anderson, personal communication). A matched filter was applied to the acoustic water column data using an idealized replica signal. For all data, range from the transducer face was computed using the mean harmonic sound speed based on the nearest in time CTD profile. Range data were converted to depth by accounting for the static vessel draft.

### ADCP (Acoustic Doppler Current Profiler)

All data from the shipboard ADCP were processed in MATLAB 2021b using script package provided by the Leibniz Institute for Baltic Sea Research, Germany (V. Morholz, personal communication). From previous surveys, it is known that the ADCP is mounted with a slight angular offset to the aft-bow axis of the vessel, and a mounting alignment bias of  $-5.477^\circ$  was applied. Data was averaged over time in 10 second bins. To get a sense of the average current speed and direction during the survey, the data was averaged in three equidistant sections over each survey line in two separate depth intervals: from the surface to 45m depth and between 45 and 55m depth.

### CTD (Conductivity Temperature Depth)

The CTD data were processed with Sea Bird's processing software (SBE Data Processing Win32\_V7.26.2) and binned into 0.1 dbar vertical averages. Using the binned data, salinity profiles were converted to absolute salinity following the International Thermodynamic Equation of Seawater (IOC, SCOR and IAPSO, 2010) with the GibbsSeaWater (GSW) Oceanographic Toolbox for MATLAB (<http://www.teos-10.org>). Depth vectors were then calculated from the pressure, temperature and absolute salinity profiles. CTD profile data are shown for individual stations in this report as well as for average profiles ( $\pm$  one standard deviation) where the data were first interpolated to a common 1 cm depth grid.

### Multi sensor core logging (MSCL)

The unopened sediment cores were logged on a Geotek Multi-sensor core logger (MSCL) in the Sediment (Lake and Marine) Laboratory (Slamlab) at the Department of Geological Sciences, Stockholm University. The MSCL setup for unopened cores implies that the sensors are oriented in the horizontal direction. Measurements of the gamma ray derived bulk density, compressional wave velocity (p-wave) and magnetic susceptibility were acquired at a down core resolution of 1 cm.

Gamma-ray attenuation was measured using a  $^{137}\text{Cs}$  source with a 5 mm collimator and a 10 s count time. Prior to logging, calibration of the system used a machined piece of aluminium that was fit within a section of core liner. The calibration piece has 4 different thicknesses of aluminium with diameters of 2, 3, 4, and 4.45 cm. Distilled water was filled in the calibration piece and left to equilibrate with room temperature ( $\approx 20^\circ\text{C}$ ) before being placed between the  $^{137}\text{Cs}$  source and detector on the MSCL track. The number of gamma rays passing through each Aluminium/water sections, as well as through water only, are logged over a course of 30 s. The known bulk density of the aluminium/water mixture at each calibration step is linearly fitted with the natural logarithm of the measured counts per second in providing a calibration function to determine the sediment bulk density from measured counts of gamma-rays per second.

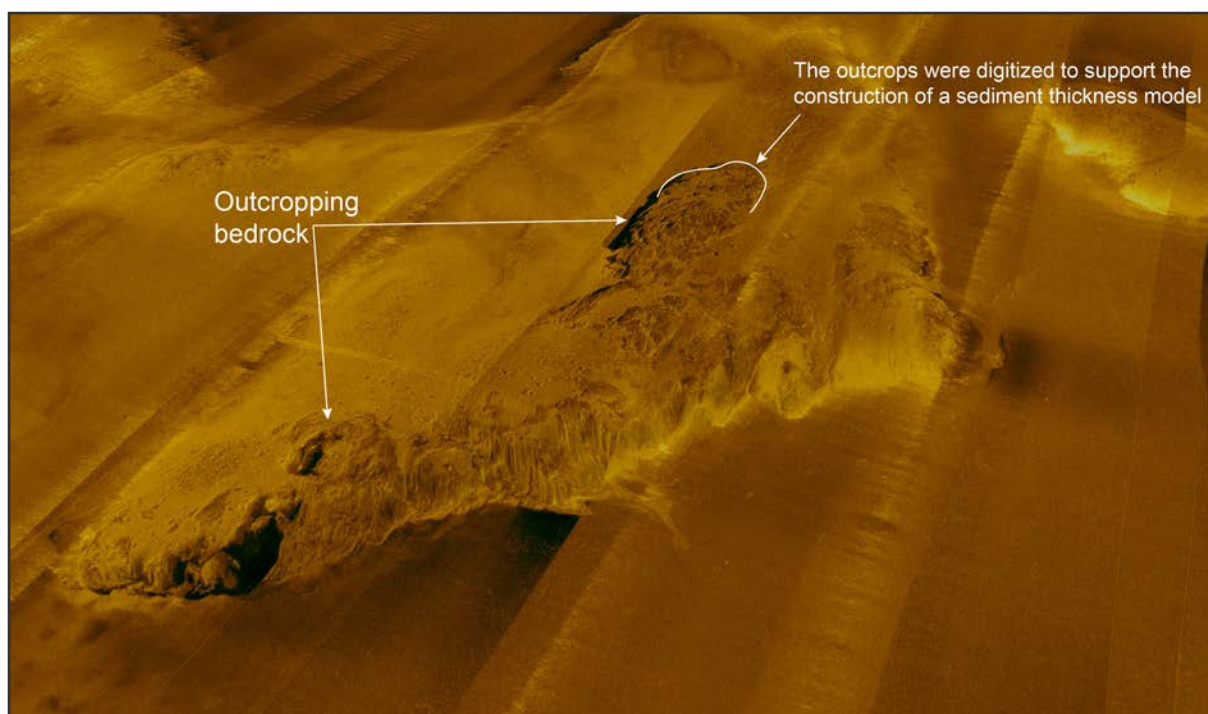


Figure M5. Side-scan mosaic draped on the multibeam bathymetry. Outcropping bedrock was clearly identified in the side-scan imagery and digitized in order to constrain the compilation of a gridded sediment thickness model of the area.

The MSCL has a pair of automated spring-loaded rolling transducers that are used to measure the compressional (p-wave) velocity of a submitted acoustic pulse through the sediments. The time it takes for the p-wave to pass through the sediment core is logged. Since the distance between the transducers is measured, the velocity can be calculated after calibration considering delays introduced by the electronic circuitry and the passage of the p-wave through the PVC core liner. This calibration was performed by measuring the travel time through a core liner filled with distilled water at a known temperature. A theoretical travel time through the distilled water inside the core liner is calculated and compared with the logged total travel time in order to determine the delays caused by the PVC liner and electronic circuitry.

The MSCL has a 125 mm Bartington loop sensor for measurements of magnetic susceptibility. An acquisition time of 1 s was applied. An integrated susceptibility signal over the entire diameter (110 mm) of the core and along the effective sensor length of generally 4–6 cm is acquired. No mass or volume corrections were made to the magnetic susceptibility measurements.



Figure M6. Fall Cone setup, shown before the cone is released into the sediment.

### Fall Cone

Undrained shear strength ( $S_u$ ) was calculated from the average of three fall cone measurements acquired at  $\sim 15$  cm intervals on split cores. A cone with a known mass and angle was placed just at the surface of the sediment and locked in place (cone tip angle/mass:  $30^\circ/128.95$  g,  $60^\circ/58.21$  g or  $108.21$  g) (Fig. M6). The cone was released to penetrate the sediment and then locked in place again  $5 \pm 1$  s after the cone became stationary in the sediment. After recording the penetration depth, the cone was removed from the sediment and cleaned before repeating the procedure. If the penetration was greater than 20 mm, either a lighter mass or a blunter cone was selected. If the penetration was less than 5 mm a heavier or sharper cone was used. The undrained shear strength was calculated using the cone mass ( $m$ ), cone tip angle and penetration depth ( $i$ ):

$$S_u = c \cdot g \cdot \frac{m}{i^2} \quad \text{Equation M1.}$$

where  $c$  is a constant dependent on the cone tip angle ( $c=0.8$  for  $30^\circ$ ,  $c=0.27$  for  $60^\circ$ ) and  $g$  is the gravitational acceleration ( $9.82 \text{ m s}^{-2}$ ) (ISO/TS 17892-6, 2004).

### LOI (Loss on Ignition)

The total amount of organic carbon (TOC) was primarily analyzed to provide an indication of whether or not samples to be measured for grain size required pre-processing before application of the particle size analyser (PSA). TOC was measured using loss on ignition (LOI). The samples were dried, weighed, burned, and then weighed again in order to estimate how much organic matter had been combusted (BenDor and Banin, 1989). To keep the sample levels consistent between different measurement types (e.g. the fall cone measurements), the cores were sampled every 15 cm, which resulted in 39 samples in total. Both sections of core EL21-Estonia-PC01 were excluded from the LOI process due to a too high sand content for the PSA. Samples from these sections were instead sieved to establish the grain size.

All samples analyzed for TOC were placed in an oven at  $105^\circ\text{C}$  (overnight or at least  $>4$  h) to dry. Once dry, the samples were weighed before they were placed in a furnace, which was gradually raised to a temperature of  $550^\circ\text{C}$  over two hours and then kept at that temperature for eight hours. After eight hours, the temperature was reduced to  $105^\circ\text{C}$  where it remained until the next day when the samples were retrieved from the furnace and weighed again. The TOC is determined by dividing the burned mass ( $M_b$ ) with the dry mass ( $M_d$ ) of the samples:

$$TOC (\%) = 1 - \frac{M_b}{M_d} \cdot 100 \quad \text{Equation M2.}$$

## Grain Size

Two methods were used for grain size analyses: 1) Laser diffraction, 2) Sieving. For sediment with particles <1 mm, a Mastersizer 3000 particle size analyser (PSA) from Malvern Panalytical was used. The device applies laser diffraction to estimate the grain size range. The LOI measurements showed that core EL21-Estonia-PC02 contained >2–5% organic matter, which is too much for the Mastersizer to output a reliable result as this will cause aggregation of particles. Therefore, the samples from this core were treated with hydrogen peroxide ( $H_2O_2$ ), with a concentration of 30%, before being put through the Mastersizer 3000 PSA. Small samples (<3 g) were placed in 10–15 ml of water and stirred up to separate the sediment particles. 21 ml of  $H_2O_2$  were then added, 5 ml the first three times with >1.5 h in between each addition. Due to the still visible reaction, the sample tubes were then placed in hot water ( $\geq 50^\circ C$ ) where an additional 3 ml of  $H_2O_2$  was added. This was repeated until there were no visible reactions. To clean the samples and remove the remaining  $H_2O_2$  before the subsequent PSA analysis, the test tubes were placed in a centrifuge (model Mega Star 1.6 from VWR) at 4000 rounds per minute (rpm) for ten minutes. The clear solution could then be removed due to the sediment accumulation at the bottom of the test tube. Deionized water was added to the samples that were shaken to stir up the sediment before being placed in the centrifuge again. This process was repeated three times to ensure that the sediment was clean and free from  $H_2O_2$  (samples that were still “murky” after this procedure were run again in the centrifuge until the solution was clear). Once clean, the remaining water was drained and replaced with new deionized water, so the total volume of the sample was 10 ml. With the use of a pipette and a stirrer (model REAX top from Heidolph) the sediment was mixed vigorously, sucked up in the pipette and emptied into the PSA until the obscuration was between 5 and 15%. 3 ml of sodium metaphosphate, with a concentration of 10%, was added as a dispersant and the PSA was now ready to run. Two separate measurements were performed on each sample to ensure a reliable result. Core EL21-Electra-PC03, which contained <2% organic matter, could be analyzed directly without preparation, but otherwise following the same procedure as EL21-Estonia-PC02 in the PSA.

Core EL21-Estonia-PC01 mainly contained sand, which through ocular observation was estimated to be >1 mm. This core was sieved. Three samples from each section were extracted (top, middle, bottom) and placed in an oven. Once dry, the samples were sieved during 10 minutes in a sieve range from 4 mm to 63  $\mu m$  (4 mm, 2 mm, 1 mm, 500  $\mu m$ , 250  $\mu m$ , 125  $\mu m$  and 63  $\mu m$ ) and the size fractions were calculated by dividing the remaining material in each sieve size by the total dry sample mass.

## Moored ADCP

Raw data were converted to ascii through the Nortek *Aquadopp Profiler v1.35* software. The relevant time series, during which the ADCP was pinging from the bottom, was determined from looking at auxiliary sensor data, including heading, roll, pressure and temperature.

## Results and interpretation

### Seafloor and water column mapping with acoustic methods

#### Multibeam bathymetry

The multibeam mapping can be divided into a survey aimed to give a general bathymetric overview of the surroundings of the shipwreck and surveys dedicated to provide maximum resolution of the shipwreck and its nearest surroundings (Fig. MB1). A first detailed survey began on July 9, but was aborted due to bad weather with rapidly increasing wave heights that resulted in unstable ship movements and caused bubbles to be drawn in under the hull and ship, that together degraded the acquired data quality (Fig. MB2). Furthermore, the waves and strong winds prevented RV *Electra* to maintain a slow enough survey speed (<2 knots) needed to obtain an adequate number of depth measurements on the seafloor along track for our high-resolution requirements. When this survey was aborted, RV *Electra* was brought to shelter at Hangö (see Appendix 1: Expedition daily notes). The overview survey was run on July 12 along with the side-scan operations further described below. The swath-width was set to 50°×50° as planned and the survey lines were run with 100% overlapping swaths. The processed data, gridded with a cell-size of 1.5×1.5m, covers an area of 5.3km<sup>2</sup> (Fig. MB1). A second detailed survey of the shipwreck was started directly after the overview survey on July 12 in good weather conditions with smooth sea. This survey was successfully completed on July 13. The swath width was reduced to 25°×25° in order to increase the resolution across track and RV *Electra* was moved forward along the survey lines at the slowest speed possible (occasionally down to 1 knot) to maximize the data resolution along track. A few additional lines were run with a maximum swath width of 70°×70° in order to get depth recordings from the sides of MS *Estonia*, which partly lies in an acoustic shadow due to her listing and a trench that has been formed in the seafloor along its northern and western sides. This trench is further described below. A set of lines diagonally across the shipwreck were also completed in order to approach it at different angles for maximum data coverage (Fig. MB1). The acquired data could be gridded at a resolution of 0.25×0.25m, albeit with some small holes in the grid coverage, which could be filled by interpolation from neighbouring cells. This detailed 0.25×0.25m grid has a smaller cell-size than the foot print of the individual beams in the water depth of 75m and 85m at the wreck site, which should be considered when interpreting details (see Methods for the achievable foot print at these water depths). The final grid of the detailed survey covers an area of 0.25km<sup>2</sup> (Fig. MB3). Larger sized maps of the surveys at higher resolution are shown in Appendix 2.

The mapped area is characterized by an undulating seafloor terrain with bathymetric highs, mostly shallower than 70m, separated by valleys of which some are deeper than 90m (Fig. MB1). There are two pronounced valleys striking from SW to NE in the southeastern part and one running from E to W in the western section. The deepest mapped location is in the northeast where the seafloor reaches depths >105m.

The seafloor morphology in the vicinity of MS *Estonia* is rather characteristic for areas in the Baltic Sea where the underlying bedrock consists of igneous rocks. Patches of till are in those areas commonly found on top of the bedrock. This till was deposited by the Scandinavian Ice Sheet, which completely filled the Baltic Basin during the Last Glacial Maximum approximately 19000–26000 years ago (Andrén et al., 2011) and thus flowed over the bedrock. The ice sheet retreated from the MS *Estonia* site at about 12000 years ago (Hughes et al., 2016). Glacial clay was subsequently deposited on top of the bedrock/till during the ice-sheet retreat. This clay has the characteristic varved appearance as finer grain sizes were deposited during winter and coarser during summer when more melting and erosion took place. The annual rhythm in clay deposition during ice-sheet retreat resulting in varves was discovered over 100 years ago (De Geer, 1912). When the Scandinavian Ice sheet had disappeared from the Baltic Basin, the deeper

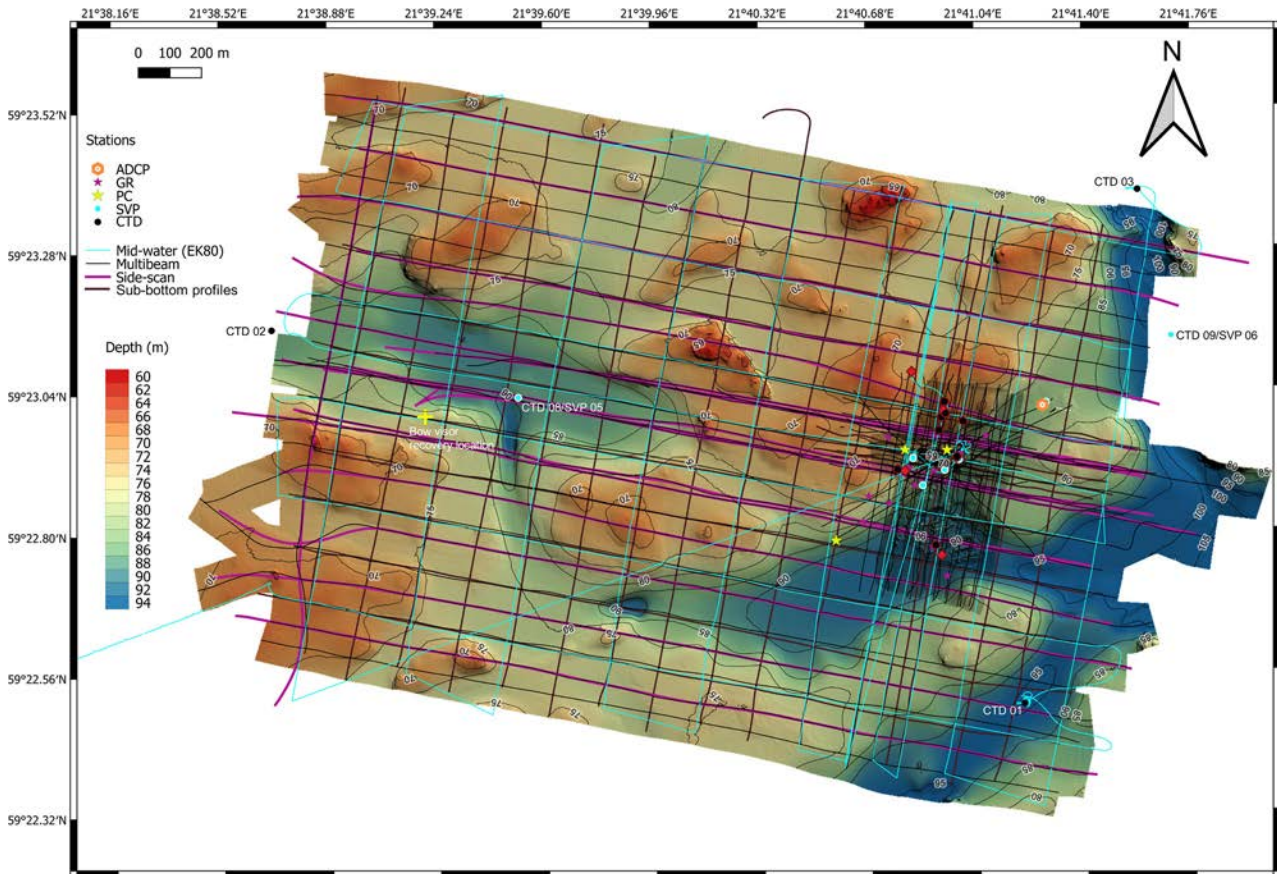


Figure MB1. Stations and completed survey lines with the different acoustic mapping systems. ADCP-data were acquired along with the EK80 collection of mid-water acoustics and the multibeam was run simultaneously with the side-scan for the overview survey. Only labels for the stations falling outside of the detailed map are shown in this map, Figure MB3 displays labels for the rest of the stations. ADCP=Acoustic Doppler Current Profiler mooring; GR=Grab Sampler; PC=Piston Corer; SVP=Sound Velocity Profiler; CTD=Conductivity, Temperature, Depth. A larger version of this map is found in Appendix 2.

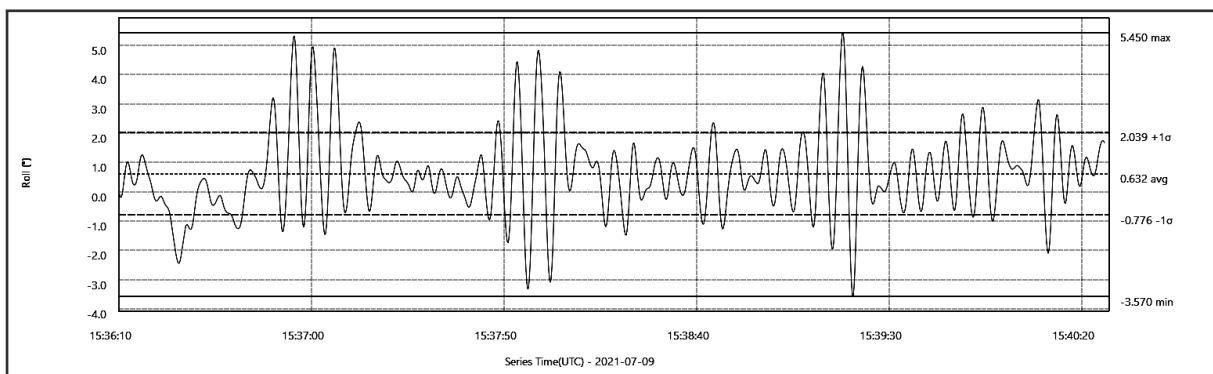


Figure MB2. RV Electra's roll captured by the motion sensor of the multibeam system during the first detailed survey of the shipwreck, which was aborted due to bad weather on July 9. RV Electra is equipped with a gyro stabilizer, which greatly reduces vessel motions. The gyro is most efficient with respect to reducing the roll.

valleys and basins were continued to be filled by clay, although without the varved appearance. This clay is commonly referred to as postglacial clay, which in the upper layers often has high organic content resulting in biogenic gas production. The geological maps previously compiled of the area around MS *Estonia* show this classical Baltic Sea seafloor geology (Fig. I2). The geological layers are not uniformly distributed because of influence of bottom currents and seafloor dynamics such as mass wasting implying for example that bedrock can be exposed without a blanket of overlaying till or glacial clay.

A slope map compiled using the detailed bathymetry shows that MS *Estonia* rests on a seafloor generally sloping between about 5 and 10° towards southeast (Fig. MB4). This conforms to previous coarser bathymetric surveys where the general slope where MS *Estonia* is situated was found to be between about 7 and 10°. The 75–80m depth interval is outlining the steepest seafloor. Beginning midship at the northern side of the shipwreck and continuing north-eastward, this depth interval becomes steeper than 10° (Fig. MB4).

The shipwreck itself is for the most part well imaged by the detailed multibeam survey (Fig. MB5). The exceptions are the aft part of the shipwreck and the contact between the hull and the seafloor along the northern side (Fig. MB5). This is due to a pronounced trench formed along the shipwreck in these areas, which caused an acoustic shadow, i.e. the beams of the multibeam are blocked from reaching the hull's contact with the seafloor. The trench is clearly visible in both the bathymetry and slope maps (Figs. MB5–MB6). It is roughly 6 m wide and 4 m deep along the aft of the shipwreck. The trench widens to >8m and deepens to about 7 m along the northern side (Fig. MB5). Following the trench for about 55 m from the aft, the bottom of the trench becomes shallower and the wall is less steep (Fig. MB5). The shallowest part of MS *Estonia* is the port bottom furthest aft, which rises to a depth of about 57 m (Fig. MB5). There are several elongated marks seen in the multibeam bathymetry, of which three are visible in the hull, two of them clearly and one a bit vaguer (Fig. MB6). These resemble scrape marks after a dragged object, similar to when an anchor is dragged across the seafloor. The holes for the bow thrusters are also possible to distinguish in the detailed multibeam bathymetry (Fig. MB6).

The Swedish Geotechnical Institute (SGI) has summarized the geotechnical data available from previous studies (Rudebeck and Kennedy, 2021). They concluded from published reports that at least four mass-wasting events have occurred to the east, west and south of the shipwreck. A first slide is proposed to have been triggered by MS *Estonia*'s impact with the seafloor. The sediments then gave away just south of where MS *Estonia* impacted. Two slides encompassing seafloor areas of 800 m<sup>2</sup> occurred when sand was dumped on the seafloor to reinforce the eastern and western part of the area to be covered. Finally, a fourth slide is proposed to have occurred after the filling was stopped to the south of the shipwreck.

Our detailed multibeam survey reveal several clear signs of mass wasting on the seafloor (Figs. MB6). However, it is difficult to exactly link the visible mass-wasting features with the previously reported events. An approximately 150 m long slide scarp is visible to the east of MS *Estonia*, with corresponding mass-wasted material piled-up downslope in the form of small transverse ridges. This slide occurred along the steepest section of the sloping seafloor in water depths between about 75 and 80 m (Fig. MB7b). Within approximately the same water depth range, a 230 m long slide scarp is mapped west of MS *Estonia*. The mobilised sediments are found downslope where they form lineations in addition to being piled-up in lateral ridges at the bottom of the slope. The form of the upper slide scarp appears to correspond to the edge of the geotextile placed on the seafloor, making it tenable to suggest that it is the dumped sand that slid downslope on top of the geotextile (Fig. MB8). Approximately 100 m southeast of the shipwreck, a slide scarp begins and continues due south for about 170 m. Mass-wasted material below this scarp is evident also

here. Finally, slightly over 300m south of MS *Estonia*, a series of transverse ridges are mapped that likely are formed from mass-wasting. There is however not a slide scarp evident upslope of these ridges.

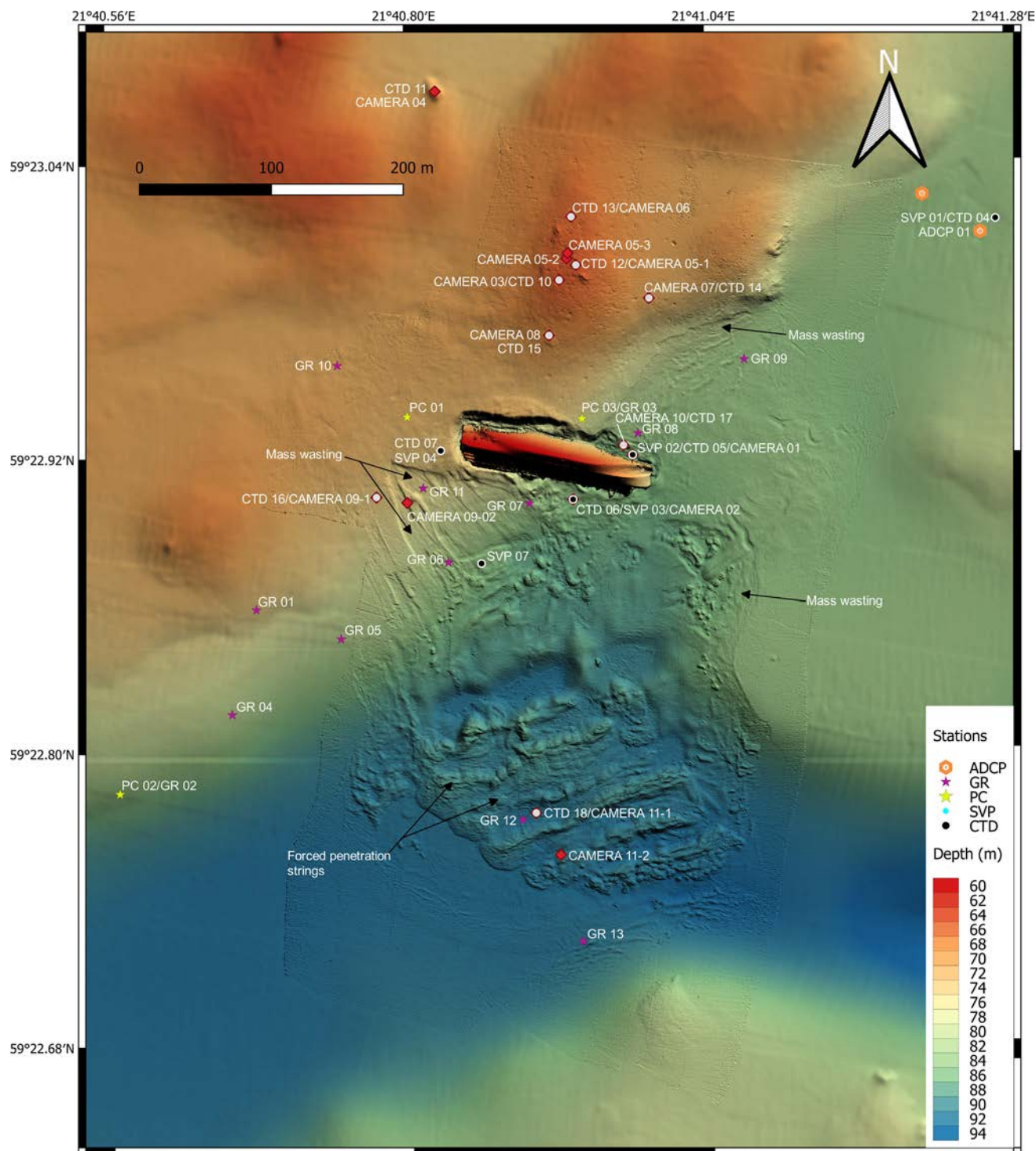


Figure MB3. Bathymetric map created using the high-resolution grid (cell-size: 0.25×0.25 m) based on the detailed multibeam survey completed on July 13. Acquired stations are shown on the map. Where more than one device was deployed at a station, the symbols cover each other. In these cases, the labels next to the visible symbols show the sampling accomplished. The forced penetration strings as well as signs of mass wasting are clearly visible in the bathymetry. The morphology is further shown along with interpretations in Figure MB7. A larger version of this map is found in Appendix 2.

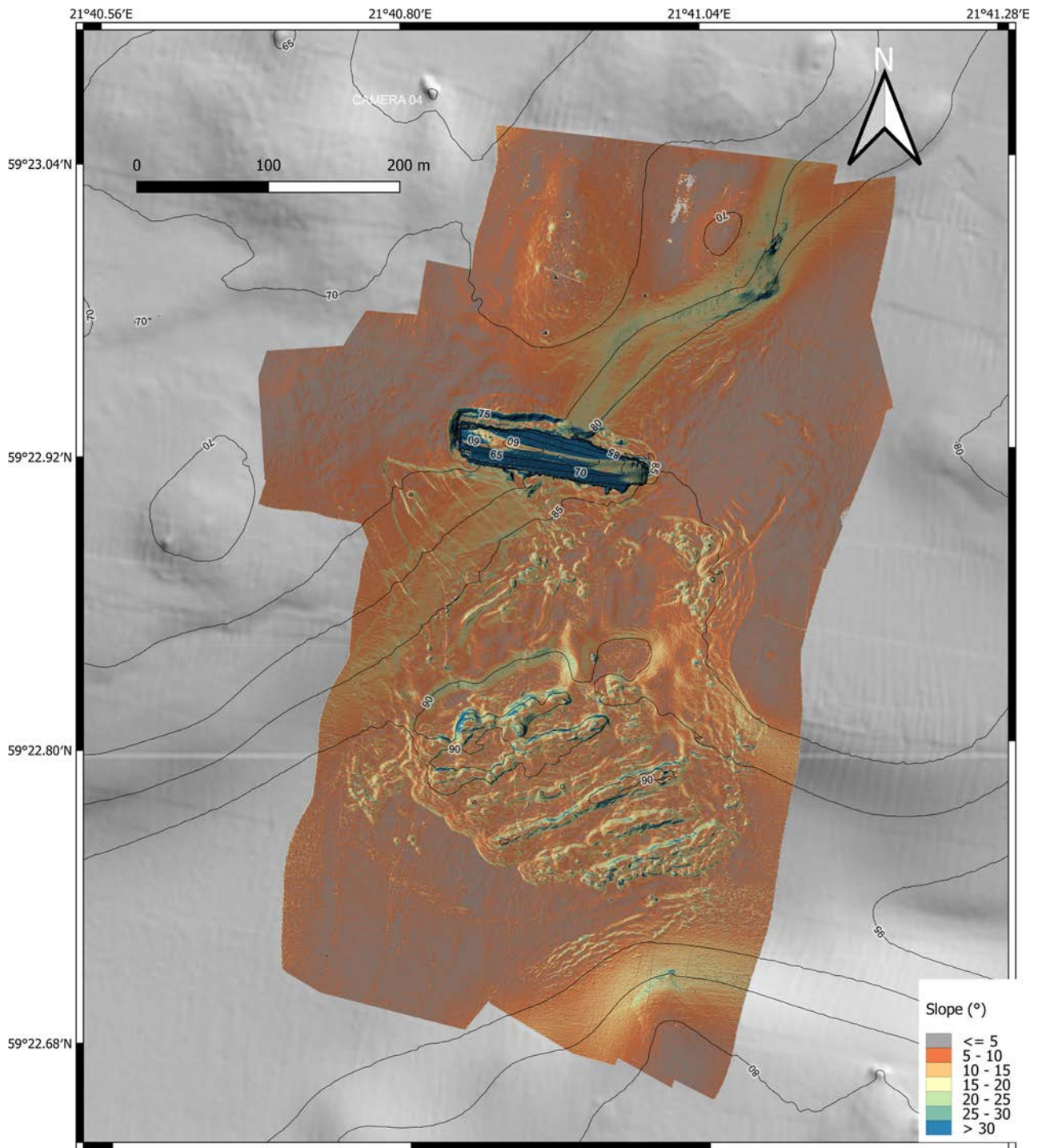


Figure MB4. Slope map created using the detailed multibeam high-resolution grid (cell-size: 0.25x0.25 m) based on the detailed multibeam survey. A larger version of this map is found in Appendix 2.

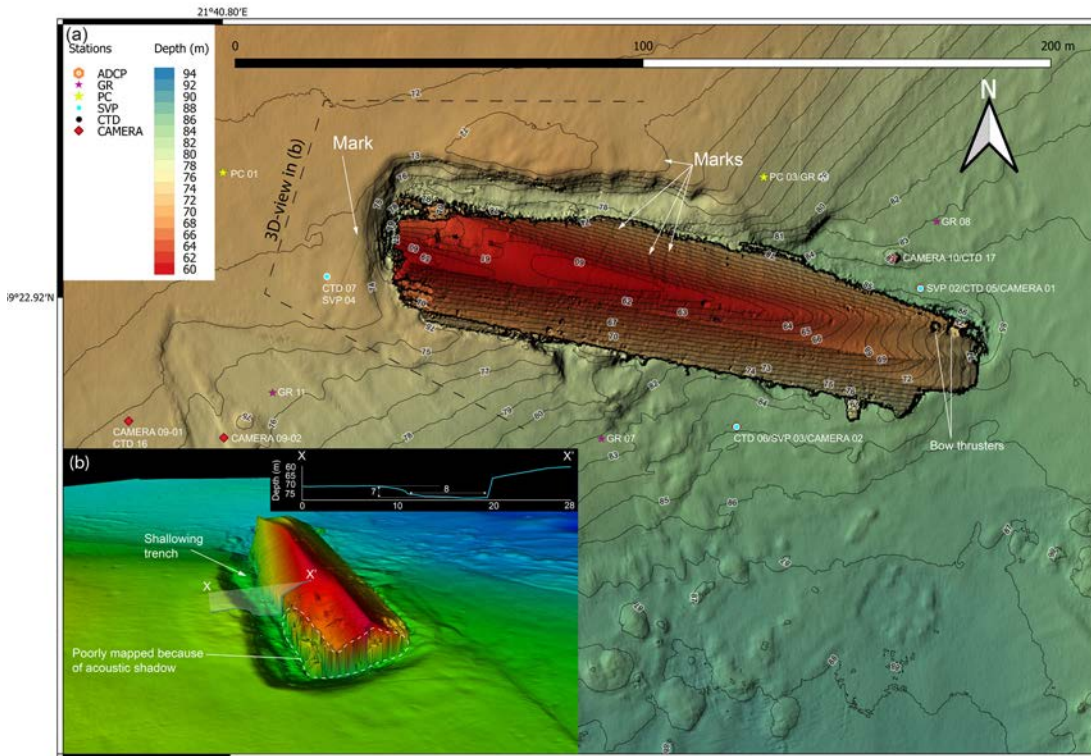


Figure MB5. The shipwreck of MS Estonia portrayed with the detailed multibeam high-resolution grid (cell-size: 0.25×0.25 m). A 3D-view looking towards the aft is shown in (b). This view clearly reveals the trench formed along the shipwreck. The most poorly mapped part of the shipwreck is indicated with a stippled line. A larger version of this map is found in Appendix 2.

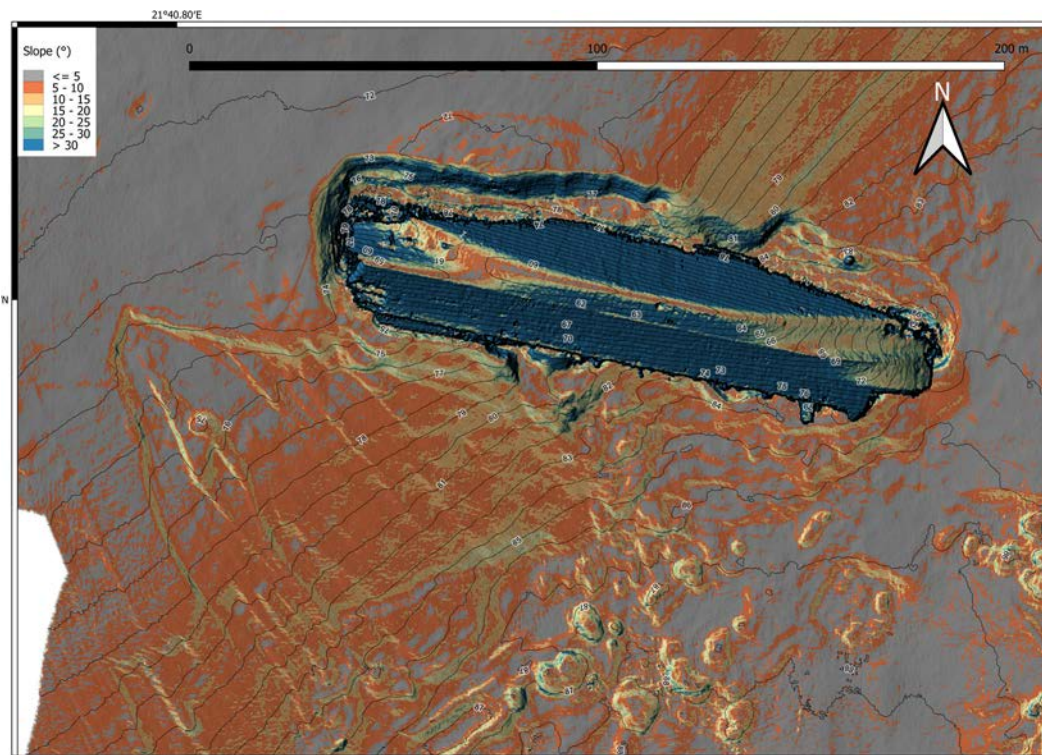


Figure MB6. Slope map created using the detailed multibeam high-resolution grid (cell-size: 0.25×0.25 m) based on the detailed multibeam survey. A larger version of this map is found in Appendix 2.

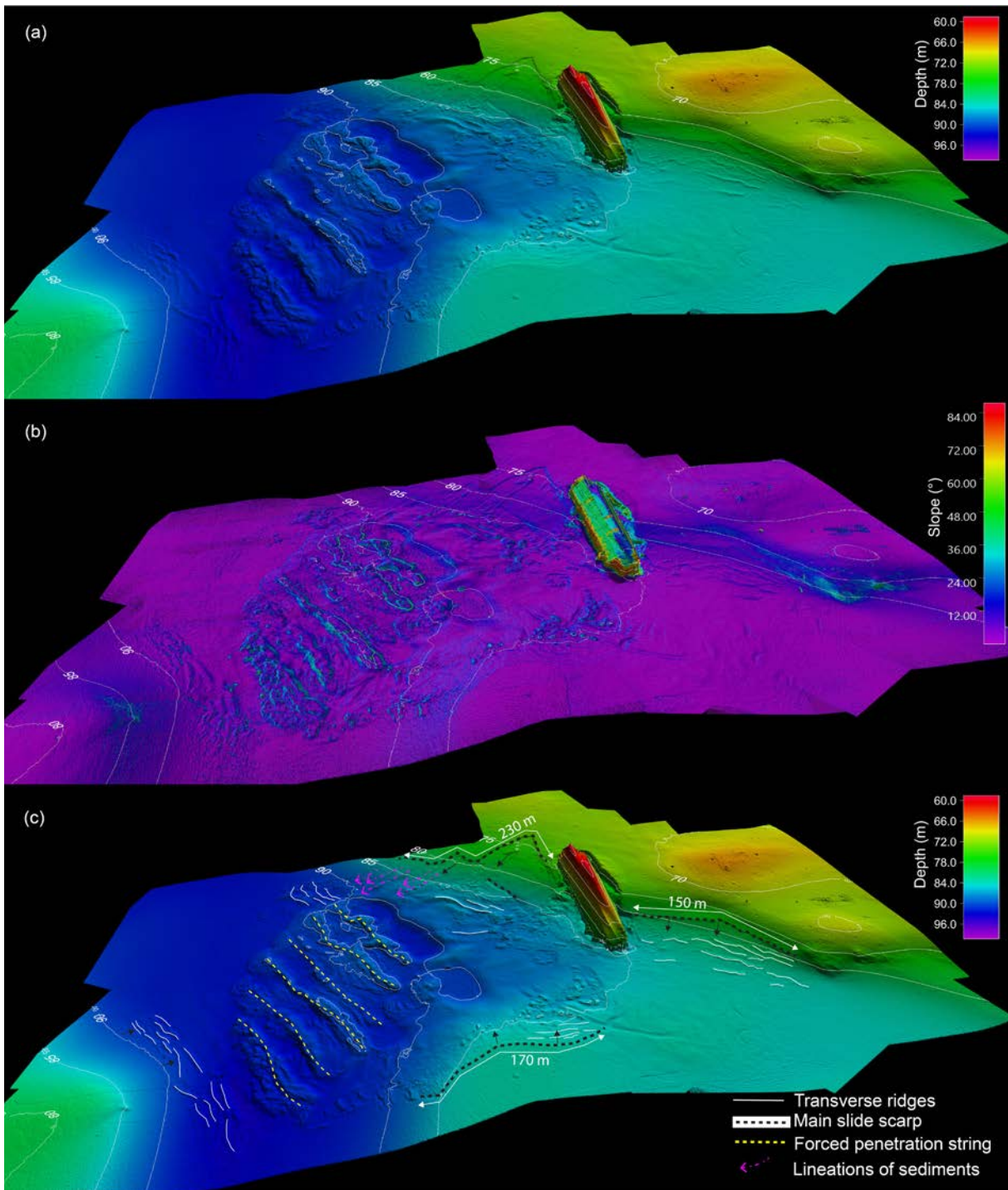


Figure MB7. 3D-views based on the detailed survey and the compiled grid with a cell-size of 0.25×0.25 m. (a) Bathymetry. (b) Slope derived from the bathymetry. (c) Interpretation of the seafloor morphology. A larger version of this illustration is found in Appendix 2.

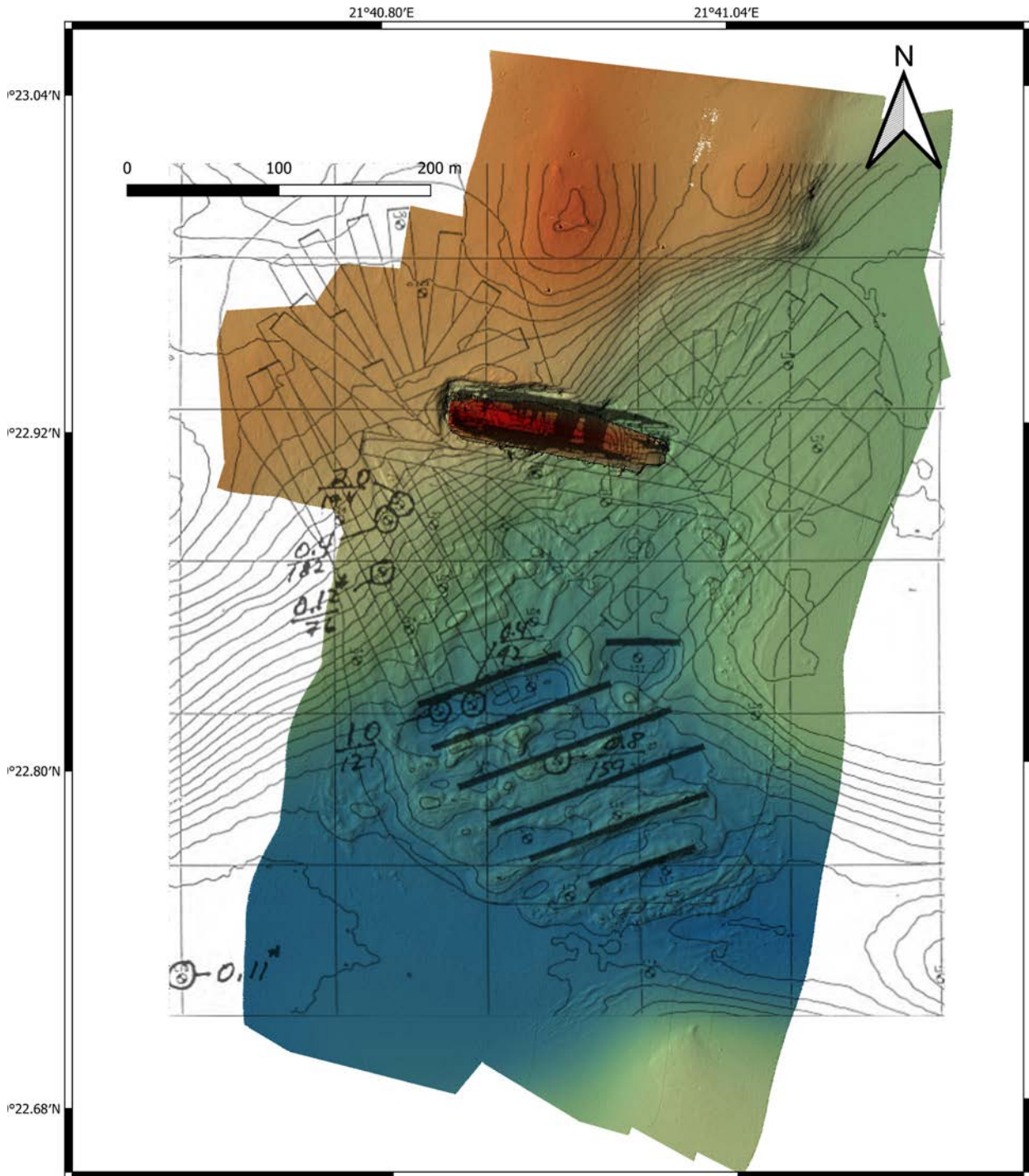


Figure MB8. Map from Delft Geotechnics (1996-09-19) showing the location of the forced penetrations strings, geotextiles and sediment samples measured for geotechnical parameters overlaid on top of the multibeam bathymetry. This shows clearly that the drawing of the forced penetrations strings fits with the seafloor morphology. The western part of the geotextile that is located along the shipwreck on the southern side seems to correspond to the slide scarp visible in the bathymetry.

## Multibeam backscatter

The backscatter information from the multibeam contains information about the seafloor characteristics and one area can be compared to another if the backscatter is radiometrically and geometrically corrected properly (Fonseca and Calder, 2005). The software tool used in this project (QPS FMGT) applies the appropriate corrections for the backscatter data acquired with the EM2040 multibeam system. After the necessary processing, the backscatter values will provide insights into sediment type and characteristics such as roughness and impedance (Lurton et al., 2018). There is generally a correlation between high backscatter values and hard seafloor.

A backscatter mosaic with a resolution of  $0.25 \times 0.25$  m was created for the entire area (Fig. MB9). However, it should again be noted that the water depths in the survey area are deeper than 60 m yielding multibeam foot prints with diameters  $>0.4$  m, which implies that objects as small as  $0.25 \times 0.25$  m cannot be expected to be identified (see previous discussion). The bathymetric highs are generally associated with high backscatter values while the deeper areas show lower values (Fig. MB9). Overlying the boundaries from the geological map compiled by Nuorteva (1995) shows that the backscatter pattern broadly fits some of the inferred geological boundaries, although it is clear that a much more nuanced view is provided by the backscatter mosaic due to its full spatial coverage. A geological map based on sparse data will provide a much more generalized view and details will be left out. MS *Estonia* is resting across the boundary between postglacial clay and glacial clay, which generally follows a marked transition from lower to higher backscatter values (Fig. MB9). This is even better seen on a backscatter mosaic where mean values have been calculated for grid cells of  $4 \times 4$  m (Fig. MB10). Most of the areas shown as till or bedrock on the geological map coincide with high backscatter, although some

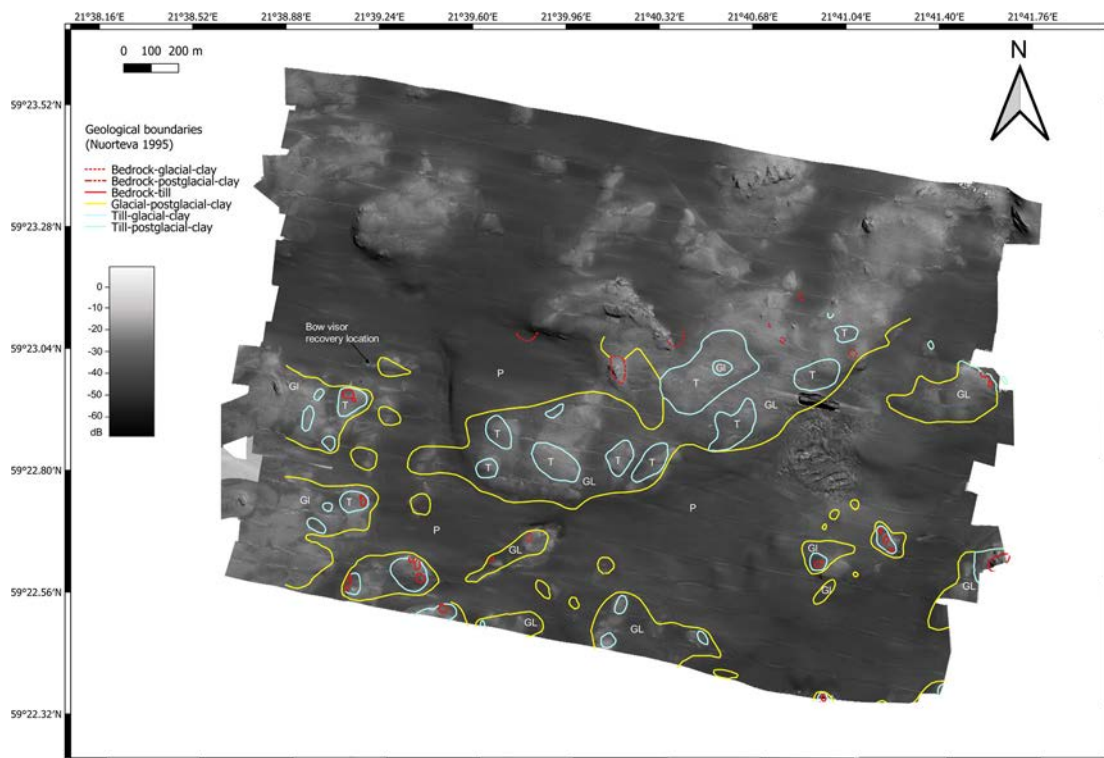


Figure MB9. Backscatter mosaic created at a grid cell-size of  $0.25 \times 0.25$  m using the multibeam data from the overview survey. The geological boundaries from the map compiled by Nuorteva (1995) are inferred. Letters indicate the seabed deposition shown on the geological map: P=Postglacial clay; GL=Glacial Clay; T=Till. The red enclosed areas are shown as bedrock on the map by Nuorteva (1995). The bathymetry is used to apply a shading from the northeast in order to give a better perception of the terrain. However, this has the downside of darkening the image behind high up sticking objects, such as along the southern side of MS *Estonia*. A larger version of this map is found in Appendix 2.

seem to be located with an offset. To a certain extent, this could be due to misregistration of the geological map, which is seen when comparing the location of MS *Estonia*. However, the offsets are not systematic in some directions, which rather point to issues with positioning of samples and geophysical data that served as a base for the geological map.

The detailed survey provides backscatter data of the highest quality in the vicinity of MS *Estonia* (Fig. MB11). In this area, it is possible to compare the sediment surface samples and camera observations with the backscatter and thereby calibrate the geological interpretation. This is done below in a separate section where the samples and camera observations are described. The two maps shown in this section in Figures MB11 and MB12 are without any additional overprinted information in order to not clutter the details (see Appendix Results for larger sized maps). The detailed backscatter provides additional information on the mass-wasting features discussed in the context of the seafloor morphology and multibeam bathymetry presented in Figure MB7. Sediment deformation features are a bit more clearly visible southwest of the forced penetration strings, which in fact are encircled by the slides and smaller signs of mass-wasting. Furthermore, the backscatter accentuates that the large slide west of MS *Estonia* is different in character compared to the other slides. It seems tenable to suggest that the unique appearance of this slide suggests to that it may entirely be comprised of the dumped sand that slid downslope on top of the geotextile. The area north of MS *Estonia* is characterized by numerous up sticking features on the seafloor, which will be further discussed below along with the camera observations that targeted several of them.

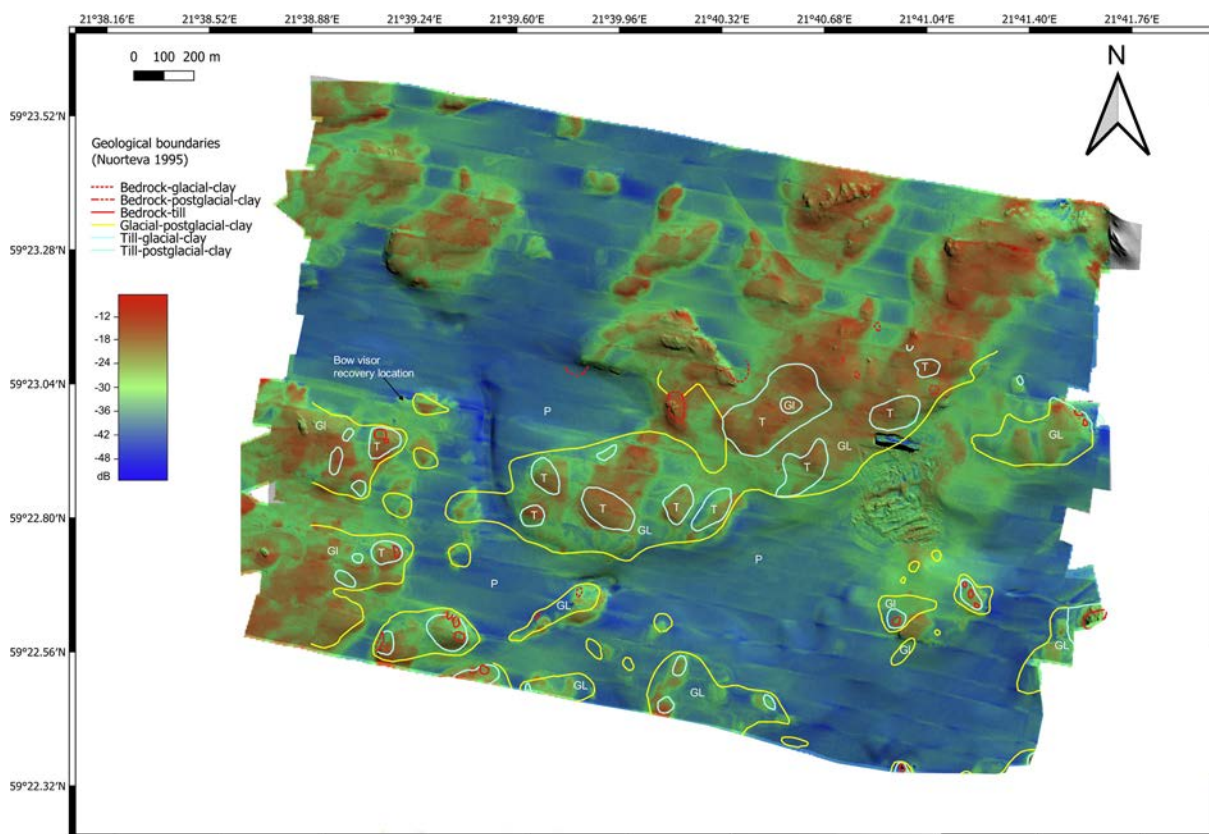


Figure MB10. Backscatter mosaic showing the mean backscatter within grid cells of 4×4 m. See Figure MB9 for description of the geological boundaries. The bathymetry is used to apply a shading from the northeast in order to give a better perception of the terrain. However, this has the downside of darken the image behind high up sticking objects, such as along the southern side of MS *Estonia*. A larger version of this map is found in Appendix 2.

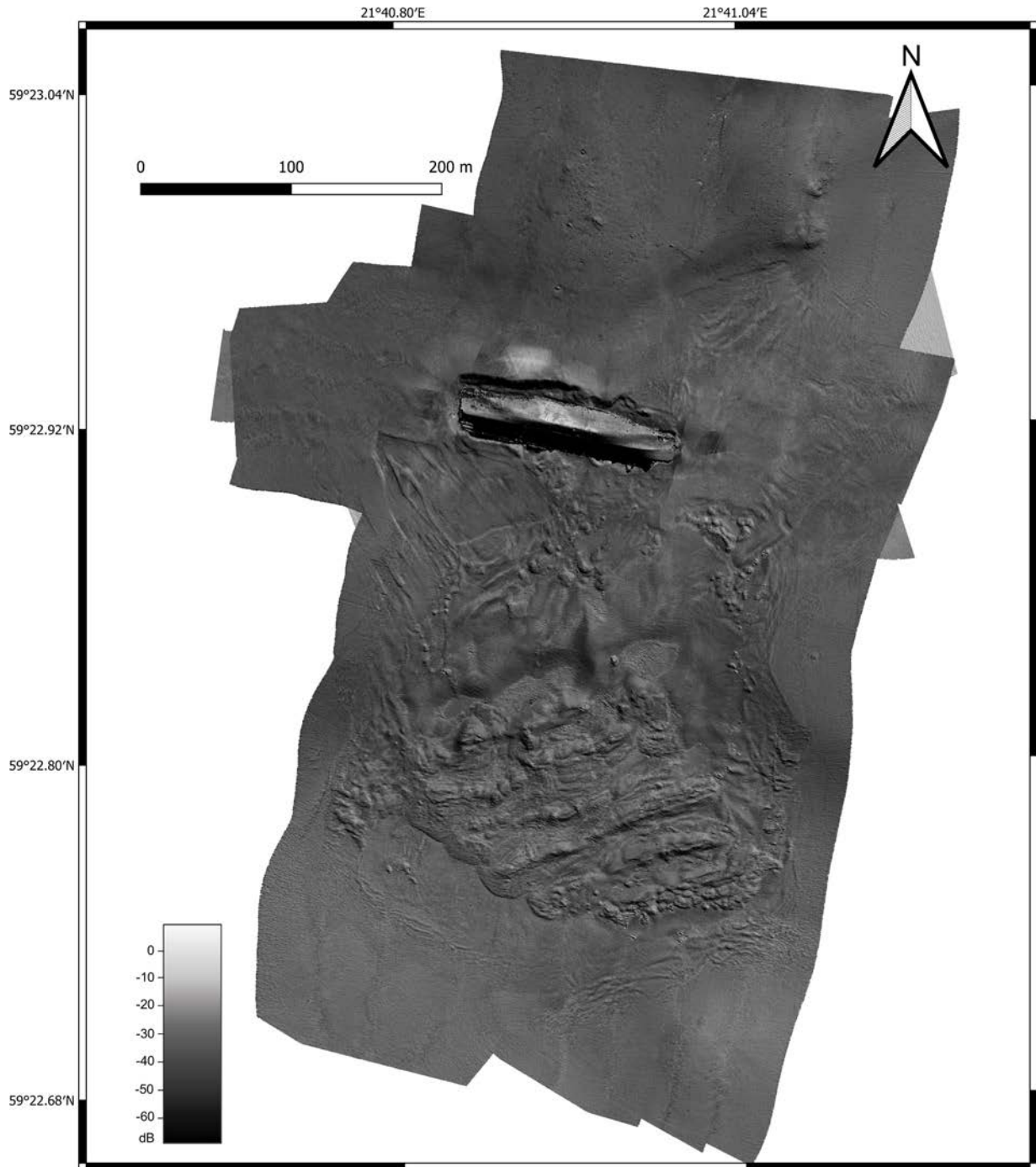


Figure MB11. Backscatter mosaic compiled at a grid cells size of 0.25×0.25 m. The bathymetry is used to apply a shading from the northeast in order to give a better perception of the terrain. A larger version of this map is found in Appendix 2.

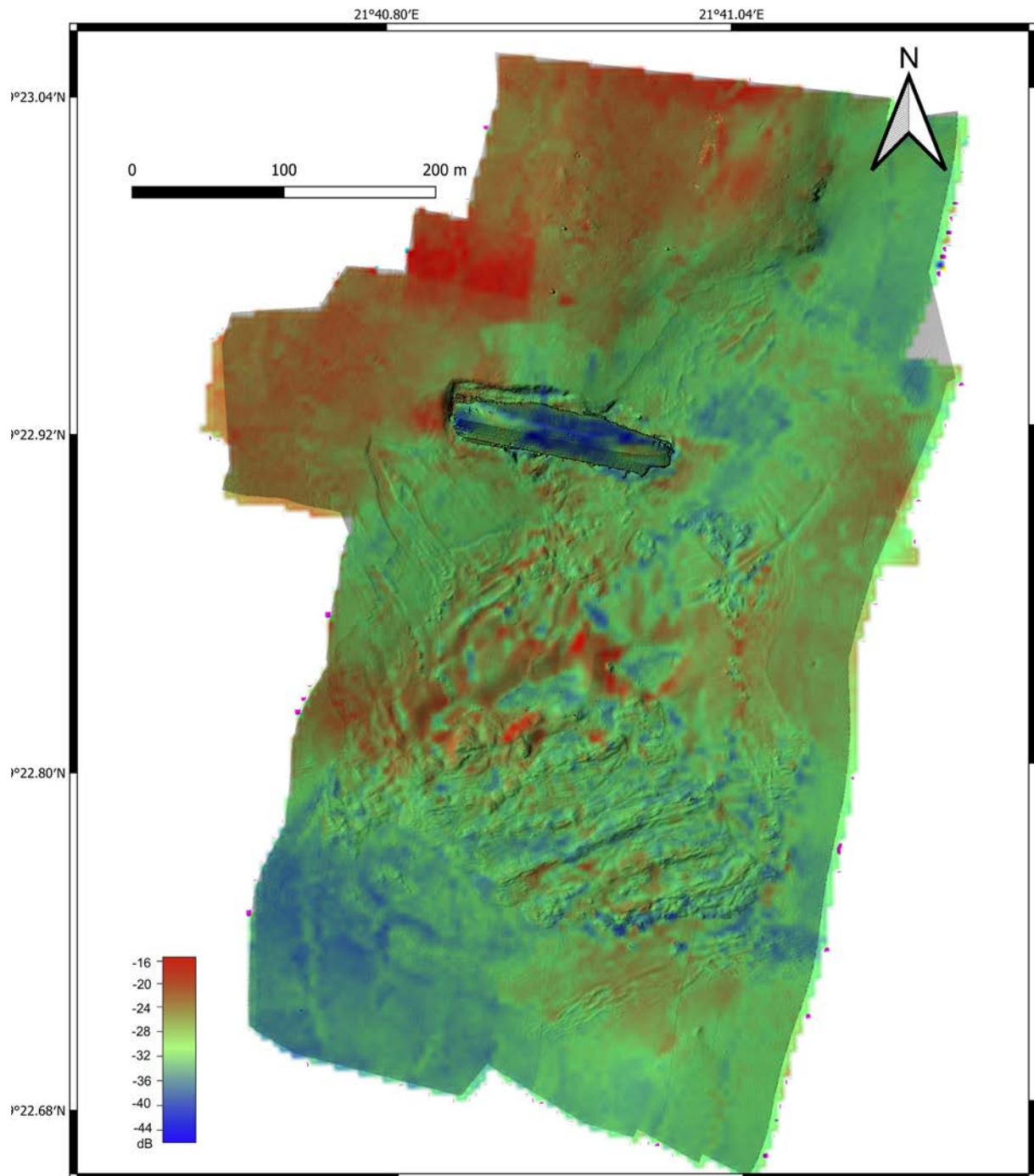


Figure MB12. Backscatter mosaic showing the mean backscatter calculated within grid cells of 2×2 m. The bathymetry is used to apply a shading from the northeast in order to give a better perception of the terrain. A larger version of this map is found in Appendix 2.

### Sub-bottom profiling

Sub-bottom profiles were acquired on July 10, 2021, with a spacing of about 160 m both in east-west and north-south direction to form a regular grid covering the survey area, and with tighter spacing between 25–40 m across the shipwreck (Fig. SB1). The sub-bottom profiles provide an acoustic overview of the sediment stratigraphy above the acoustic basement (AB), which in the area likely is comprised of till or bedrock, which acoustically are not possible to distinguish with any certainty. The focus in this study has been to identify the AB in order to compile a sediment thickness that can be used to assess how stable *MS Estonia* is on the seafloor. The proximity of bedrock close to or at the seafloor has also been one of the basic questions this pre-study set out to investigate. All acquired sub-bottom profiles are shown in Appendix 3, both with and without the interpretation of the AB. The vertical scale is displayed in milli-seconds two-way travel time for the uninterpreted profiles and in meters below sea level on the interpreted. A flat sound velocity of 1450 m/s was used to convert from milli-seconds to depth in order to make the depth scale as close as possible to the multibeam bathymetry. The stratigraphy is briefly presented and discussed in this section. The sub-bottom topic is re-visited below when the compiled sediment thickness model is presented and discussed.

A sub-bottom survey was carried out by the Netherland Institute of Applied Geoscience TNO in 1997 (Mesdag, 1997). An Edgetech chirp sonar was used with an SB-408 tow fish set to transmit a 1–6 kHz 40 ms long pulse. Bad weather hampered their survey by making it difficult to tow the chirp along desired track lines and by inferring heave artefacts. In total, 26 lines in north-south direction and 7 in east-west were completed (Fig. SB2). All of the south-north profiles crossed the hull of *MS Estonia* apart from one, while only one of the east-west lines crossed. The report by Mesdag (1997) concludes that a till surface could be mapped in several profiles near the shipwreck with confidence. Their general interpretation of the sediment sequence suggests that partly

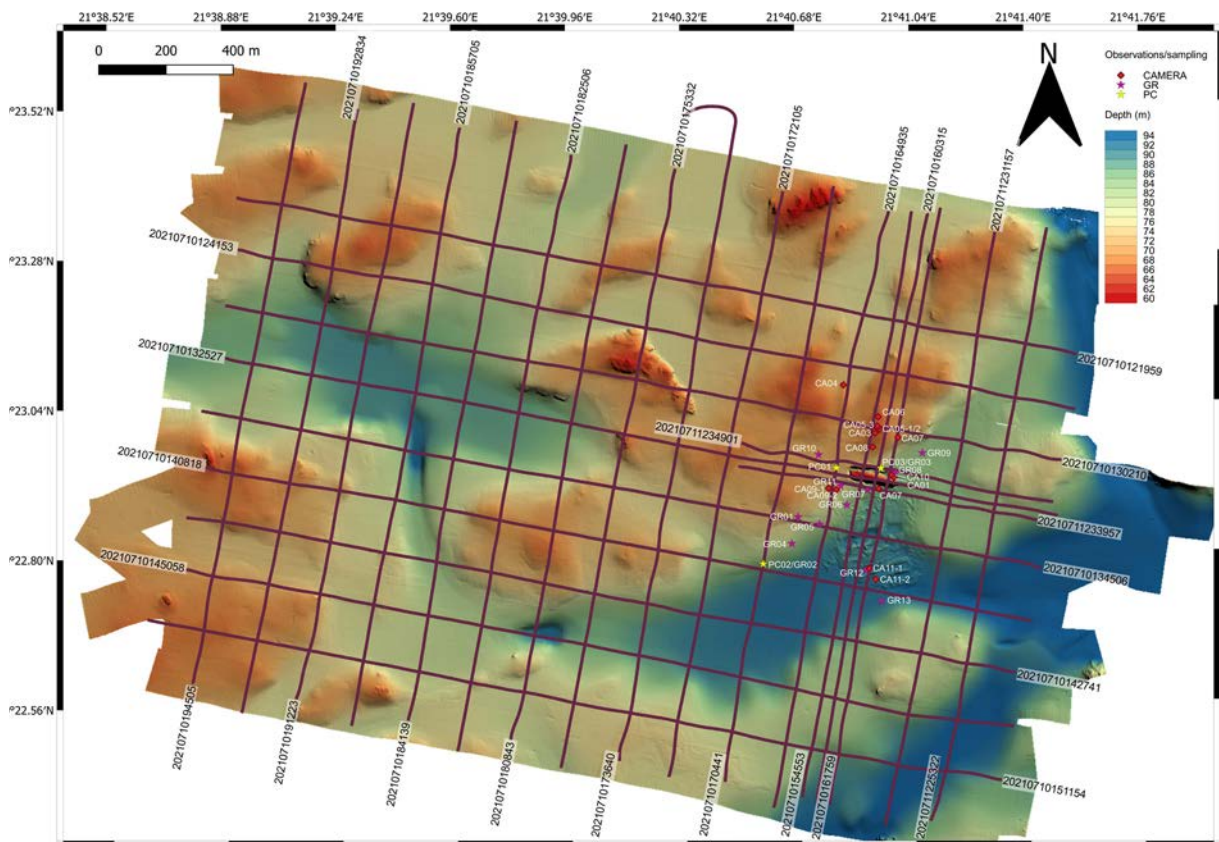


Figure SB1. Sub-bottom profiles acquired on July 10, 2021, during EL21-Estonia survey with RV Electra. A larger version of this map is found in Appendix 3.

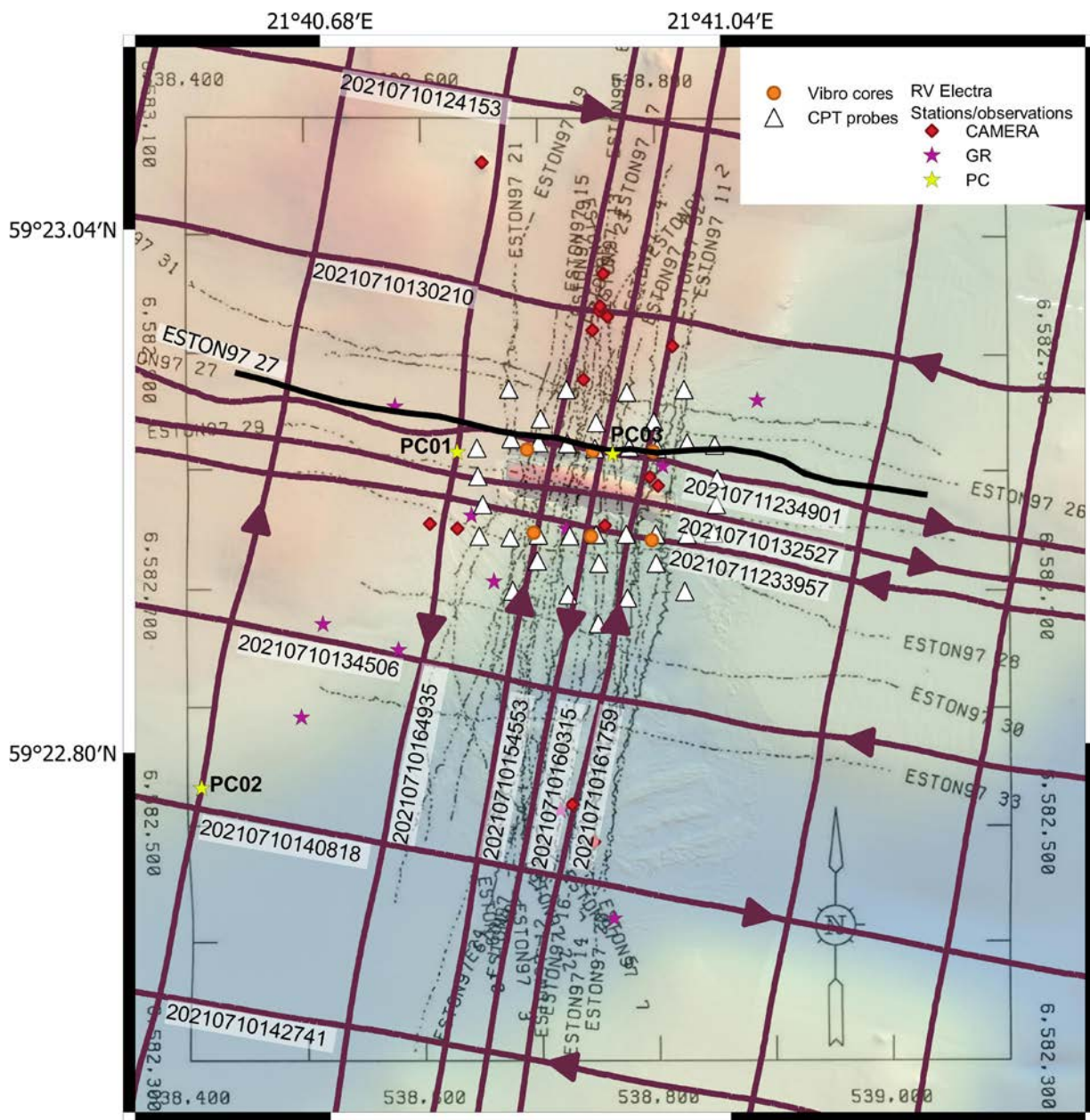


Figure SB2. Map from the report “Seismic survey at Estonia site” by Mesdag (1997) showing acquired sub-bottom profiles by the Netherland Institute of Applied Geoscience TNO in 1997. The map is made semi-transparent and overlaid the multibeam bathymetry acquired in this work in order to show where MS Estonia is located. Sub-bottom profiles from the field work with RV Electra are shown with brown lines as well as the locations of piston and gravity cores and camera observation sites. In addition, the locations of vibro-cores and CPT (Cone Penetration Test) probes from the investigations by Delft Geotechnics 1996 are shown.

laminated mud and clay overlies a glacial till consisting of generally fine-grained sand with clay, gravel and cobbles. The presence of varved clays is noted and proposed to have been deposited on top of the till during the late-glacial period. The interpreted till surface in the sub-bottom profiles is compared (and adjusted when required) with the results from the Cone Penetration Test (CPT) probes and sediment coring made by Delft Geotechnics in 1996. The interpreted “till surface” by Mesdag (1997) undoubtedly conforms to our defined AB (Fig. SB3). However, since our survey covers a much larger area we have been able to trace the AB in some profiles up to the seafloor where we find exposed bedrock in the side-scan and backscatter imagery (Fig. SB4). This confirms that we cannot with certainty tell apart whether the AB reflects bedrock or till on top of bedrock. We find acoustically stratified units in our profiles that most likely are representing varved glacial clay (Fig. SB4). Postglacial clay with high organic content in the uppermost sections has been shown to fill the low lying basins in the area, and Mesdag (1997) reports gas blanking in profiles capturing these units. We also find gas blanking in several profiles across the deeper basins filled with softer sediments (Fig. SB4). The gas blanking is preventing the identification of an AB in some of our profiles and thus also a final sediment thickness estimation in those areas. However, where this occurs, the sediment thicknesses are commonly rather large, >20m, consistent with the findings by Mesdag (1997) for the basin south of MS *Estonia*.

The question whether bedrock or till outcrops, or lay close to, the seafloor underneath MS *Estonia*'s mid-section has been raised. The investigation by Delft Geotechnics in 1996 found a minimum thickness of sediments above a firm till in the area north of the shipwreck midship. Two of their CPT-probes located approximately 18 and 25m north of the shipwreck yielded sediment thicknesses of 4.7m and 3.6m respectively (Fig. SB5). Our acquired sub-bottom profiles close to and across MS *Estonia* are consistent with these results, although the sections of the profiles closer to the shipwreck suggest that the AB come even closer to the seafloor or may be outcropping (Fig. SBP6). The general assumption of a hard surface which the shipwreck is resting on is supported by our sub-bottom profiles. However, the geology directly below the hull is not possible to decipher because the hull itself disturbs the acoustic records. The ROV investigations during the *EL21-Estonia expedition* are however able to shed additional light on whether bedrock or till reach the surface along the northern section of the hull midship, which will be reported below.

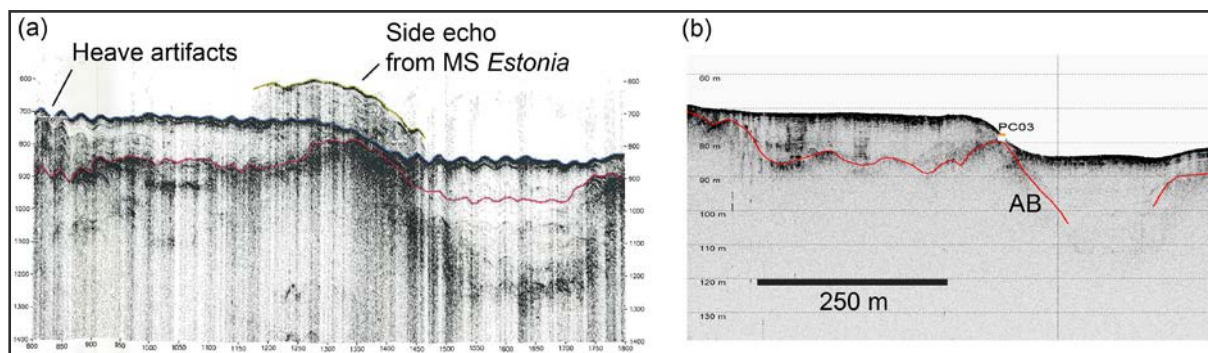


Figure SB3. Sub-bottom profile ESTON97 27 acquired by the Netherland Institute of Applied Geoscience TNO in 1997 (a). This profile runs along the path of 20210711234901 (b) with an offset to the north between about 0 and 25 m. The profile locations are shown in Figure SB2. The interpretation of a till surface inferred by Mesdag (1997) is shown in (a) with a red line while our interpretation of an acoustic basement is shown (b).

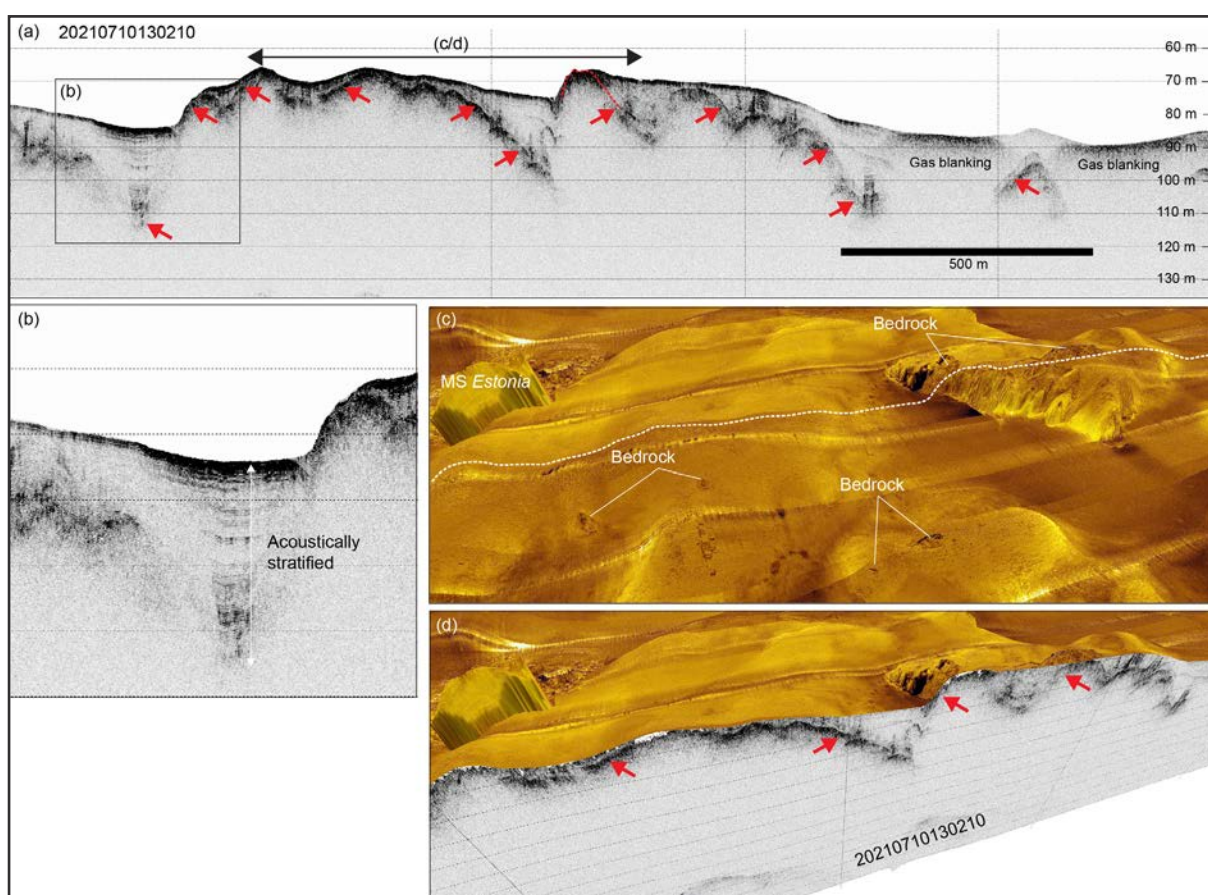


Figure SB4. (a) Sub-bottom profile 20210710130210 is shown to illustrate the occurrence of acoustically stratified sediment, interpreted to be comprised of varved glacial clay and in the uppermost part laminated postglacial gyttja clay, gas blanking and the interpretation of an acoustic basement (AB, red arrows). (b) Enlarged section with acoustically stratified sediments. (c/d) Side-scan imagery over the section of profile 20210710130210 showing where bedrock is exposed on the seafloor. This information has been used in our interpretation of the AB. In (d), the side-scan imagery is cut along profile 20210710130210.

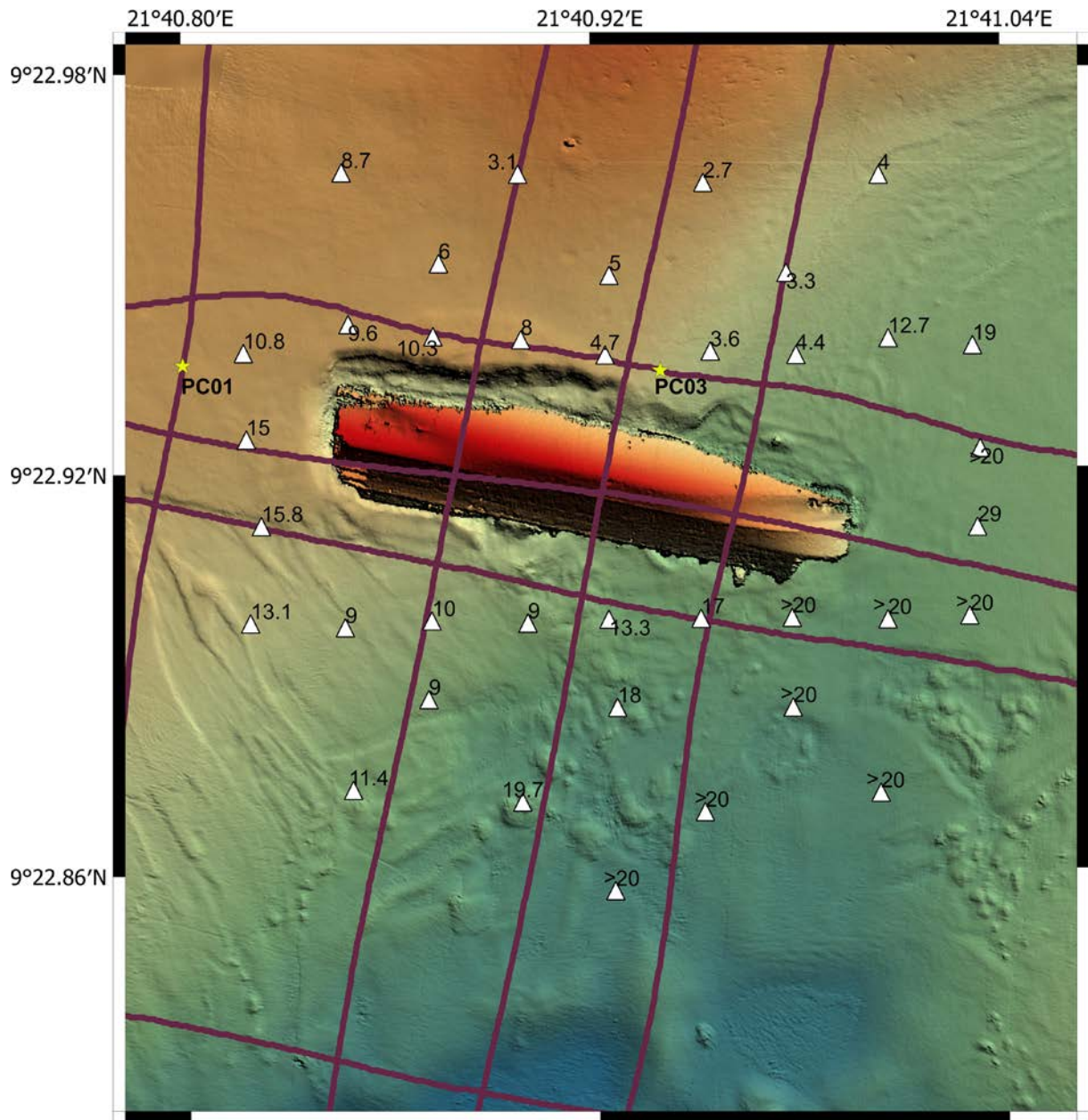


Figure SB5. Sediment thicknesses inferred from CPT probes made by Delft Geotechnics in 1996.

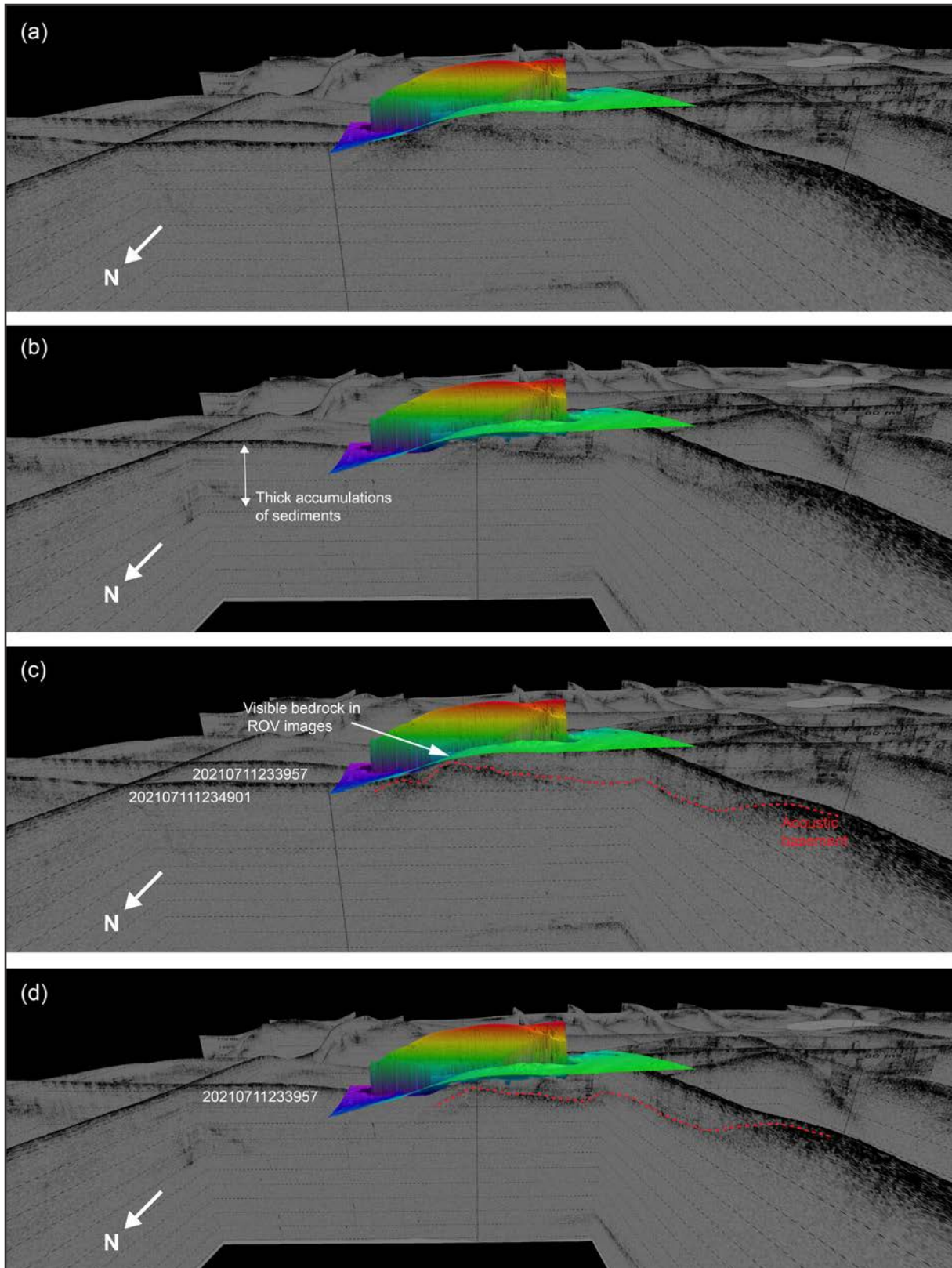


Figure SB6. 3D visualizations of the sub-bottom profile acquired with RV *Electra* running close to MS *Estonia*, which is shown on its right location with the multibeam bathymetry. The AB is seen to come up close to the seafloor, or even outcropping, in the closest profile 20210710130210 just north of the shipwreck.

## Side-scan sonar

In this section an overview of the side-scan results is presented with a focus on the general seafloor geology, i.e. sediment composition and bedrock. Objects identified in the side-scan records that were investigated with camera are further described in the section *Sediment sampling, bottom inspection and mooring*.

The side-scan survey was hampered because the tow fish could not be winched up and down swiftly to maintain an optimal tow-height above the seafloor of about 10–20 % of one channel's horizontal range. With our total range set to 2×100 m (100 m coverage to each side), the tow fish height above the seafloor should be around 10–20 m. This was not always managed because of the winching difficulties. Instead of winching in and out we had to alter the tow fish height by modifying the ship speed; the tow fish goes deeper with lower speed and vice versa. The entire survey area was mapped by east-west side-scan lines distanced with approximately 160 m (Fig. SS1). One line was run in south-north direction in the western survey area. There was an issue with getting a good focus on the starboard channel during the first lines, implying that only the port channel from these lines was used to create the complete mosaic at a resolution of 20×20 cm pixels shown in Figure SS2. A tiled higher resolution mosaic at 10×10 cm was also produced to be used for detailed maps.

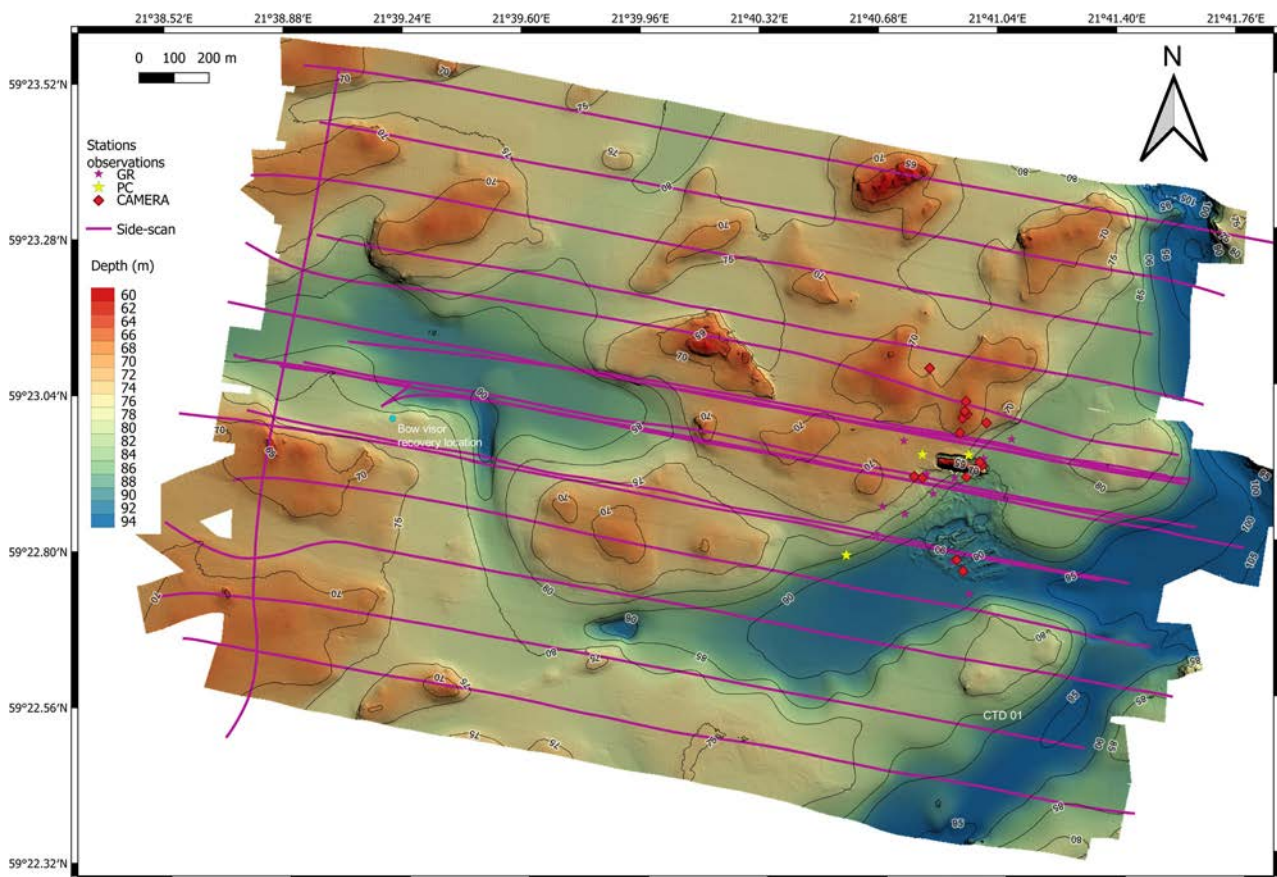


Figure SS1. Track lines of the side-scan survey. Several passed over MS Estonia were made. A larger version of this map is found in Appendix 4.

A general pattern with high reflectivity on the bathymetric highs and lower in the deeper areas is observed (Fig. SS2), i.e. similar to what is observed in the backscatter data. Areas with exposed bedrock at the seafloor are readily identified at numerous locations (Figs. SS3 and SS4). These areas were digitized to be used together with the interpretation of an AB in sub-bottom profiles for the compilation of a gridded sediment thickness model described below under a dedicated section. Boulders and other objects are also seen in the side-scan imagery, which will be further addressed in the section describing the camera observations. The site where the bow visor of MS *Estonia* was recovered according to the JAIC final report shows a nearby high reflectivity area where till most likely makes up the seafloor geology and boulders may be present (Fig. SS5). There are no clear signs of an imprint in the seafloor from the bow visor itself in the side-scan images. The reported coordinates are assumed to be referenced to WGS84. However, coordinates of the bow visor location were also reported by the Finnish navy in the Finnish KKJ datum. These coordinates were here converted to WGS84 and are shown on the map in Figure SS5. A feature is here seen on the side-scan imagery that may be the imprint of the bow visor in the seafloor.

The shipwreck of MS *Estonia* was passed several times both on the starboard and port side and with slightly different tow fish levels. MS *Estonia* is sticking up as much as 16m from the seafloor, which made the shipwreck difficult to image with the side-scan. None of the side-scan images provide a stellar image of the shipwreck, mainly because of an abundance of side-echoes, although some details such as the balconies and some rows of windows can be made out (Fig. SS6).

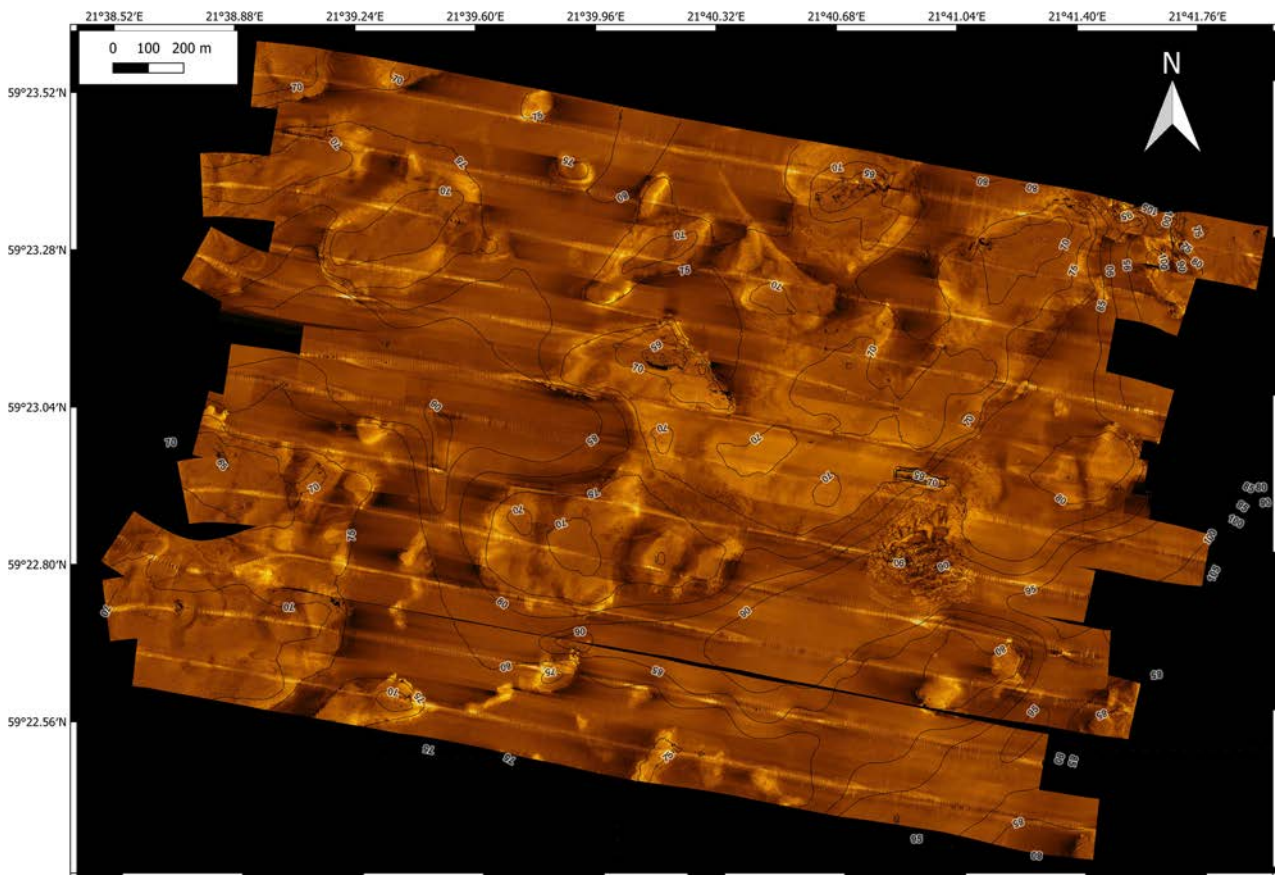


Figure SS2. Side-scan mosaic compiled at a pixel-size of 20×20 cm. A larger version of this map is found in Appendix 4.

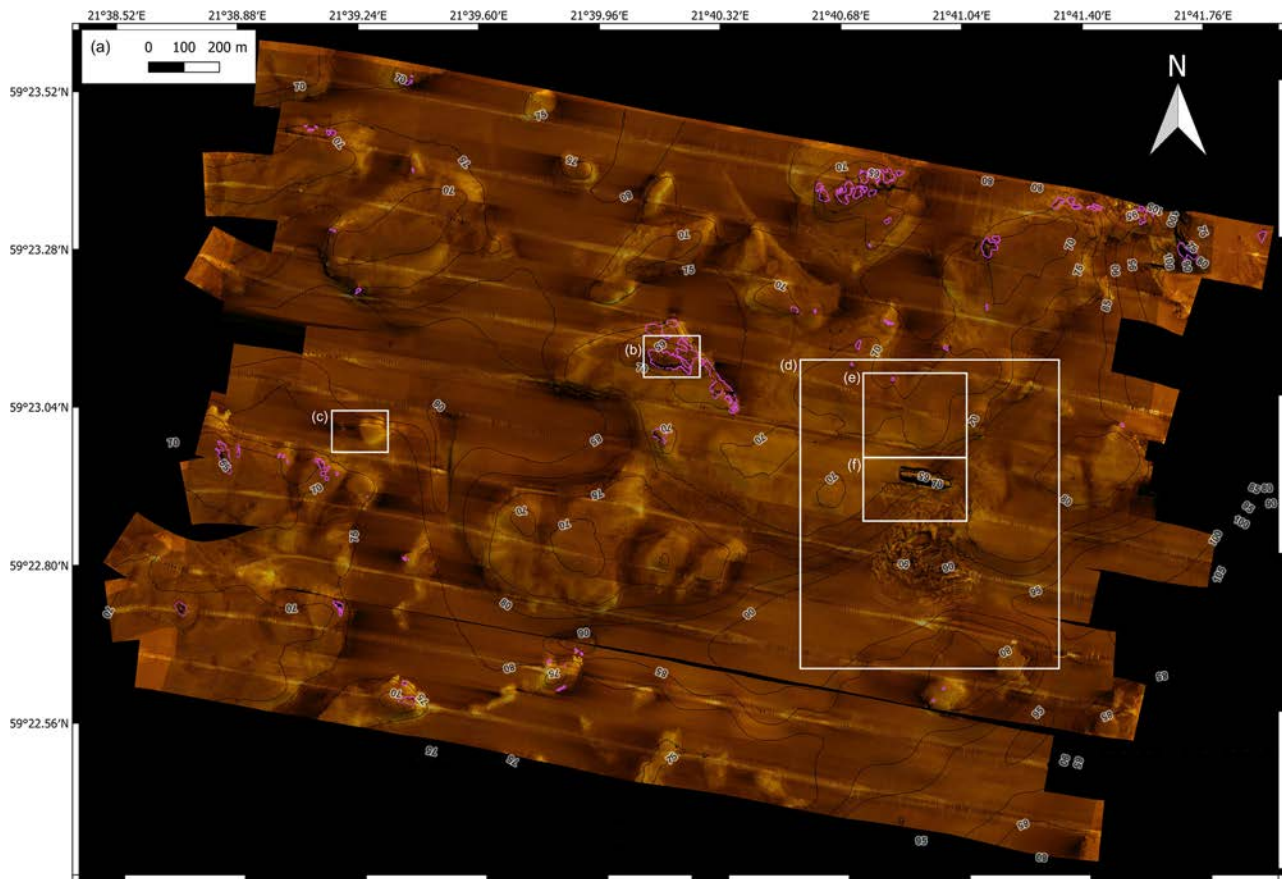
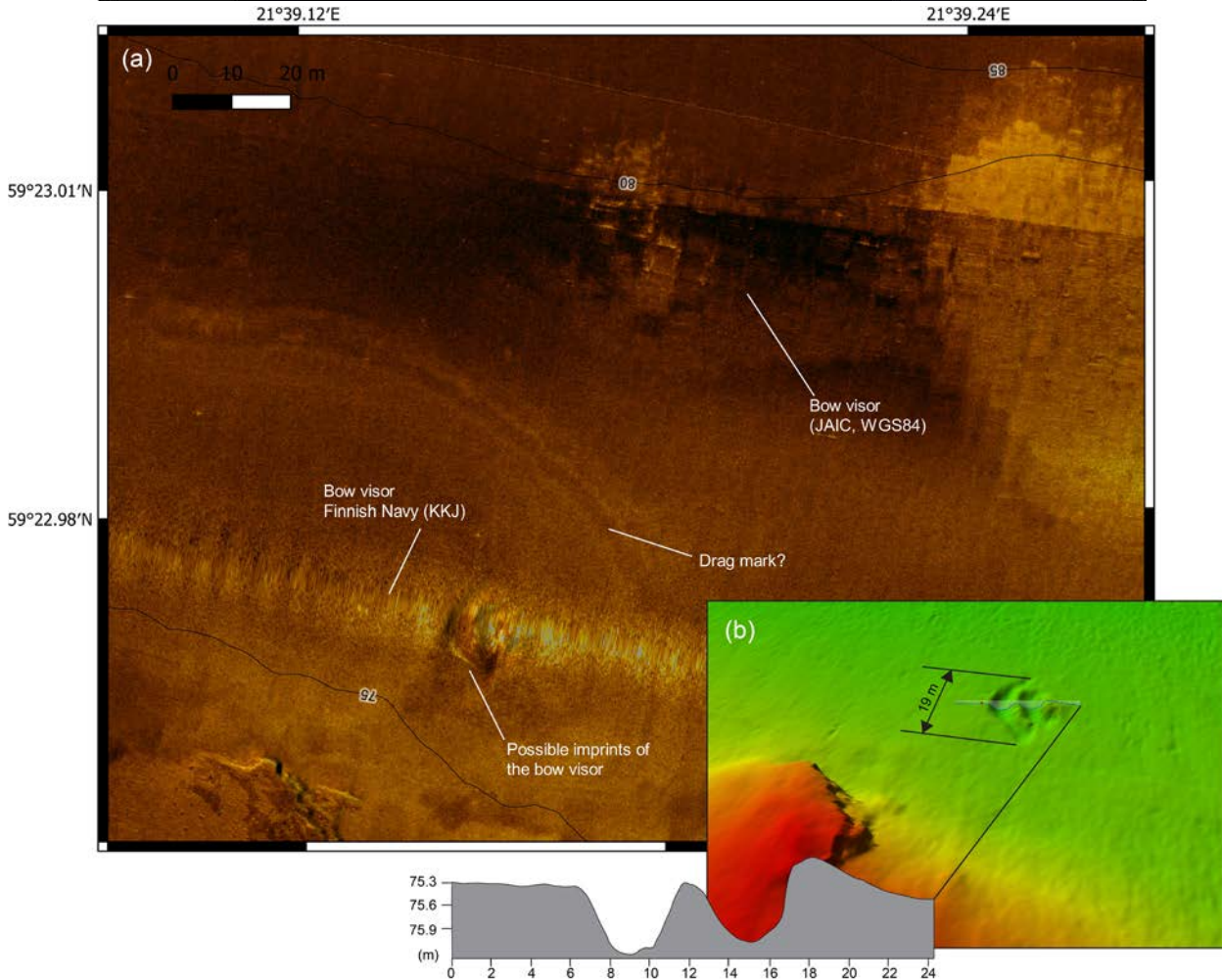
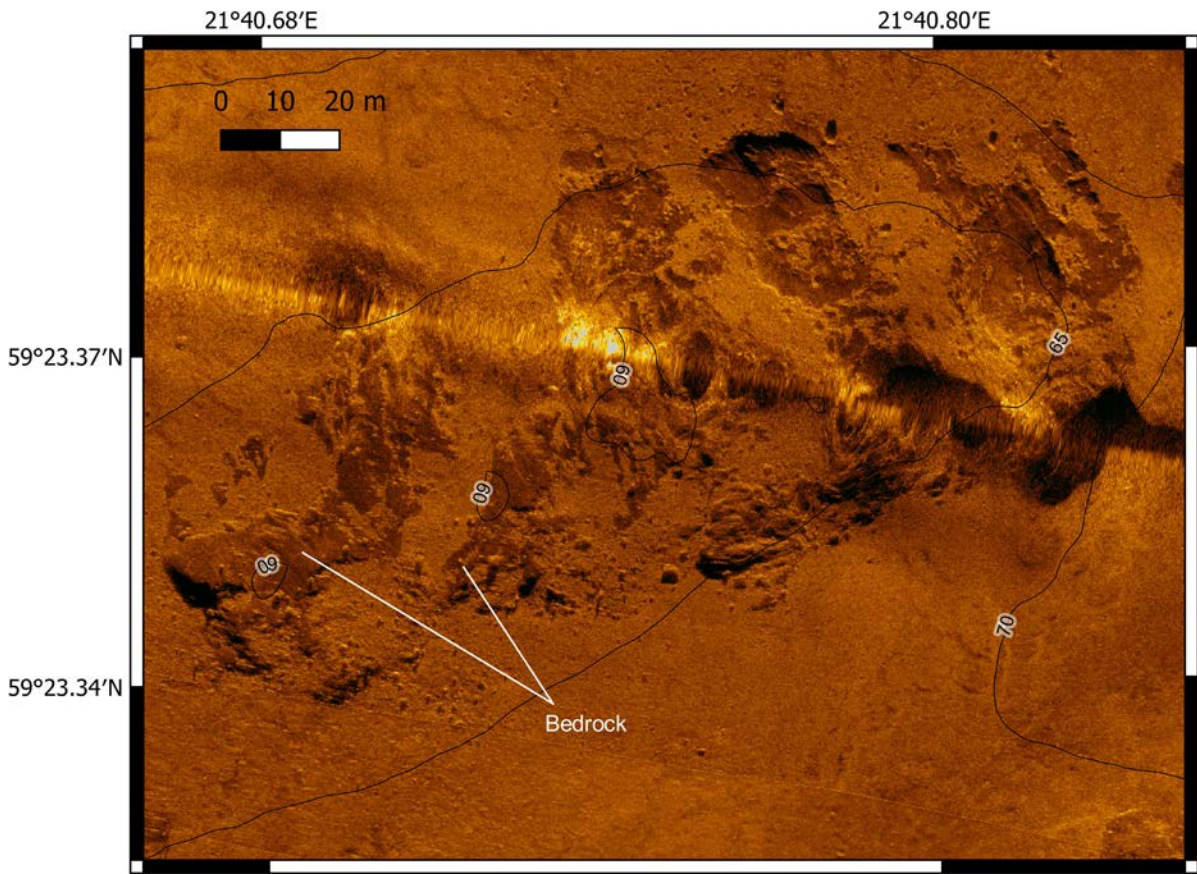


Figure SS3. (a) Same side-scan mosaic as shown in Figure SS2, but made semi-transparent in order to make the shading from the multibeam bathymetry shine through to get a depth perception. Bedrock at the seafloor is outlined with purple dots. (b) An area with bedrock at the seafloor shown in the detailed map in Figure SS4. (c) Detailed map of the visor recovery location shown in Figure SS5. (d). Detailed map of the shipwreck location shown in Figure SS6. (e and f) Extent of maps shown in the section “Sediment sampling, bottom inspection and mooring”. A larger version of this map is found in Appendix 4.

Top right: Figure SS4. Side-scan mosaic of an area with bedrock at the seafloor. The map location is shown in Figure SS3. A larger version of this map is found in Appendix 4.

Bottom right: Figure SS5. (a) Side-scan mosaic of the area where the bow visor was recovered according to the final report by JAIC (position referenced to the WGS84 datum) and the position given by the Finnish Navy reported in the Finnish KKJ datum, here converted to WGS84. The Finnish location is situated close to a feature on the seafloor that may constitute an imprint of the bow visor. The map location is shown in Figure SS3. (b) Multibeam bathymetry of the possible imprint of the bow visor. A larger version of this map is found in Appendix 4.



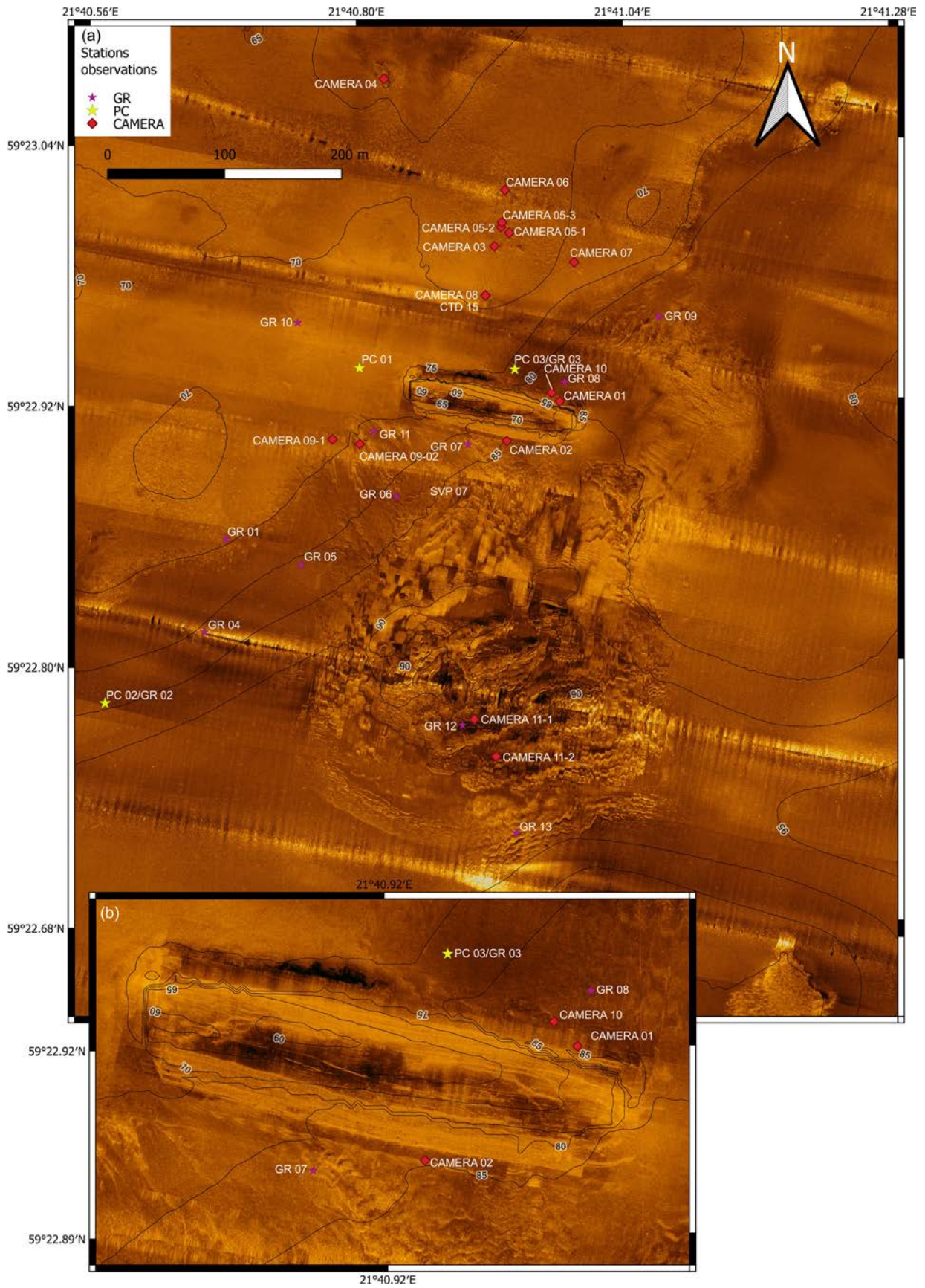


Figure 556. (a) Side-scan mosaic shipwreck site. Artifacts from tow-fish movements are seen as stripes in some lines. (b) Close up on MS Estonia.

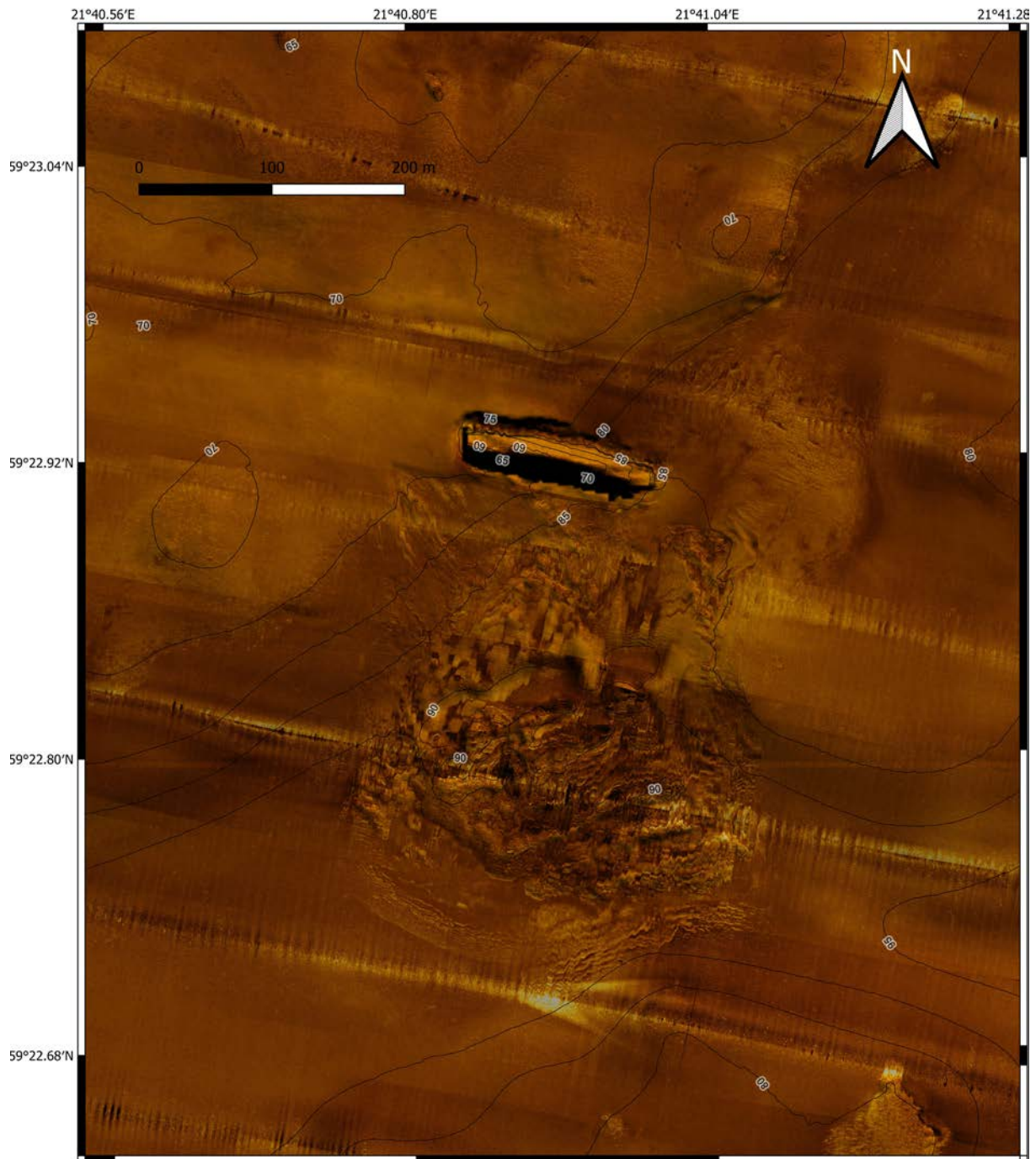


Figure SS7. Side-scan mosaic of shipwreck site made semi transparent in order to get a depth perception from the shading of the underlying multibeam bathymetry.

## Mid-water sonar

The Simrad EK80 files (.raw format) were parsed and processed in MATLAB 2021b using a series of scripts provided by Kongsberg Maritime (L. Anderson, personal communication) and corrected for range using the nearest (in time) CTD profile. Features visible in the EK80 data include rising gas bubbles, fish and fish aggregations (Fig. MW1a). Thermohaline stratification can also be identified in the acoustic data, seen as discrete horizons at ~20 and ~30 m depth (compare black dots in Fig. MW1a and dashed black lines in Fig. MW1b). The permanent halocline (Reissmann et al., 2009), situated between approximately 60 and 80 m depth (Fig. MW1b), can be seen as a banded horizontal feature in the acoustic data (Fig. MW1a). Thermohaline stratification has been observed with wideband echosounders previously in the Arctic Ocean (Stranne et al., 2017) and in the Baltic Sea (Weidner et al., 2020).

In Appendix 5, EK80 data are shown in three panels for each survey profile (in total 18 profiles). Two panels show the ES70C transducer data (45–90 kHz), one with focus on the water column and one with focus on the sub-bottom penetration. The third panel show ES200-7C transducer data (160–260 kHz) with focus on the water column (as there is essentially no penetration at these frequencies). An example survey profile is shown in Figure MW2. Note that all EK80 data are shown as uncorrected volume backscatter, meaning that quantifications based on these data are not possible (of e.g. the turbulent mixing, gas bubble size distribution etc.)

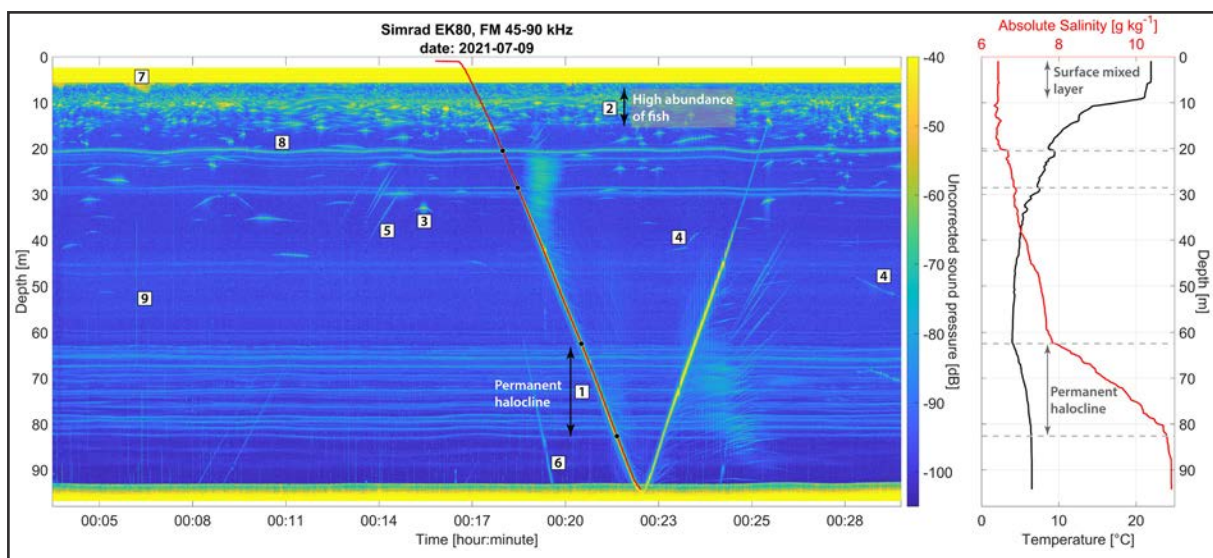


Figure MW1. Wideband EK80 data from the ES70C transducer (45–90 kHz) and concurrent CTD profile. a) EK80 echogram showing the uncorrected volume back-scatter over depth and time as Electra was at a CTD station (holding position with DP). The large v-shaped feature in the echogram is the CTD rosette going down to the bottom and then back up to the sea surface. The red line is the CTD depth plotted against CTD time and the fit between the two data sets confirms that the depth corrections (on both data sets) as well as time stamps are accurate. b) Depth profiles of absolute salinity and in-situ temperature from CTD station 1 are shown. The depths of the horizontal dashed lines correspond to the black dots in (a) and are examples of thermohaline stratification (i.e. variations in salinity and/or temperature) visible in the echosounder data. The numbered white boxes in (a) represent additional features in the acoustic water column data: 1 indicates a depth interval with horizontal banded features coinciding with the permanent halocline, 2 indicates a region down to about 15 m depth where fish (and likely other biology) are abundant, 3 shows an example of a single stationary fish, 4 (two examples) show moving fish, 5 shows a rising gas bubble from the seafloor, 6 indicates the “double return” from the CTD rosette (an acoustic artefact), 7 shows turbulence and/or noise from the ship propellers (frequently occurring when the ship is on DP), 8 indicates internal waves propagating along the stratification interface, 9 shows noise from unknown sources (potentially related to propellers).

### Acoustic Doppler Current Profiler (ADCP)

The shipboard ADCP survey was performed in parallel with the midwater sonar survey (Fig. MB1). An example transect is shown in Figure MW3 and all transects are shown in Appendix 5. The data were averaged over two depth intervals (surface-40m and 40–55m) and over three equidistant parts of each transect, in order to estimate the overall current flow velocities over the survey area during the time of the survey (Fig. MW4b and Appendix 5, p. 58). The estimated current velocities (Fig. MW4a) are based on these averages. The surface velocities in the area were generally modest during the ADCP survey. A band between about 20 and 40m depth with a slightly elevated eastward velocity can be seen, and a section in the eastern part of the transect, between about 40–60m depth, with a clear southward velocity component (Figs. MW3 and MW4).

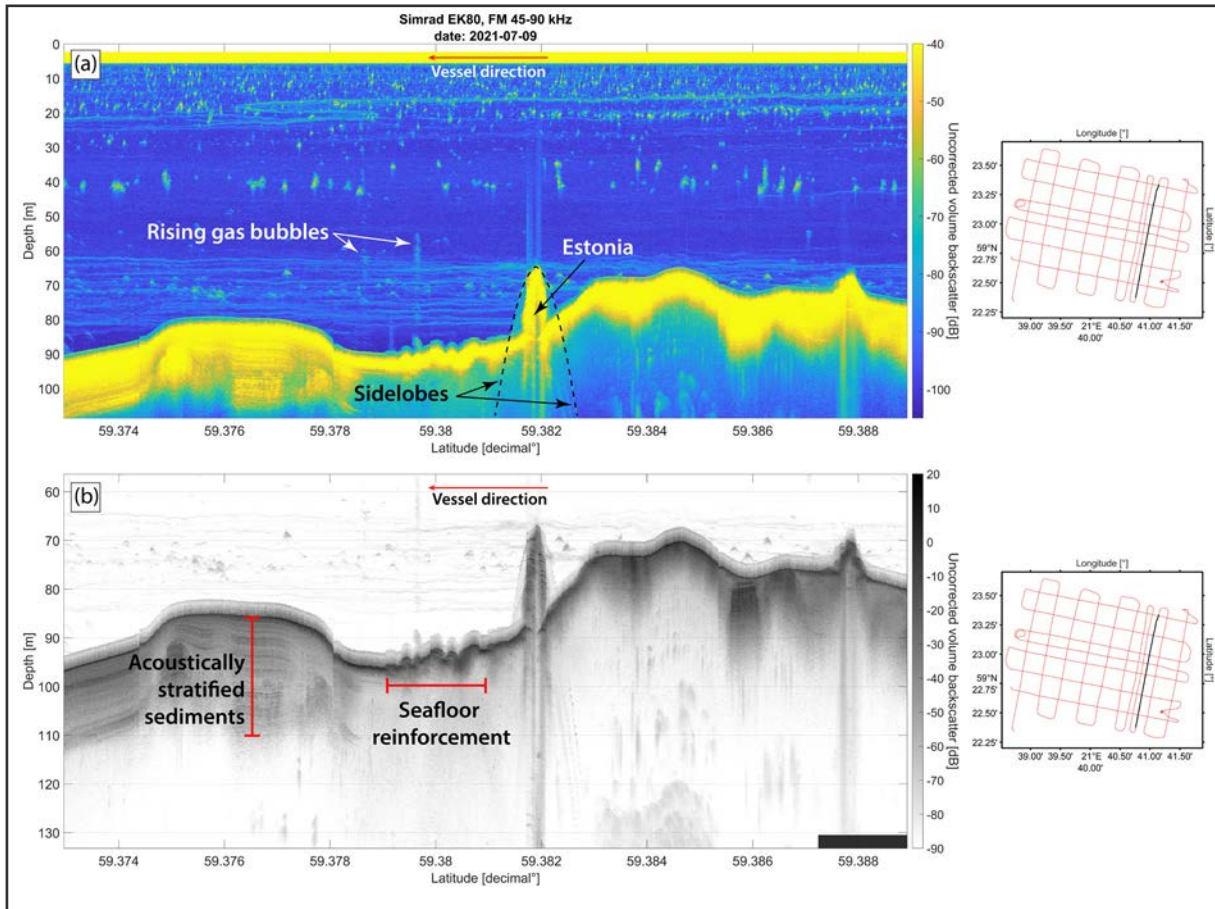


Figure MW2. Example EK80 echograms. a) Echogram across MS Estonia processed with focus on water column features. Visible features include the permanent halocline (see Fig. MW1), fish and fish aggregations, and rising gas bubbles. Also marked out is the Estonia shipwreck and associated sidelobes (acoustic artifacts from steep topography or objects). b) Echogram with focus on bottom and sub-bottom features. Visible features include, MS Estonia, acoustically stratified sediments and the manmade seafloor reinforcement south of the shipwreck. The vessel direction is shown as a horizontal red arrow. All EK80 survey profiles (including the 160–260 kHz transducer data) are found in Appendix 5.

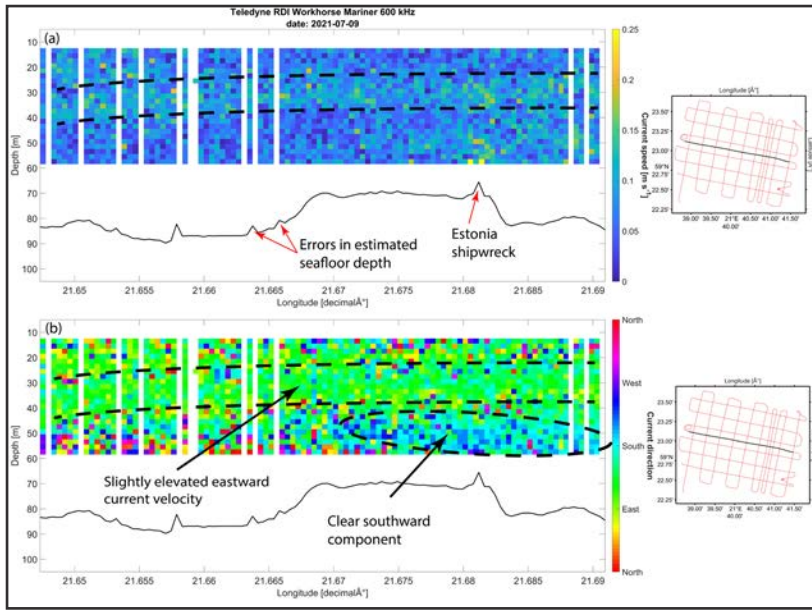


Figure MW3. Shipboard ADCP transect over the MS Estonia shipwreck. a) Current speed as a function of longitude and depth. b) Current direction as a function of longitude and depth. The range of the 600 kHz shipboard ADCP is typically around 50 m. In this figure and in Appendix 5, the Electra draft (2.3 m) is applied and the data is cropped at 60 m depth in order to not show the unreliable data beyond the range of the ADCP.

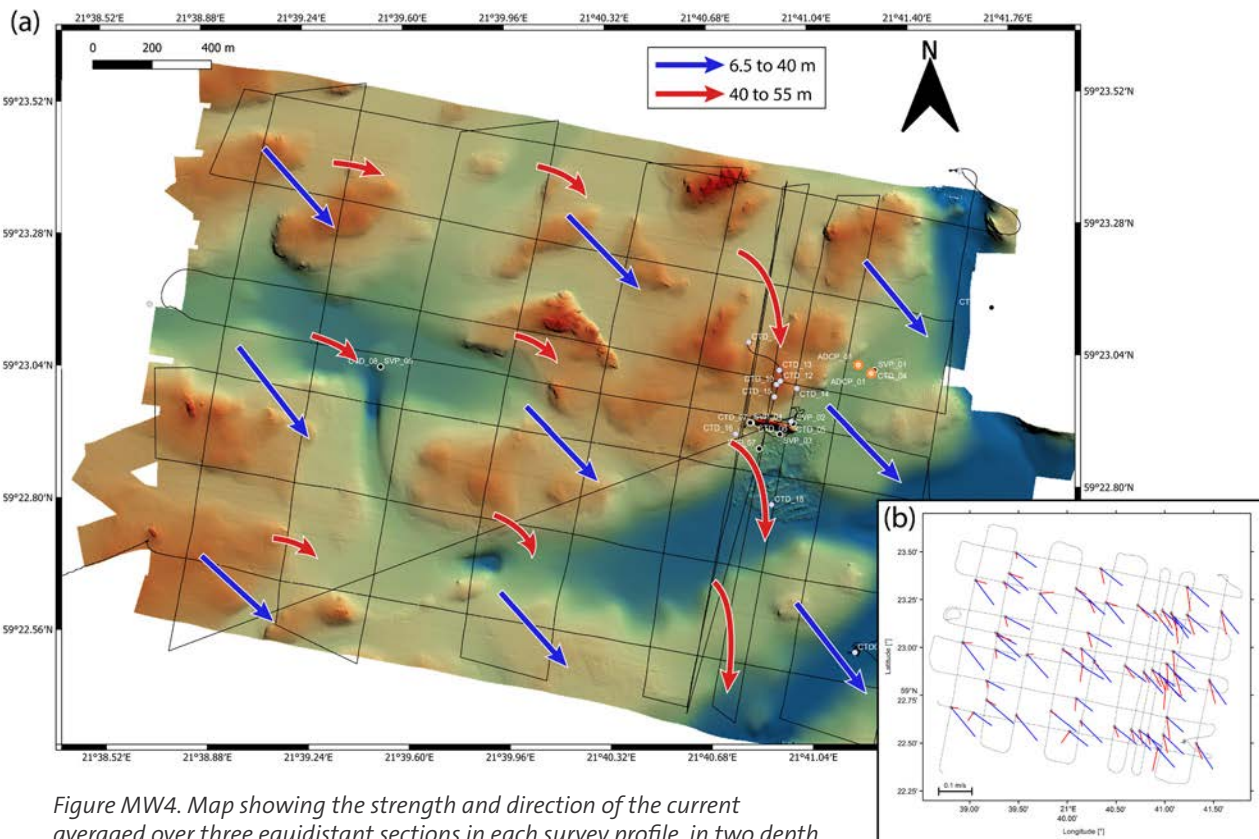


Figure MW4. Map showing the strength and direction of the current averaged over three equidistant sections in each survey profile, in two depth intervals: 6.5–40 m and 40–55 m. a) interpreted current directions from the calculated averages shown in (b). During the time of the survey, the currents in the depth interval of 6.5–40 m (blue) had a south-eastward direction with a speed of ~0.1 m/s. The currents in the 40–55 m depth interval (red) were generally weak and directed eastward in the western part of the survey area and intensifying and turning towards south-southeast in the eastern part of the survey area. Panel (b) can also be found at larger size in Appendix 5.

### Water properties (sound speed, temperature, salinity)

The CTD data is comprised of vertical profiles of temperature, absolute salinity, density (derived from absolute salinity, temperature and pressure), dissolved oxygen, fluorescence and turbidity. Data from all CTD stations are shown in Appendix 6 pp. 2–19. In Figure WP1, CTD profile data averaged over all stations and the corresponding  $\pm$  one standard deviation, are shown. Looking at the density stratification (Fig. WP1c), three different water masses can be identified: the *surface mixed layer* (surface to ~10 m), the continuously stratified *surface water* (15 to 60 m) and the well-mixed bottom water (about 85 m to bottom). The surface and bottom waters are separated by a halocline (about 60 to 80 m, Fig. WP1b). This halocline is always present in the Baltic Proper (Reissmann et al., 2009), but the depth and vertical extension can vary as result of e.g. down/upwelling events, storms and convection during the cold season.

The dissolved oxygen concentration drops drastically below the permanent halocline and below 75 m, conditions are more or less anoxic. Weidner et al. (2020) showed that in the Western Gotland Basin, the depth of the permanent halocline coincided with the transition between oxic and anoxic conditions, and that the depth of anoxia, defined as where the dissolved oxygen concentration drops below 2 ml/l, can change ~14 m over the course of about two days. Similarly, in the present data-set the halocline and oxycline coincide, and the depth at which hypoxia begins dropped about 5 m over the first 5 days of the survey (Fig. WP2).

Fluorescence is used as a proxy for the concentration of Chlorophyll A and the amount of phytoplankton in the water column. The fact that fluorescence was highest close to the surface and decreasing below the mixed layer, where sunlight is highly attenuated, seems therefore consistent with what can be expected (Fig. WP1e).

Turbidity provides a relative measure of the amounts of particles in the water column (Fig. WP1f). The turbidity is slightly elevated in the surface mixed layer which is likely related to the higher fluorescence (and presumably higher concentrations of plankton). The lowest turbidity is found in the *surface water*, below the mixed layer. The peak in turbidity in the lower part of the permanent halocline might be related to the retardation of the particle sink velocities as the density increases. An important contribution to the turbidity maximum may also come from the strong bottom currents seen in the moored ADCP data (Fig. AM2) between 70–80 m with an associated sediment resuspension forming a nepheloid layer (Yurkovskis, 2005).

A total of 7 sound velocity profiles were collected using a Valeport MiniSVP (sound velocity, pressure) sound velocity profiler that was attached to the CTD rosette. The individual profiles are shown in Figure WP3, assuming that pressure (in dbar) is equal to depth below sea surface (an error on the order of a couple of meters).

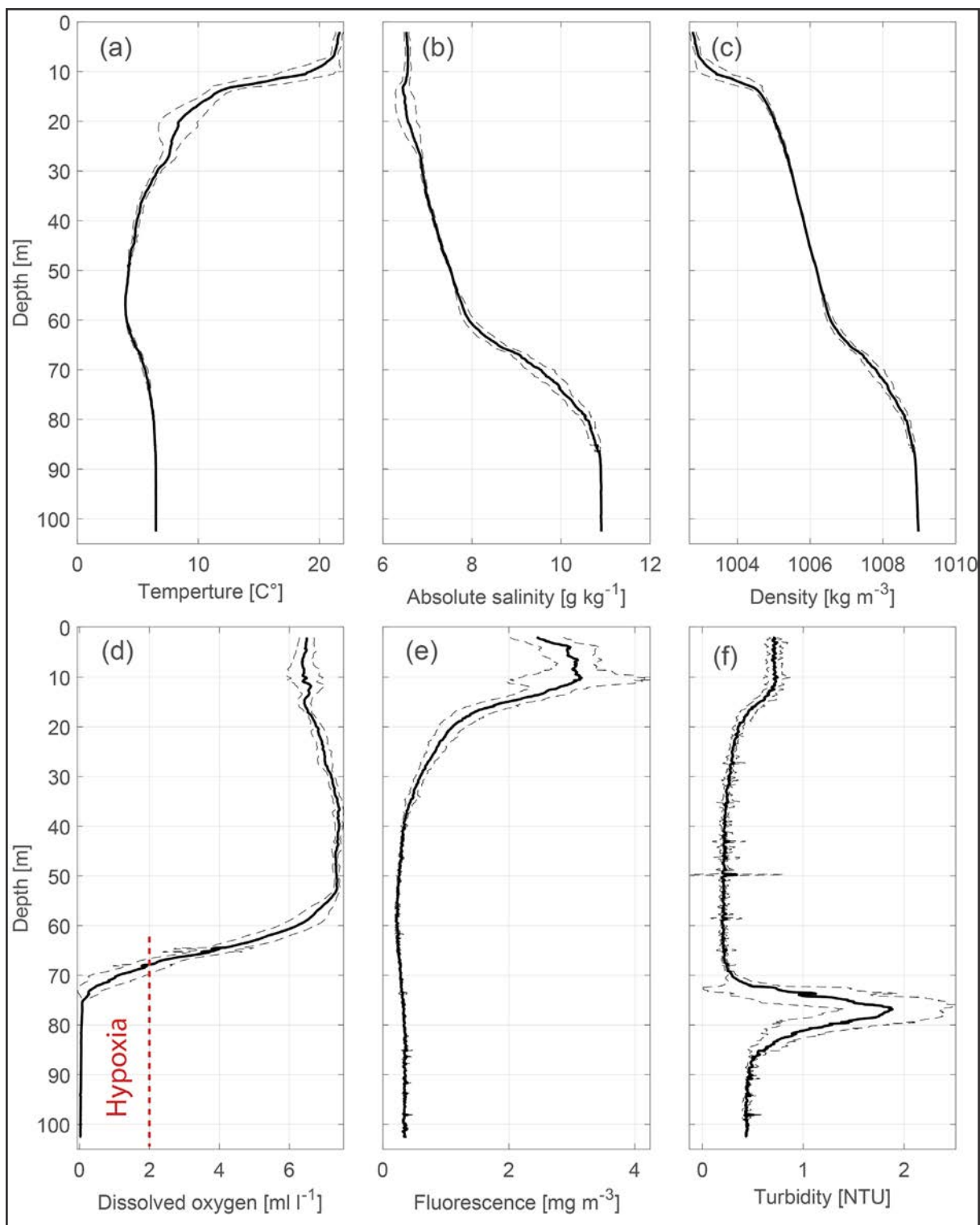


Figure WP1. Average CTD profiles. Average a) temperature, b) absolute salinity, c) density, d) dissolved oxygen concentration, e) fluorescence and f) turbidity are plotted against depth (solid black) and the corresponding  $\pm$  one standard deviation (dashed black lines).

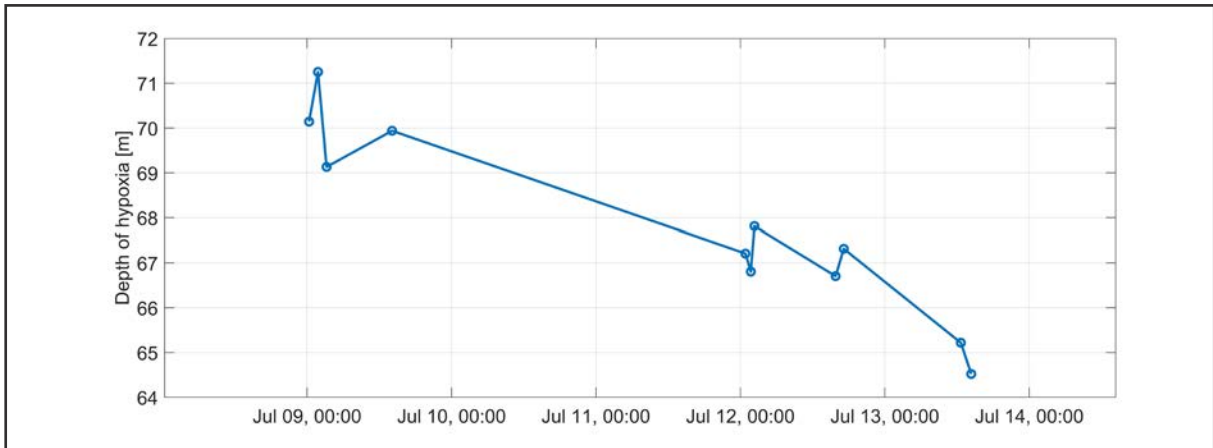


Figure WP2. Hypoxic conditions, defined as dissolved oxygen concentration  $< 2$  ml/l, are often found below the permanent halocline in the Baltic Proper. Here, the water depth at which hypoxia begins is plotted against time. The data covers the first 13 CTD stations and only CTD profiles that goes into the hypoxic zone are considered (11 stations in total).

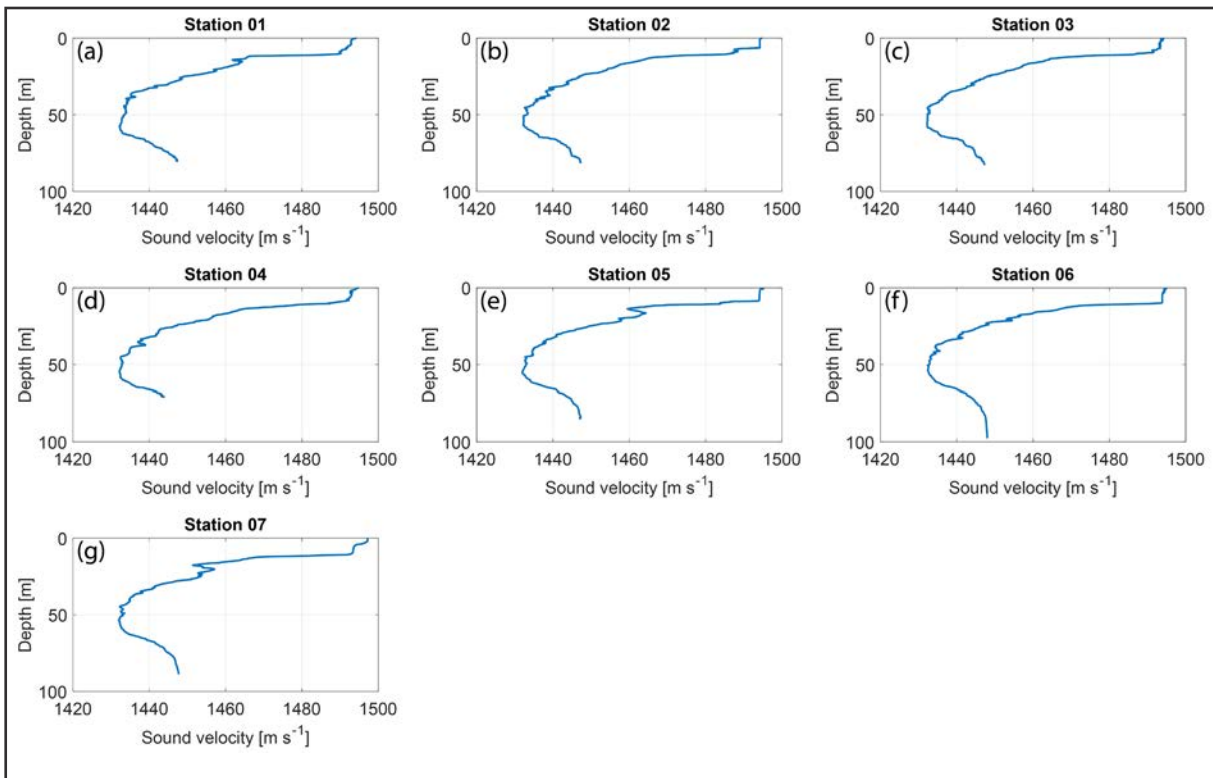


Figure WP3. Sound velocity profiles for SVP stations 1–7 (panels a–g, respectively).

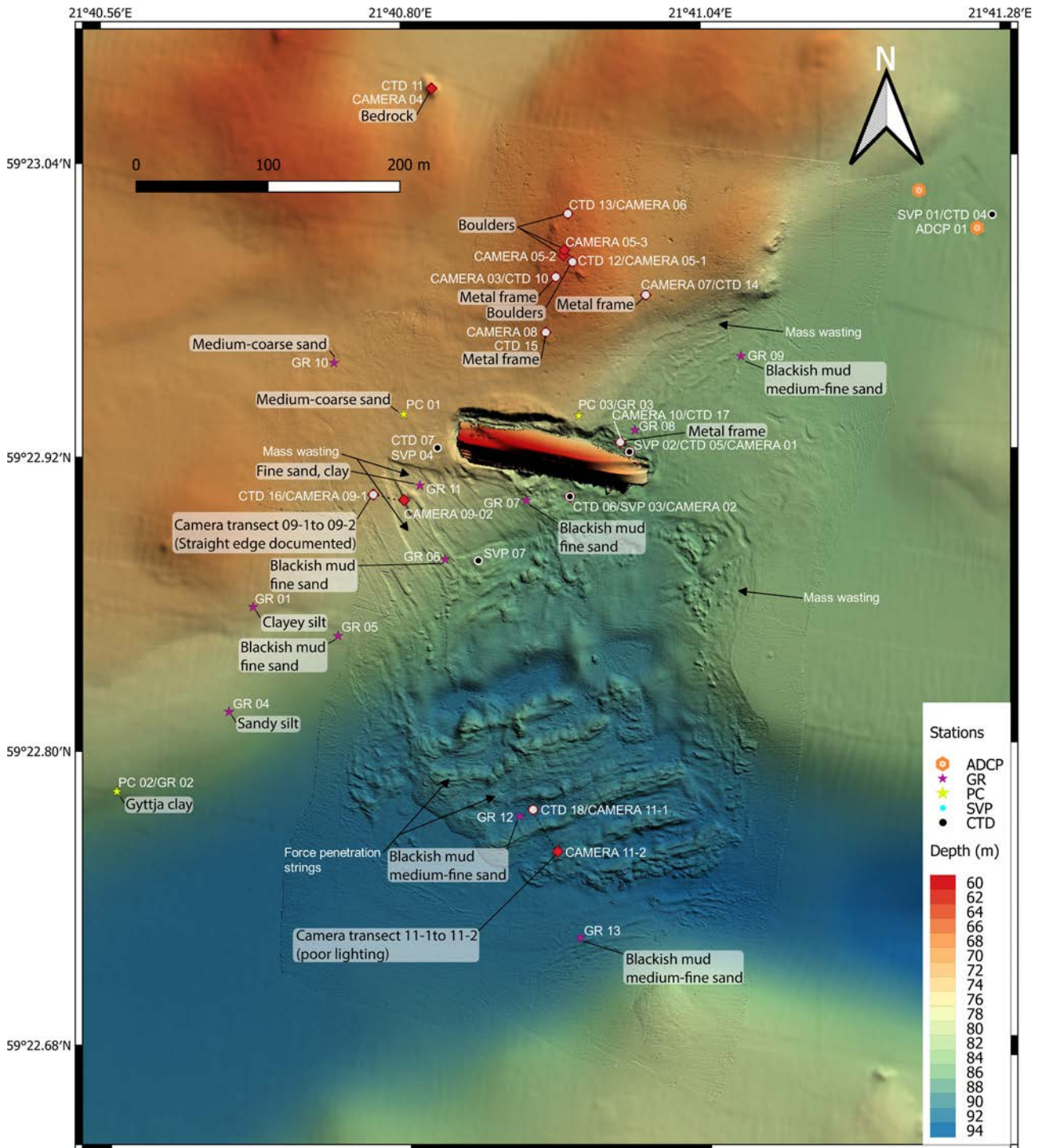


Figure SBI1. Locations of piston cores, grab samples, camera observations and the ADCP mooring site (the symbol with the station name next to it is the actual ADCP mooring site, while the other symbol shows the buoy location). Summary of the results from all bottom observations made by GoPro camera mounted on the CTD carousel and ocular inspection of grab samples are also shown on the map.

## Sediment sampling, bottom inspection, and mooring

### Piston coring

Three piston cores were acquired from the area surrounding MS *Estonia* for the purpose of ground truthing the geological interpretation of the geophysical mapping. The core locations are shown on the map in Figure SBI1. The core positions, water depths and lengths are summarized in Table SBI1. Results from analyses made on the sediment cores are presented below as well as a short summary of the core lithologies. More complete core descriptions are found in the Appendix 7.

#### Lithology

The 205 cm long core EL21-Estonia-PC01 (the suffix will henceforth be used for each core) aimed to capture the sediments west of the shipwreck in order to get an idea of the composition and thickness of the sand dumped during the covering work that later was aborted. The core captured well sorted dusky red (Munsell color nomenclature is used) medium-coarse sand that gradually coarsen downcore (Fig. SBI2). Some pebbles are found in the bottom of the core. Core PC02 retrieved 472 cm sediments that can be divided into three lithologic units (Fig. SBI2). An upper 382 cm thick unit consist of fine greenish grey gyttja clay with dark greenish black laminations. This unit transitions into a 33 cm thick siltier light olive grey clay with regular 0.5 cm thick bands of grey clay. The unit is here proposed to be comprised of glacial clay and thus we may have reached into a deglacial sequence. A water gap separated this unit from the lowermost and final unit in the core, which is comprised of a continuation of the varved clay with a higher silt content

Table SBI1. Piston cores retrieved during the EL21-Estonia expedition. Further information about the cores is included in Appendix 7.

Core	Length (cm)	Position (lat,lon)	Water depth (m)
EL21-Estonia-PC01	205	59.38227°N, 21.67999°E	71
EL21-Estonia-PC02	472	59.37972°N, 21.67612°E	82
EL21-Estonia-PC03	234	59.38225°N, 21.68233°E	77

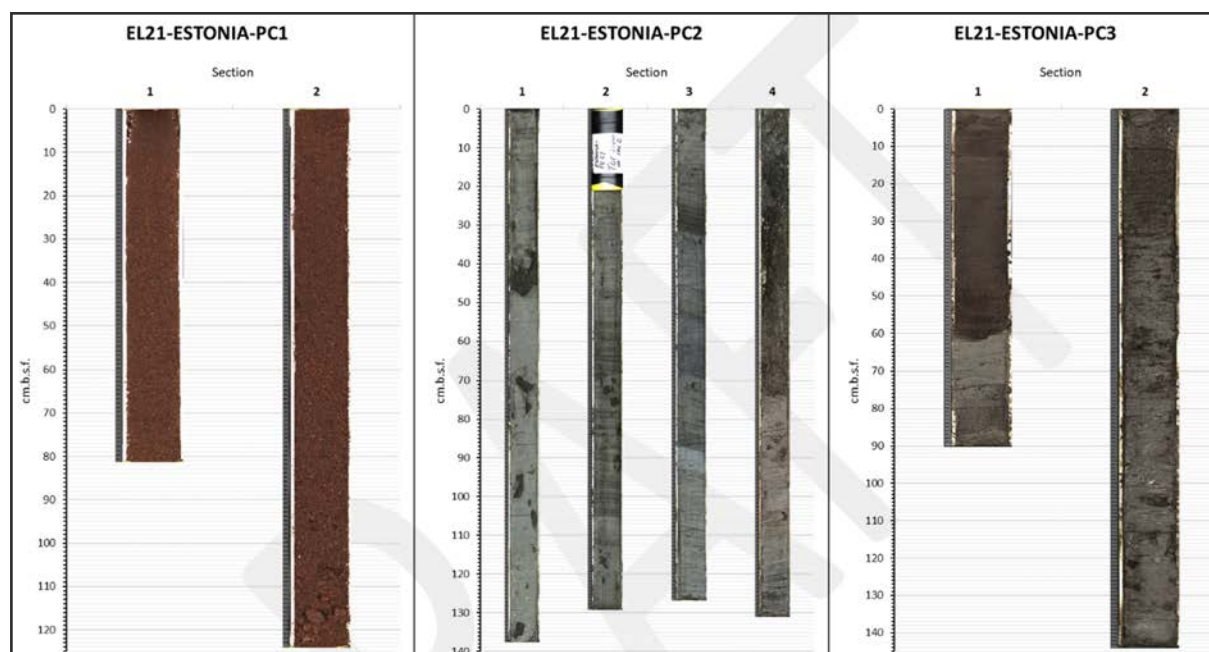


Figure SBI2. Images of the split sediment core sections. Higher resolution images are found in Appendix 7.

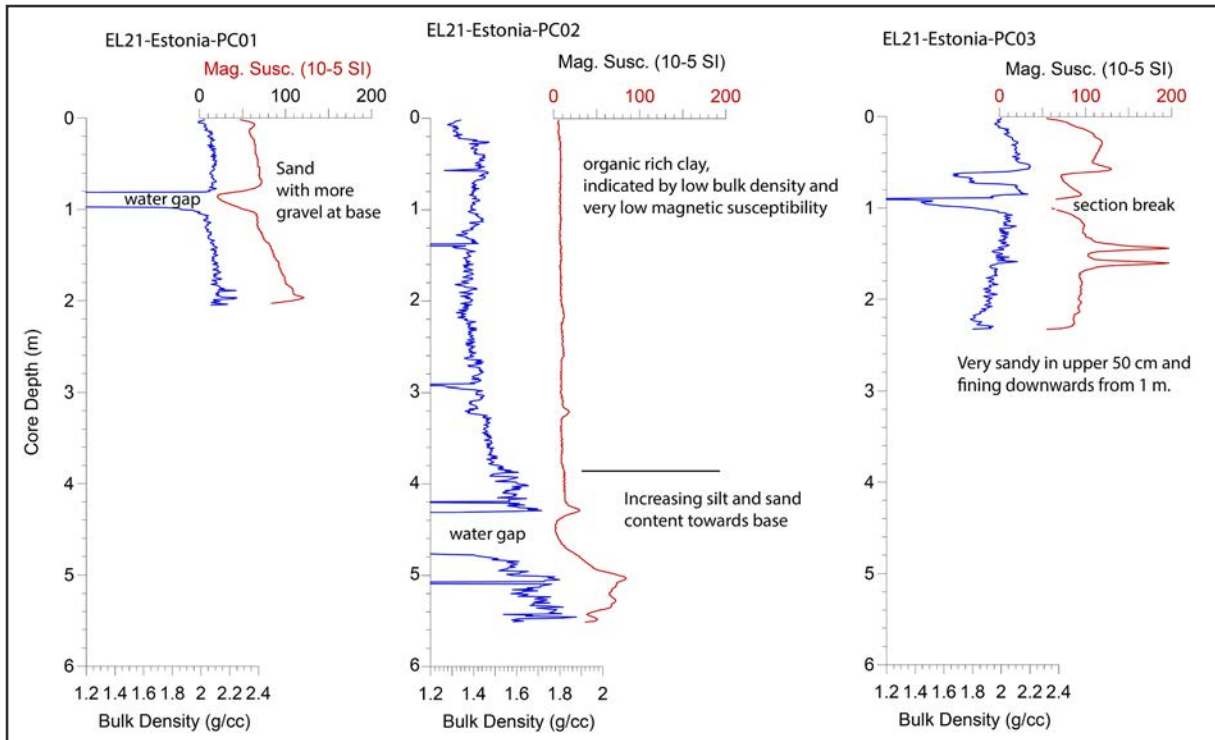


Figure SBI3. Logged magnetic susceptibility and bulk density of the three retrieved piston cores.

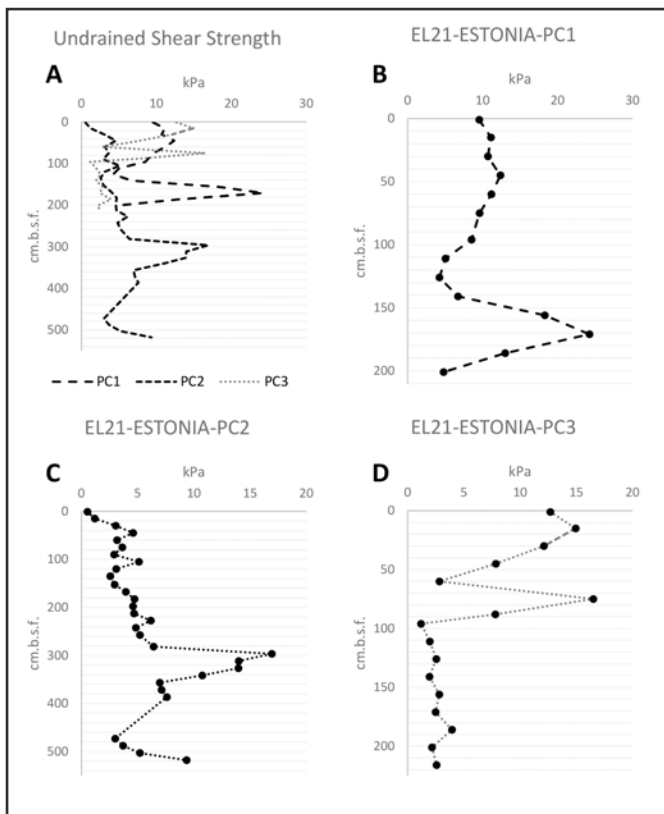


Figure SBI4. Undrained shear strength from all three cores collected from the cruise, samples taken 15 cm apart downcore. A) shows the undrained shear strength from all cores compared to each other. B), C), and D) shows the undrained shear strength from the cores individually (note the different depth scales between the cores).

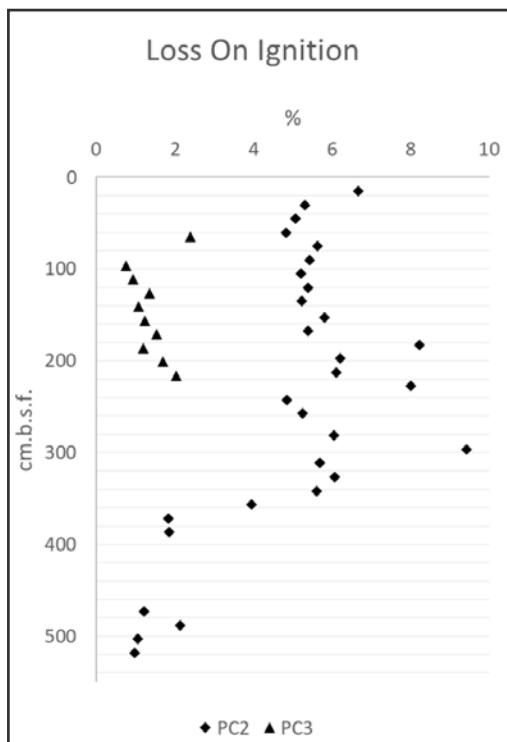


Figure SBI5. Loss on ignition results which indicated the carbon content in the sediment. Samples taken 15 cm apart downcore.

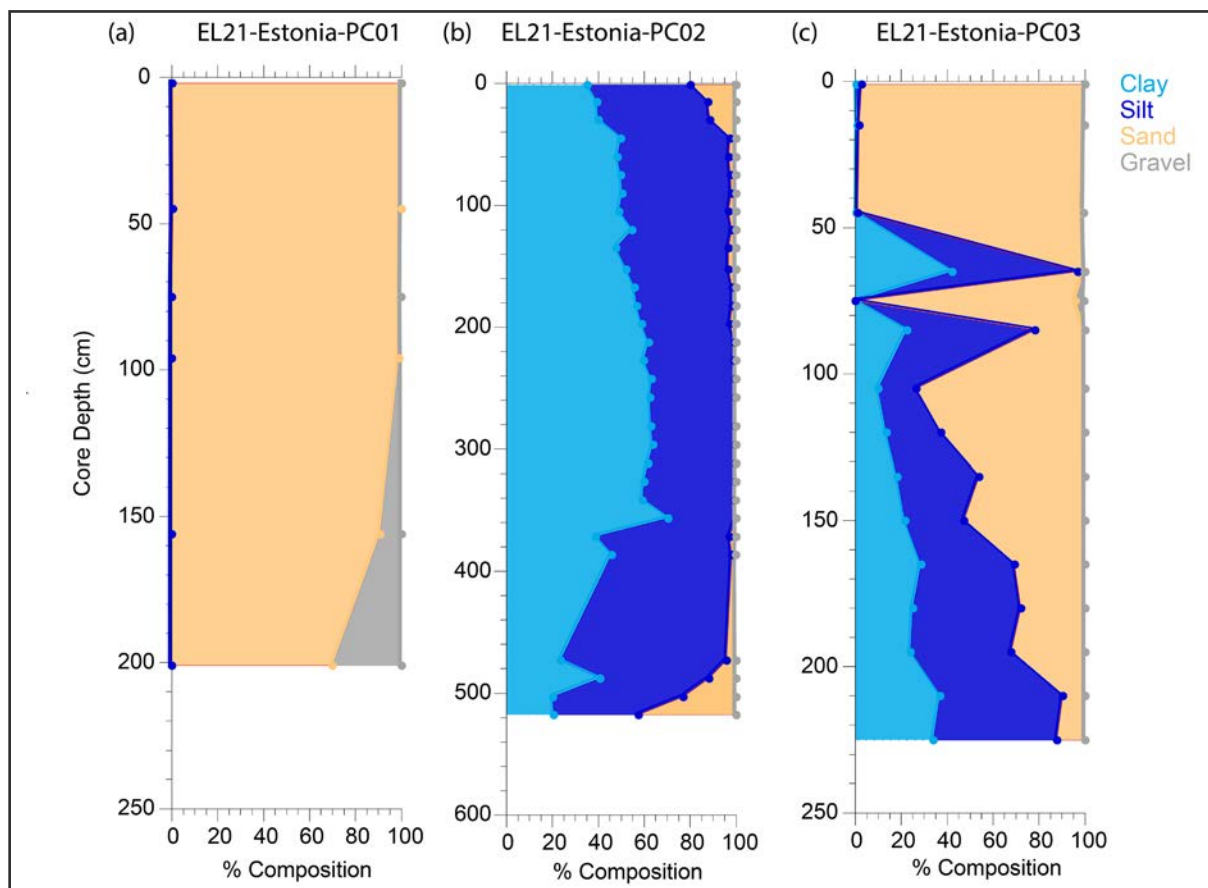


Figure SBI6. Grainsize fraction change with depth from core PC01, PC02 and PC03. (a) Sieved grain size from core PC01. (b) Measured grainsize from core PC02 using the PSA after removing organic matter. (c) Combined grainsize from sieve and PSA (without removing organic matter) from core PC03. The sediment is categorized as follows; gravel (>2.00 mm), sand (1 mm–63  $\mu$ m), silt (63–3.9  $\mu$ m) and clay (<3.9  $\mu$ m) as according to Wentworth, 1922.

Table SBI2. Descriptions of each site inspected with the GoPro camera mounted on the CTD-carousel. The locations of the inspected sites are shown in the map in Figure SBI1 and snapshots are shown in Figure SBI7-11. (WGS84 coordinates).

Observation	Water Depth	Position (Lat, Lon)	Description
CAMERA 01	85 m	59.38200°N, 21.68300°E	Site located on the northeastern side of <i>MS Estonia</i> , ~4 m from the hull. Hard lighting affects the image quality. Close up of bottom sediment, likely containing organic matter judged from black-greenish colour.
CAMERA 02	85 m	59.38170°N, 21.68220°E	Site located ~12 m south of <i>MS Estonia</i> . Only seafloor sediment visible, likely sand.
CAMERA 03	66 m	59.38319°N, 21.68204°E	Metal frame located north of <i>MS Estonia</i> , ~116 m from the hull. Appears like cables are attached on the frame. The frame has been identified to belong to transponders made by Sonardyne (model Compatt, transmitting in the frequency range of 19–36 kHz), which were placed on the seafloor during the work of covering <i>MS Estonia</i> .
CAMERA 04	70 m	59.38449°N, 21.68041°E	Bedrock visible with some small loose stones. Site is located 260 m northwest of <i>MS Estonia</i> .
CAMERA 05-1 CAMERA 05-2 CAMERA 05-3	65 m 66 m 66 m	59.38330°N, 21.68227°E 59.38334°N, 21.68214°E 59.38338°N, 21.68216°E	These three sites comprise together a camera transect beginning ~130 and ending ~137 m north of <i>MS Estonia</i> . The position of CAMERA 05–1 and 05–3 are associated with clearly visible up-sticking features in the multibeam bathymetry, while CAMERA 05–2 is located on an apparently flat seafloor. Boulders and cobbles are visible along this transect.
CAMERA 06	66 m	59.38362°N, 21.68221°E	Site is located 165 m north of <i>MS Estonia</i> . The film shows a boulder.
CAMERA 07	69 m (top of object)	59.38307°N, 21.68324°E	Metal frame located north-northeast of <i>MS Estonia</i> , ~120 m from the hull. Appears like cables are attached on the frame. Corrosion visible. The frame is of the same, or similar, type as identified at CAMERA 03.
CAMERA 08	69 m	59.38282°N, 21.68190°E	Metal frame of the same, or similar, type as at CAMERA 03 and 07. Corrosion is visible also on this frame located ~73 m north of <i>MS Estonia</i> 's hull.
CAMERA 09-1 CAMERA 09-2	74 m 75 m	59.38173°N, 21.67958°E 59.38169°N, 21.67999°E	Transect beginning ~72 m southwest of <i>MS Estonia</i> and continuing ~22 m towards the east. This transect is located across slide features visible in the multibeam bathymetry. Poor visibility. A straight elongated object is seen. It has not been possible to identify the kind of object.
CAMERA 10	82 m	59.38207°N, 21.68288°E	Located on the northeastern side of <i>MS Estonia</i> , ~9 m from the hull. This location is associated with a small up sticking feature seen in the multibeam bathymetry. The object is a metal frame.
CAMERA 11	92 m 91 m	59.37957°N, 21.68167°E 59.37929°N, 21.68199°E	Transect across the force penetration strings, beginning ~248 m and continuing towards southeast for ~37 m. Potentially a sharp block seen, but video is very dark and the seafloor is for the most part not possible to distinguish.

and alternating in colour between dark greenish grey and olive. The last core, PC03 was recovered approximately 15m north of MS *Estonia* midship for the purpose of probing the sediment depth and type. The core retrieved 234cm of sediments before reaching a hard substrate, which damaged the core cutter (Photo. SBI1). The upmost 56cm of this core is comprised of dusky red well sorted sand, which most likely was dumped at the site during the covering work. The composition is very similar to that in PC01, albeit slightly coarser. This is followed by a 10cm thick greyish brown clay unit, which in turn is followed by an additional 21cm of dusky red sand. The remaining 147cm of PC01 contains greyish brown, partly disturbed, clay with varying sand content. This lower unit may be a clayey till.

#### Measurement of sediment properties

The logging of bulk density and magnetic susceptibility for the three cores are shown in Figure SBI3 along with some comments on the results. In addition to logging, discrete measurements of undrained shear strength were carried out on the split cores (Fig. SBI4), followed by analyses of samples for total organic carbon content through loss on ignition (Fig. SBI5) and grain size (Fig. SBI6). While the results of these measurements are not further discussed here, they add to the existing database of the sediment characteristics in the area of MS *Estonia*.

#### Grab samples

In total 13 grab samples were retrieved to quickly provide information on the surface sediment composition that can be used to support the geological interpretation of the multibeam backscatter data and side-scan imagery. The results are shown on the map in Figure SBI1.

#### Bottom inspection

The sites for bottom inspections with the GoPro mounted on the CTD carousel were decided based on the seafloor mapping. In some cases, an protruding feature identified in the multibeam bathymetry led to an inspection, while in other cases a closer look at the seafloor in a specific area of interest was the reason behind lowering the camera. Examples of the latter are where the slides occurred and across the forced penetration strings. Table SBI2 summarizes our interpretations of the acquired film from each site, Figure SBI1 shows their locations on a map, and Figures SBI7–11 contain snapshots from each site. Snapshots never do justice to the original films which always are clearer and reveal more details.



ROV observations were made July 14–15, 2021, by the commercial diving company Tuukritööde OÜ and are reported separately (Tuukritööde OÜ, 2021). Snapshots of their acquired ROV films are included here as they provide information on the seafloor geology, in particular where bedrock is exposed along the hull of MS *Estonia*. The ROV did not carry an underwater navigational system. Geo-locations of the snapshots from the ROV films can therefore only be inferred roughly by identifying sections of the shipwreck.

Photo SBI1. The damaged core cutter after retrieved PC03.

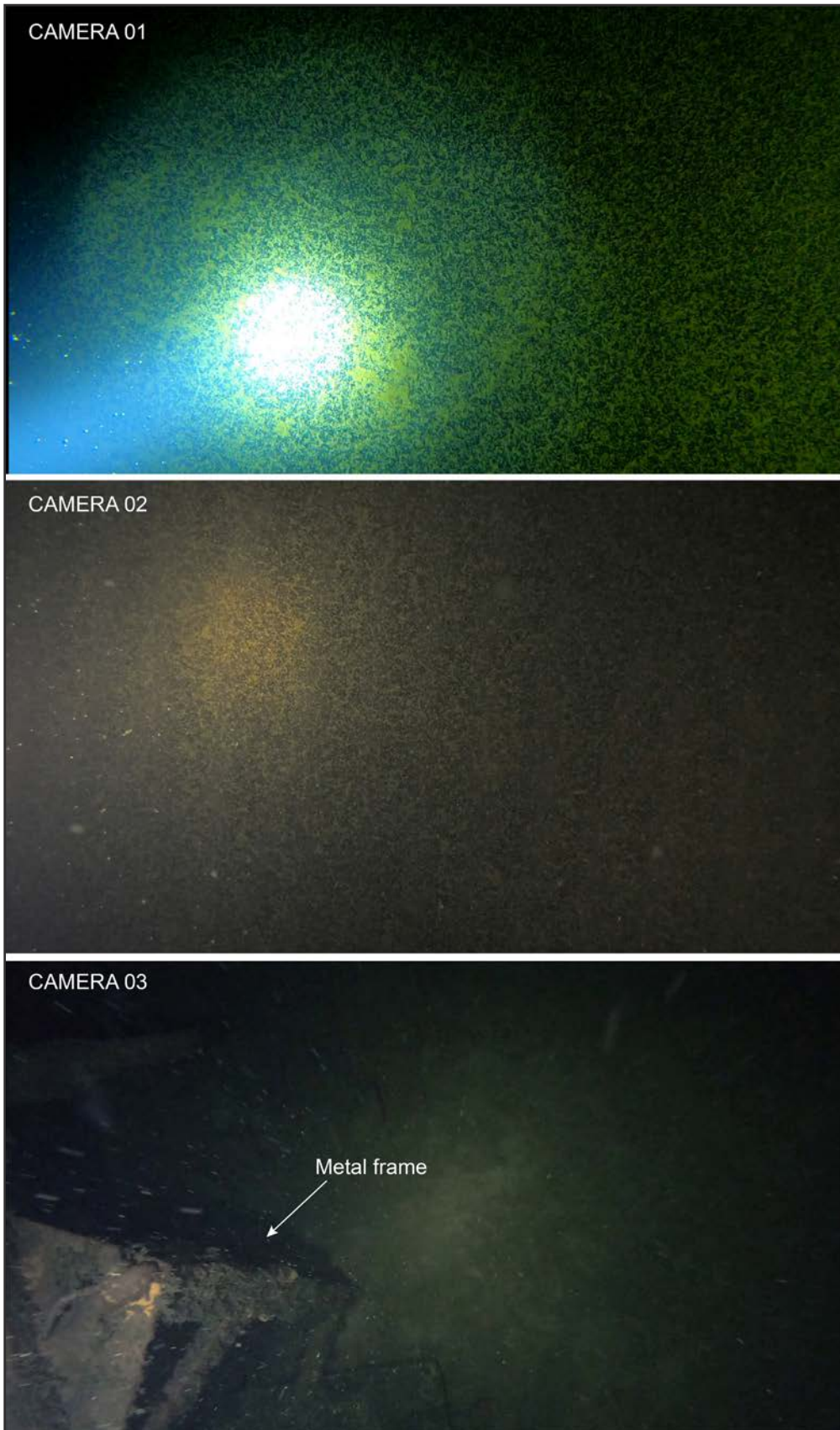


Figure SBI7. Snapshots from sites CAMERA 01, 02 and 03.

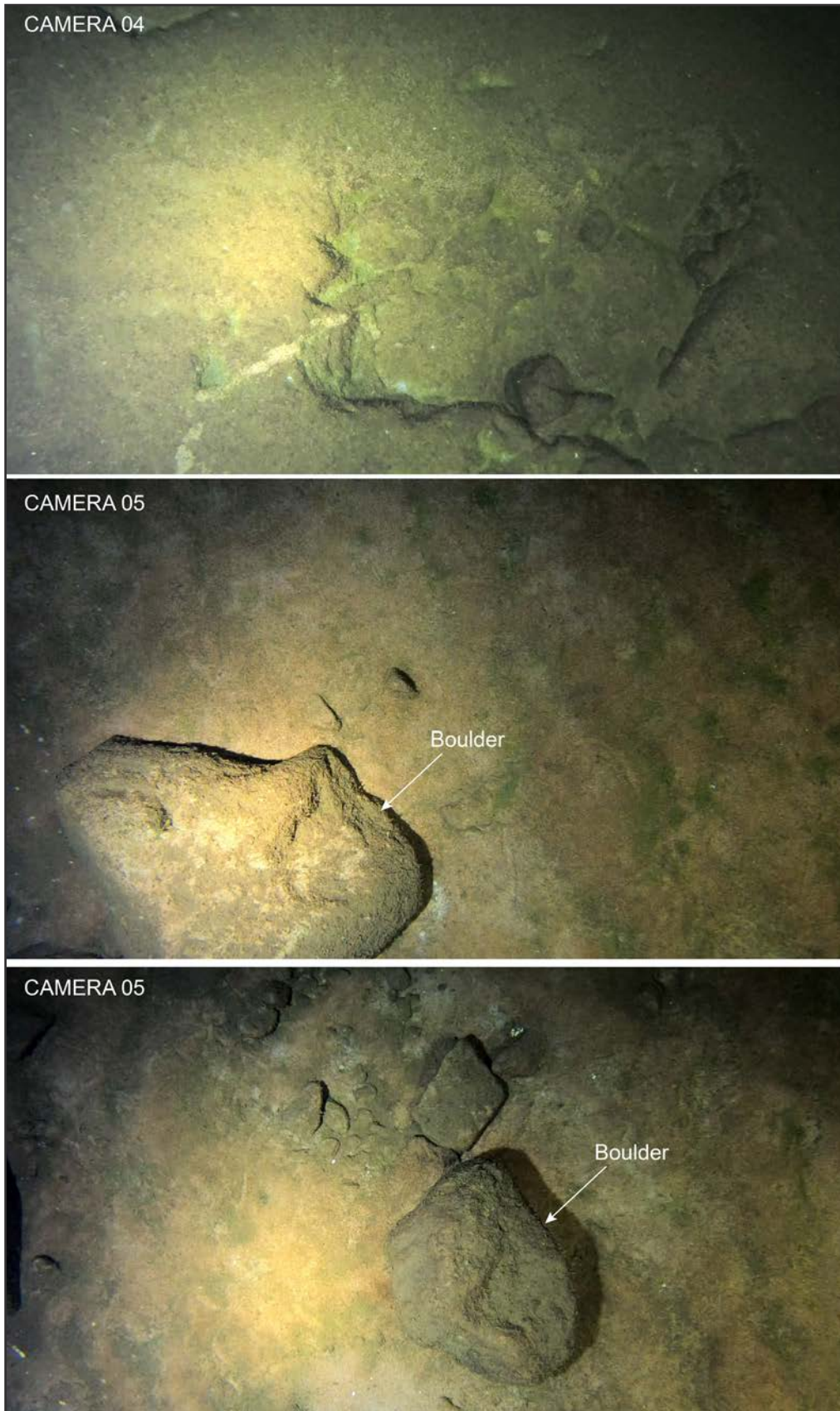


Figure SB18. Snapshots from sites CAMERA 04 and 05.



Figure SBI9. Snapshots from sites CAMERA 06 and 07.

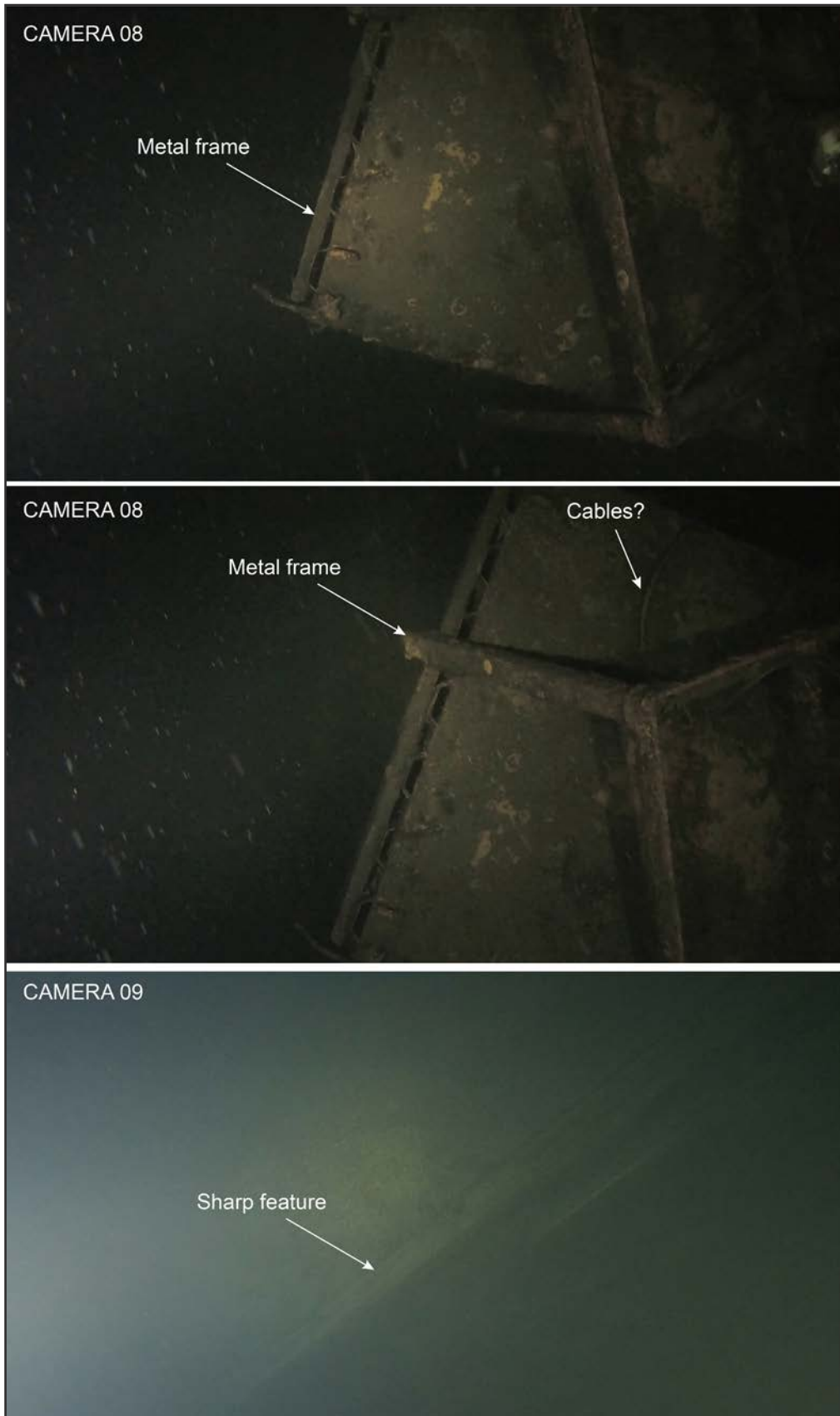


Figure SBI10. Snapshots from sites CAMERA 08 and 09.

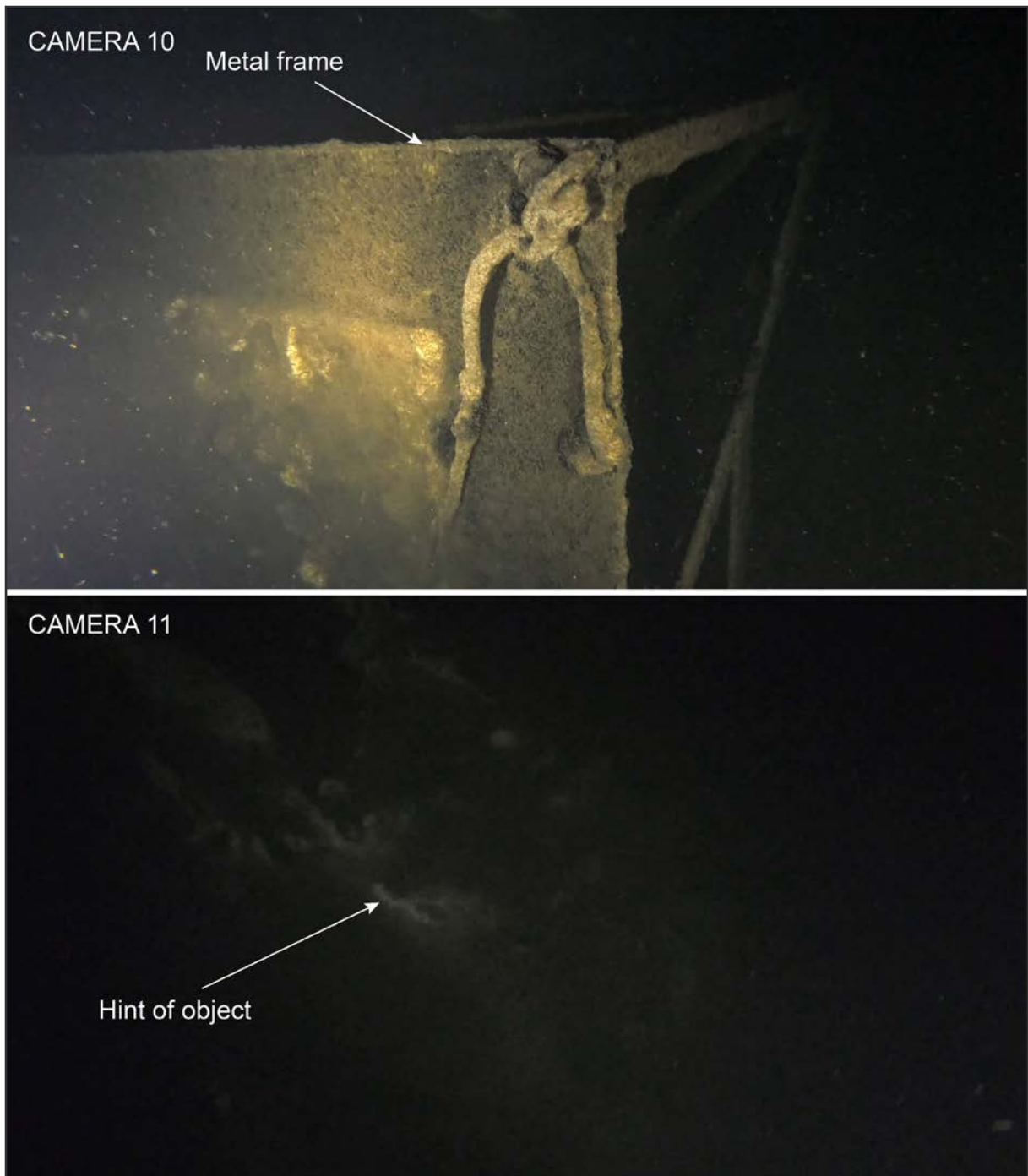


Figure SBI11. Snapshots from sites CAMERA 10 and 11.

The report by Tuukritööde OÜ (2021) includes notes of visible bedrock along the starboard side of the hull in contact with the seabed:

Dive one, page 5: “1.05.08: The movement went along the seabed, and a rupture and a crushed spot opposite a pink corner of granite was observed, that had initiated the entire survey.”

Second Dive, page 6: “16.27 The ROV moves towards the stern and at 18.00 reaches the second major damage above the granite rock.”

The notes above refer to two main areas of damage observed in the hull of MS *Estonia*, of which the one located closer to the bow was first filmed and shown in the Discovery+ documentary by Henrik Evertsson. This damage is situated approximately 89m from the shipwreck’s stern and bedrock is clearly visible in the ROV film next to it (Fig. SBI12). From the texture and parallel jointing, it appears from ocular inspection to be granite or perhaps syenite (Alasdair Skelton, Stockholm University, personal comment). The second damaged region is situated approximately 20m further towards the stern, where a large hole in the hull is seen (Fig. SBI13). The hull rests here on bedrock, which appears to be of the same composition as by the other damaged area. Furthermore, bedrock is observed between the two major damaged regions in MS *Estonia*’s hull. Where bedrock lies close to the hull it seems to have caused denting (Fig. SBI14a). Finally, the ROV films show that exposed bedrock extends a bit further than between the holes, although it is hard to infer exactly for how long as the ROV lacks a position system and there are no clear references visible (Fig. SBI14b).

The three metal frames identified to host acoustic transponders located north of MS *Estonia* are clearly visible in the multibeam bathymetry which permits measurement of their locations with respects to each other (Fig. SBI1). The frames are placed to the form a rectangular triangle with lengths of the two catheti of approximately 43m and 69m respectively. The fourth metal frame is not quite placed in a 90° angle from the 69m long “baseline” formed by the two most distal frames from the hull (Fig. SBI15). The offset is however only a few degrees. It is tenable to suggest that the fourth metal frame at CAMERA 10 located 112m from CAMERA 07 is of the same type as the other three, i.e. also hosting a transponder. From our films it is however not possible to determine as we can only see a small part of it. The discussed objects are also visible in the side-scan and backscatter imagery (Figs. SBI16–18).

### Moored ADCP

An upward-looking 400kHz ADCP was deployed on the seafloor at a bottom depth of 82m at 53°23.015’N /21°41.272’E on July 9 and was recovered on July 14. The time series covers about five days and a depth range from 80 to about 15m (Figs. SBI19 and 20). Down to about 70m depth the currents are highly variable in terms of both direction and speed (Fig. SBI19), with a large component of the variability coinciding with the inertial period (about 14 hours at these latitudes, Fig. SBI21). Such wind-driven near-inertial motions often provide an essential contribution to the spectra in the Baltic Proper (Holtermann et al., 2014). Close to the bottom, between 80 and 70m depth, there was a strong bottom current going back and forth in the south-east north-west direction (Fig. SBI20). The direction of this bottom current does not coincide with the local bathymetry which may be an indication of a problem with the compass calibration of the ADCP. If persistent, these strong bottom currents could have a significant impact on sediment transport in the vicinity of MS *Estonia* and could potentially also influence stability of the ship itself. More data (especially longer time series) and further analyses would be needed in order to draw any conclusions in these regards.

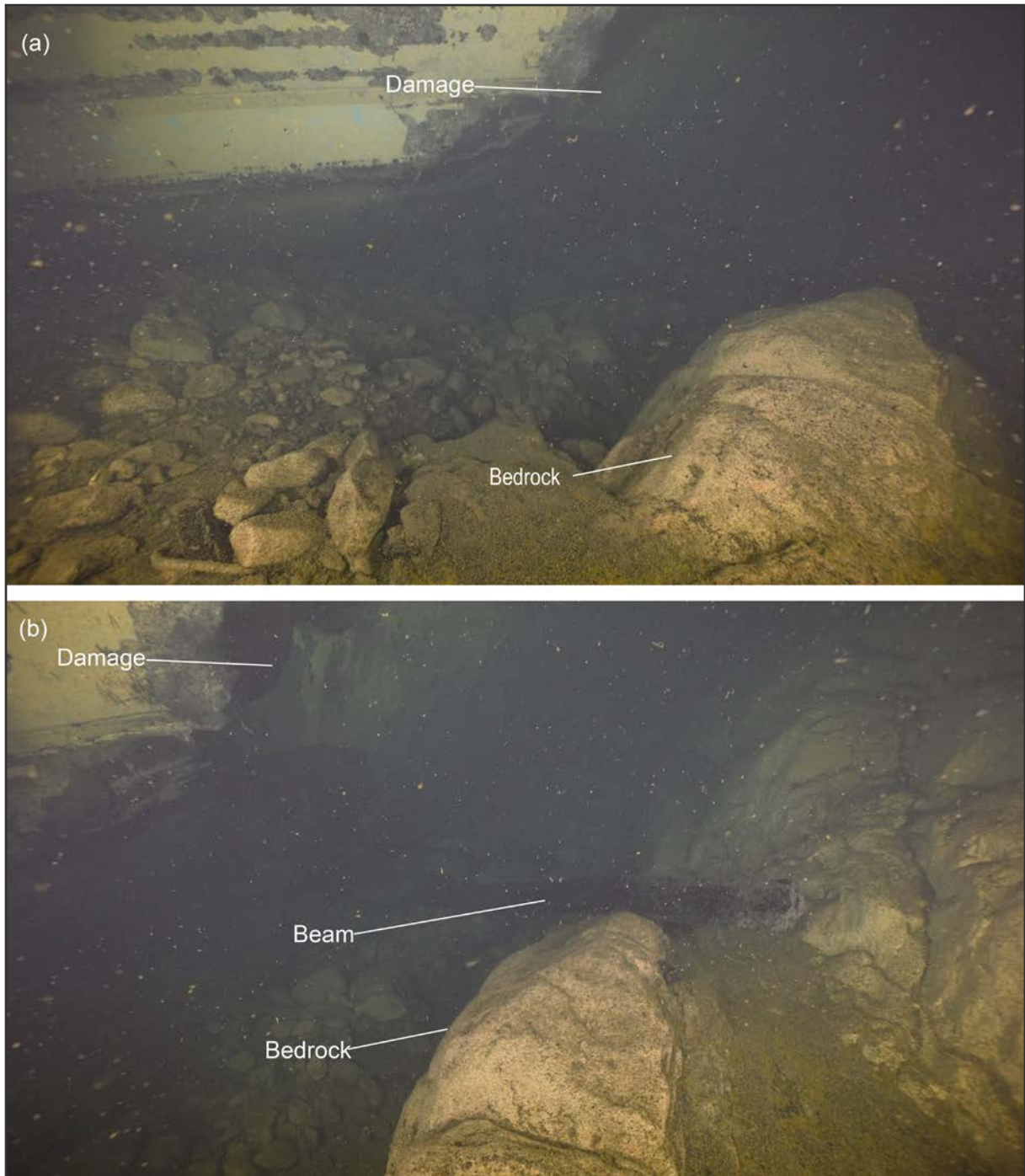


Figure SBI12. (a,b) Bedrock exposed next to the damage in hull of MS Estonia first observed in the Discovery+ documentary by Henrik Evertsson. (a) A beam has fallen out from the hole in the hull. Ocular inspection of the texture and parallel jointing of the bedrock suggest that it may be comprised of granite or syenite (Alasdair Skelton Personal communication).

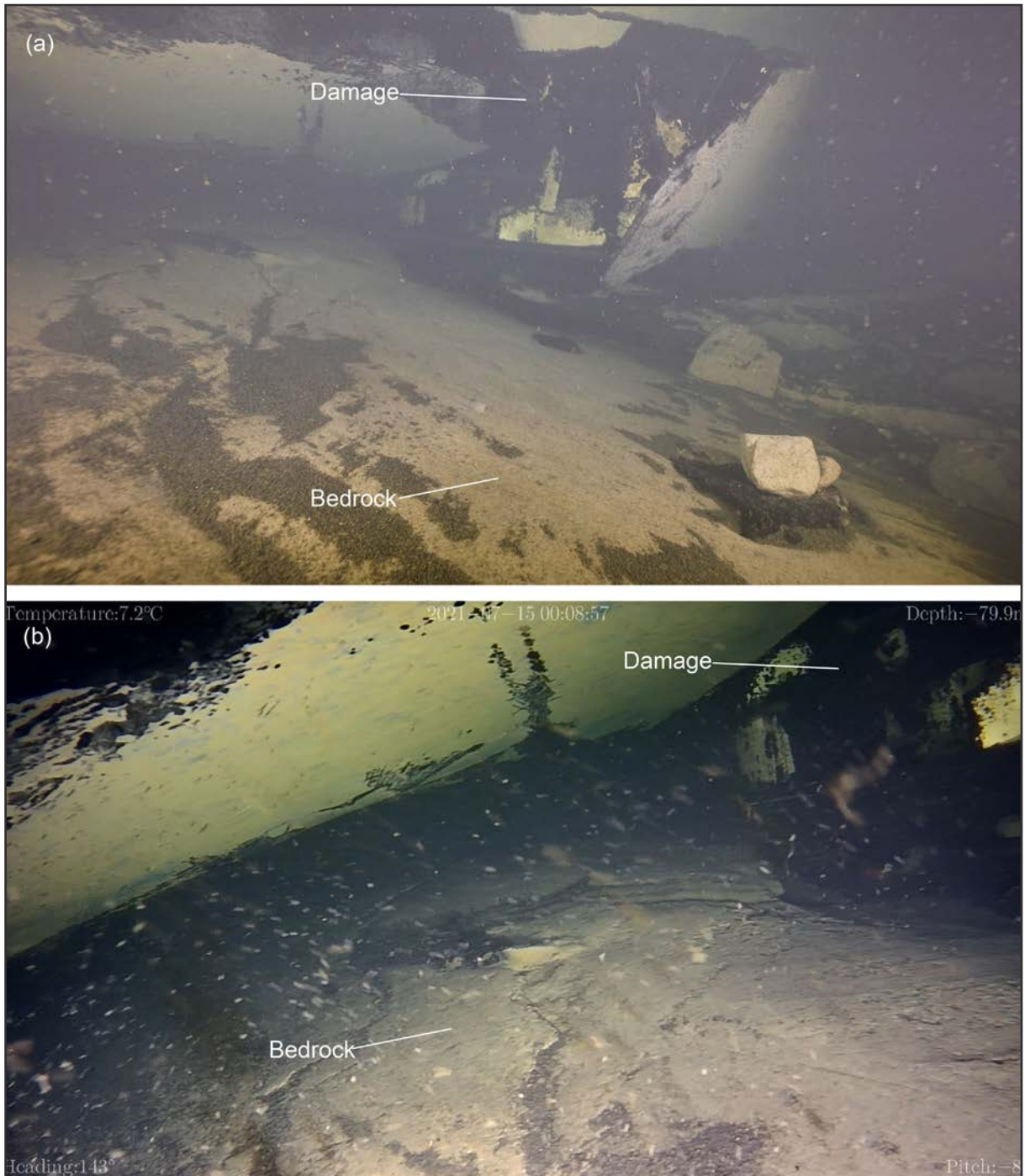


Figure SBI13. Bedrock underneath the hull of MS Estonia where another major damage is located approximately 20 m further towards the stern than first shown in Figure SBI12. (a) was filmed by Tuukritööde OÜ's using their Seaeye Falcon ROV while (b) was acquired with their smaller ROV.

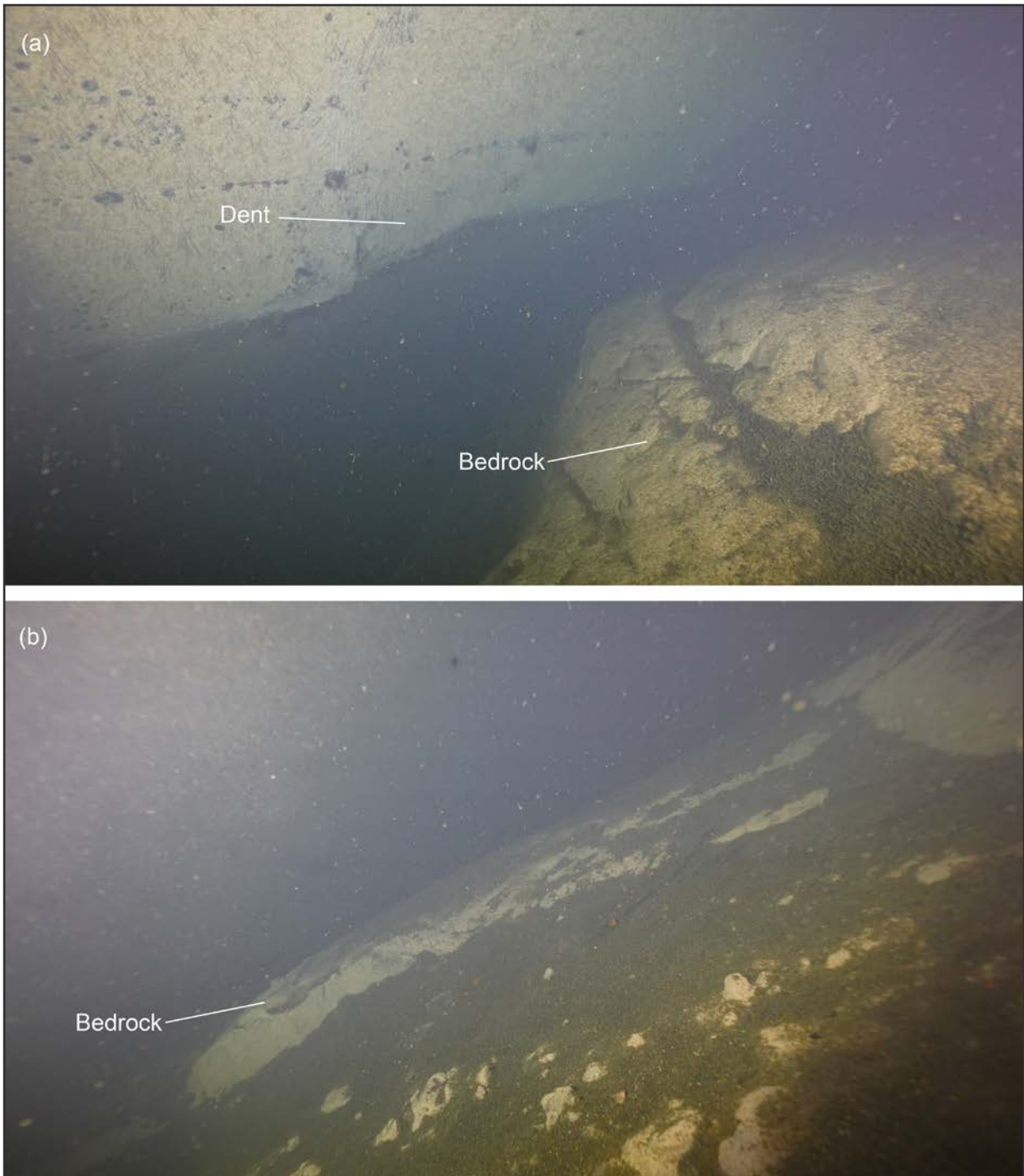


Figure SBI14. (a) Bedrock close to the hull of MS Estonia in between the two major holes shown in Figures SBI12 and 13. Denting of the hull can be seen. (b) Bedrock continuing towards the stern from the location of the rear hole.

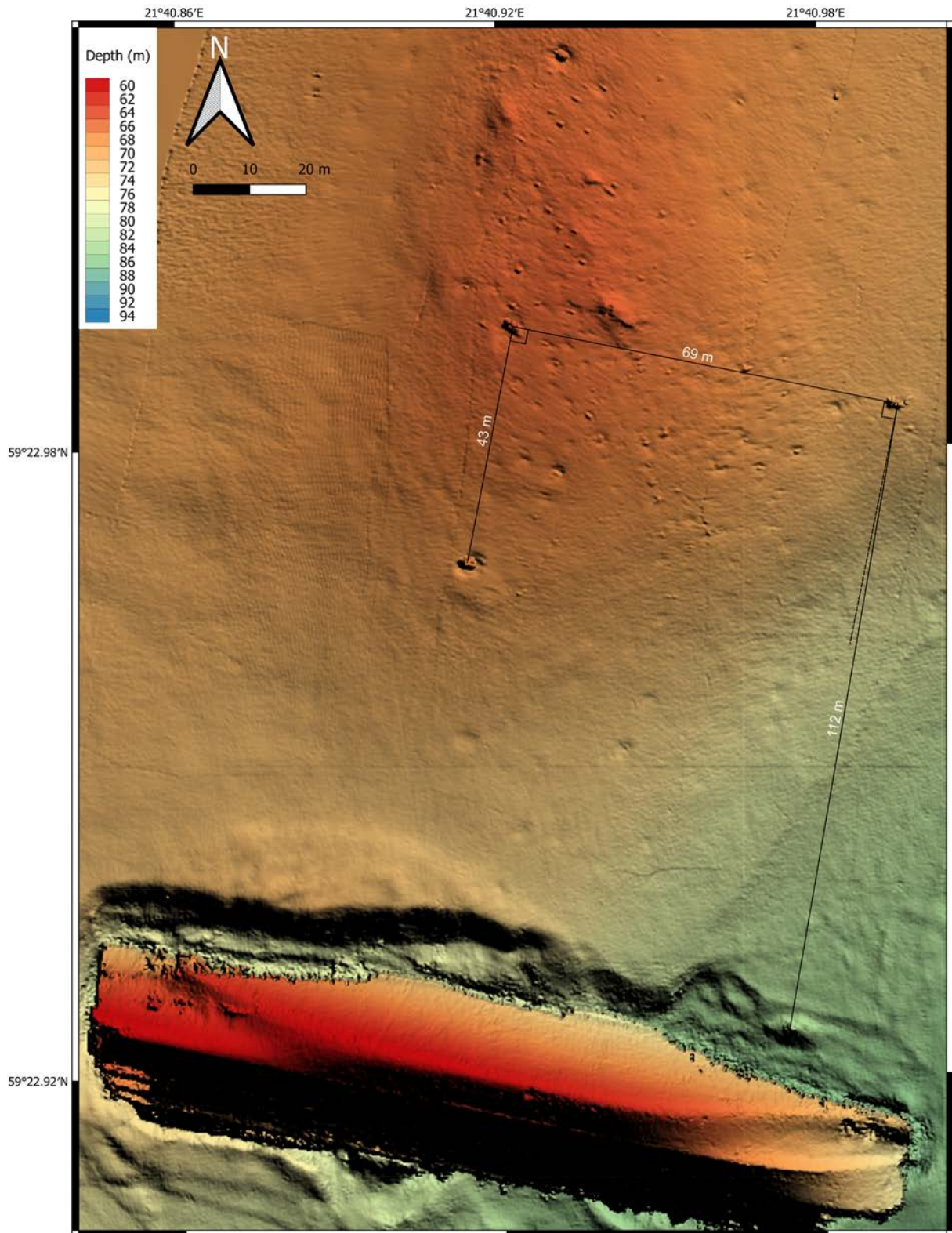


Figure SB115. Map showing the locations of identified metal frames.

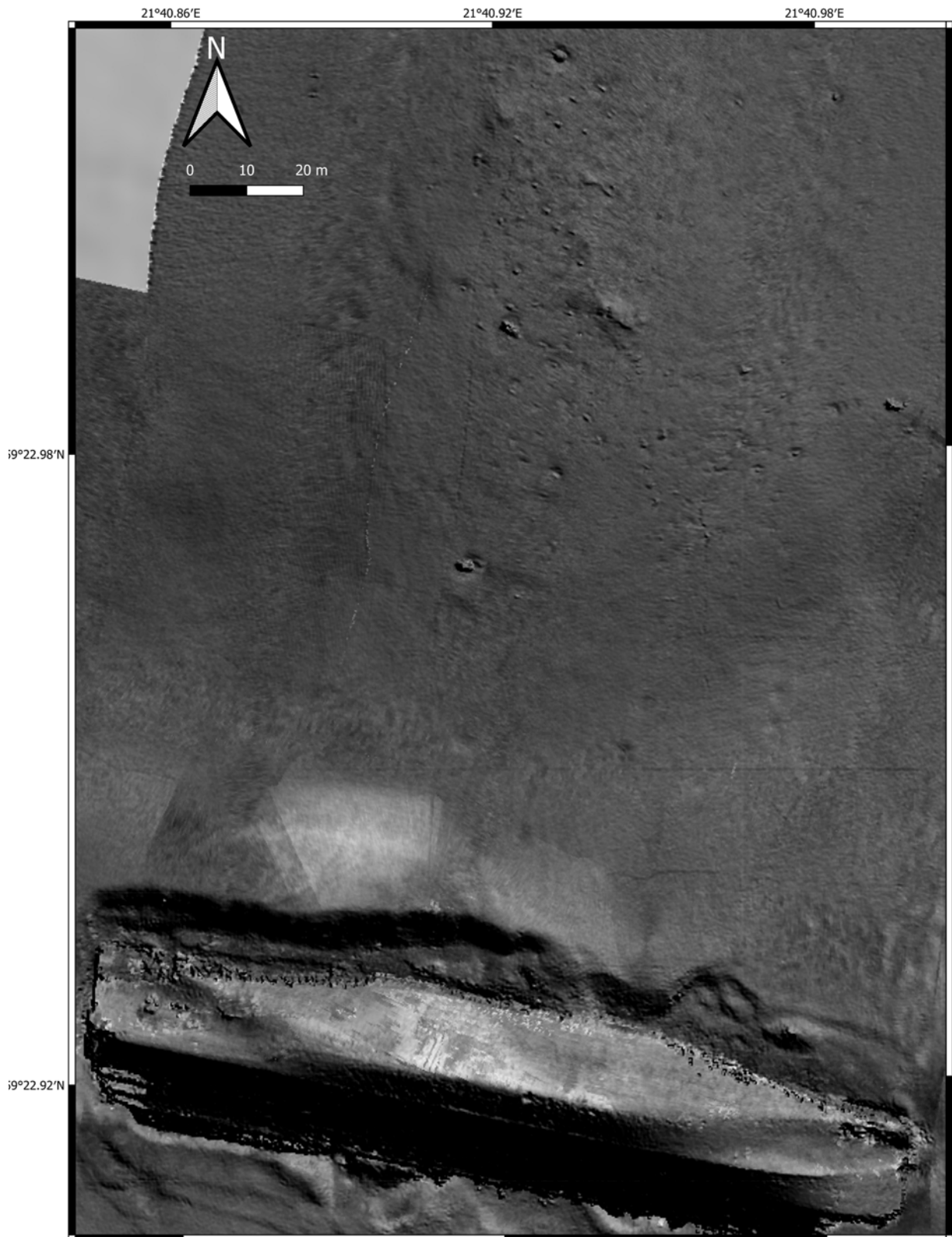


Figure SBI16. Same area shown as in Figure SBI16, but with backscatter imagery and shading from the multibeam bathymetry.

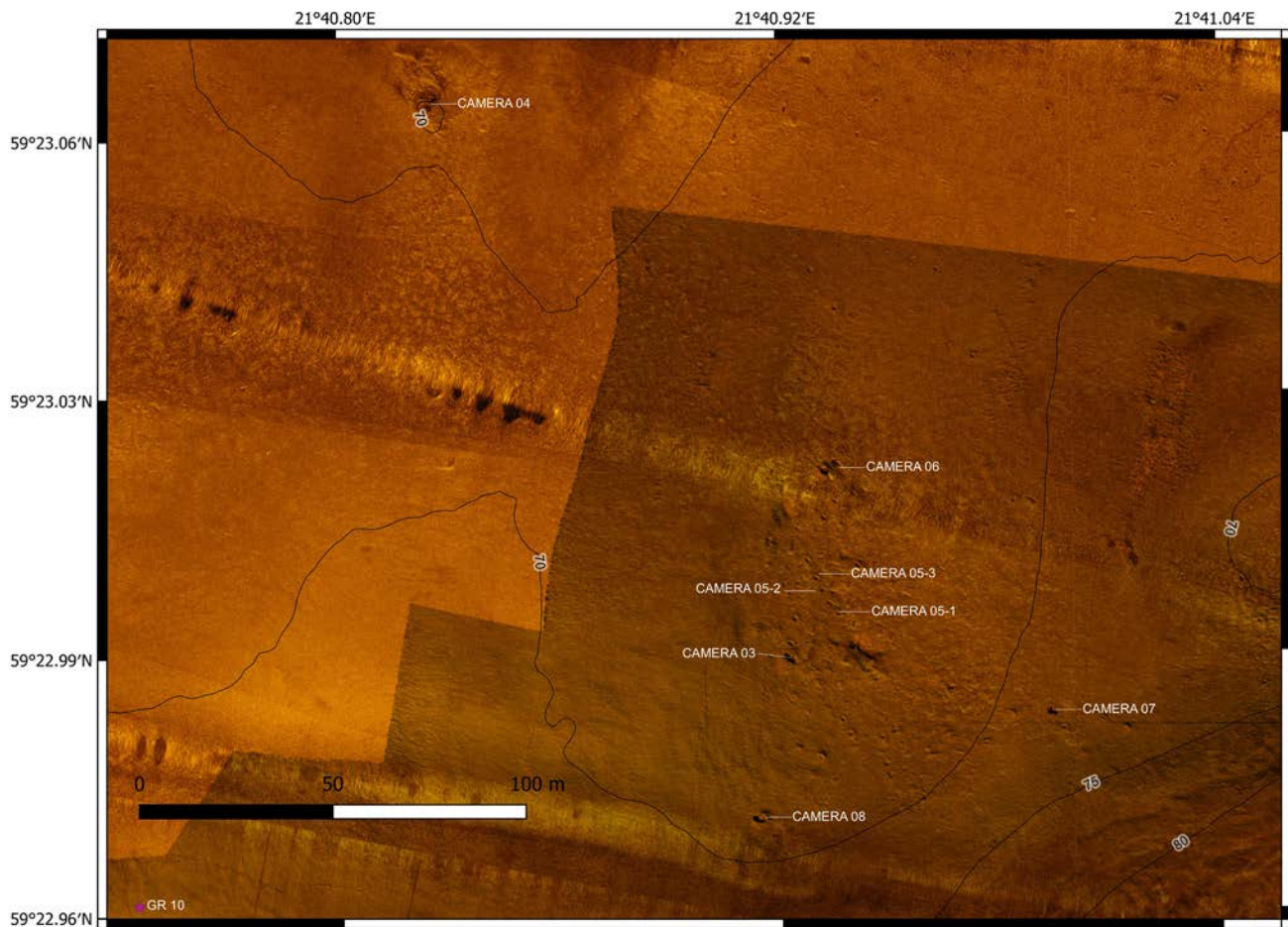


Figure SBI17. Side-scan mosaic of the area north of MS Estonia showing the locations of bottom observations with GoPro camera.



Figure SBI18. 3D-view of backscatter imagery draped on top the multibeam bathymetry in the area where the metal frames are located north of MS Estonia.

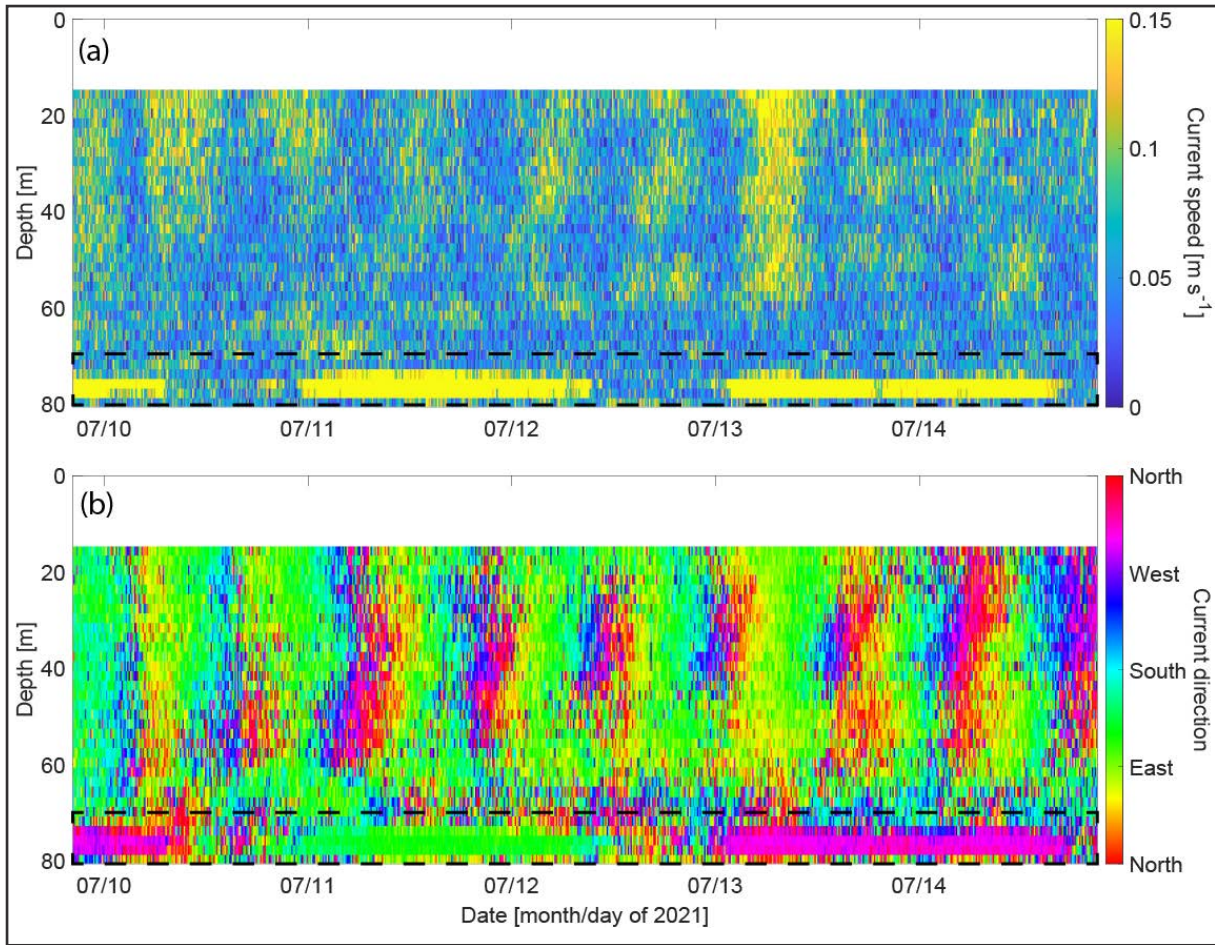


Figure SBI19. Current velocities at the mooring site. The current speed (a) and direction (b) are episodic with the dominant frequency coinciding with the inertial frequency (Fig. SBI21).

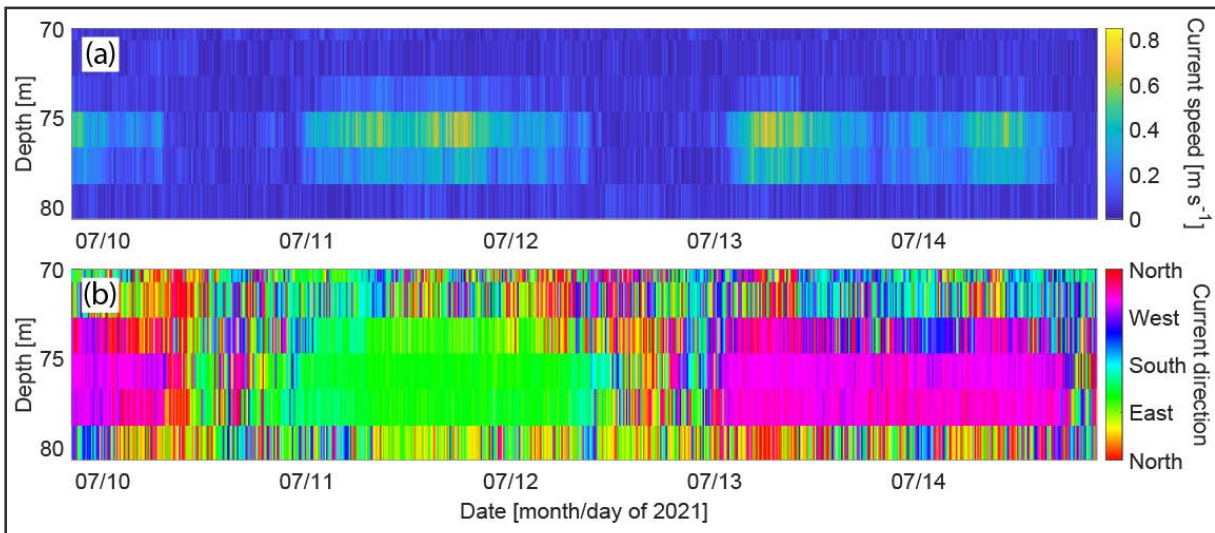


Figure SBI20. Same as Figure SB19 but zoomed into the 80 m to bottom depth interval. The current speed (a) and direction (b) are episodic. These bottom currents switch between north-west and south-east over the survey period with a speed sometimes approaching 1 m/s.

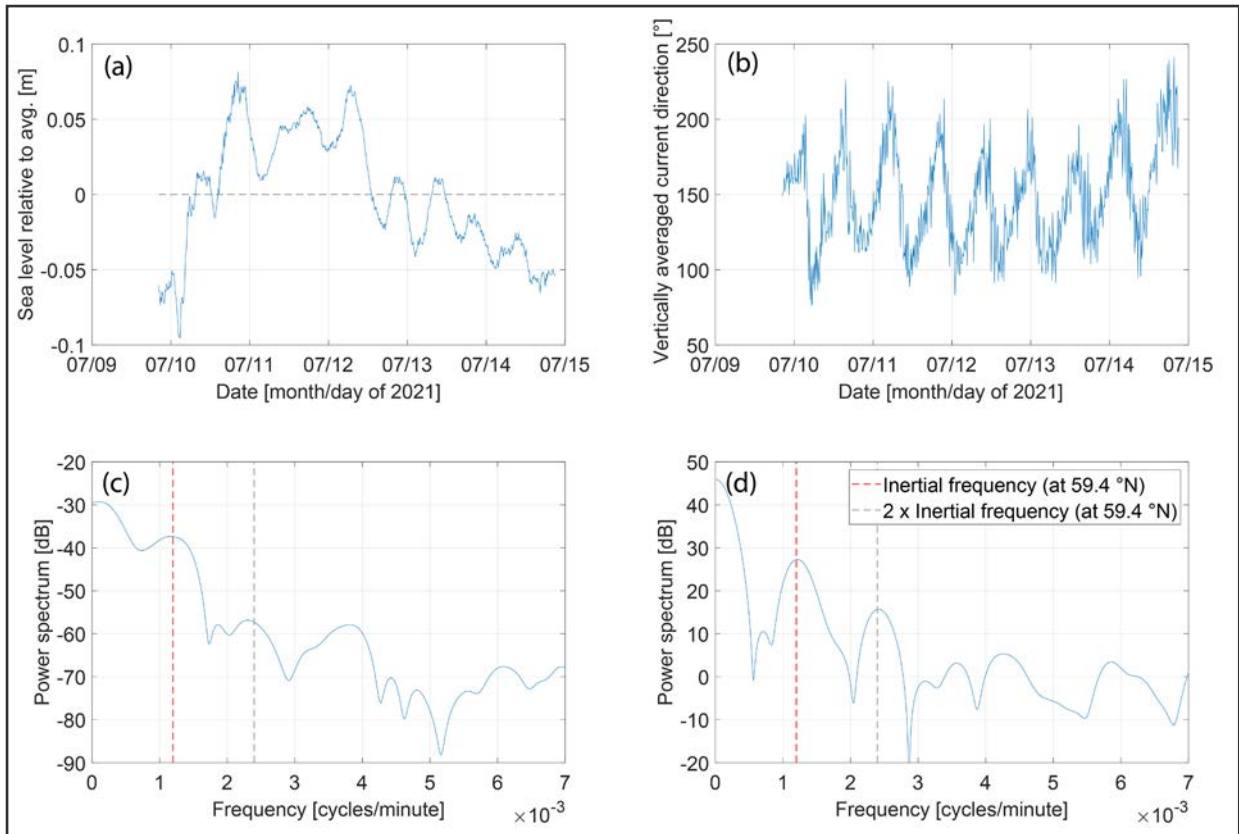


Figure SBI21. Time series and power spectrum of moored ADCP data. a) Sea level variations relative to the average, derived from the pressure sensor. b) Vertically averaged current direction. c) Power spectrum of the sea level time series (a). d) Power spectrum of the vertically averaged current direction (b). The variations in sea level and in current direction coincide to a large extent with the inertial frequency at this latitude (with a period of about 14 hours) and its first harmonic.

### Measurement of MS Estonia

Measurements of how MS *Estonia* is situated on the seafloor were made along depth profiles drawn across the hull in S-N and E-W directions (Fig. ME1). Depth values along these profiles were extracted from the detailed 0.25×0.25m grid to serve as the base for the measurements (Fig. ME2). The profiles were also used to analyse if any deformations of the hull could be detected. The measurements are facilitated by MS *Estonia* having a hull with a flat bottom and perpendicular straight sides, according to drawings (Fig. ME3). These assumptions served as a basis for the derived values in this report. The SN profiles were placed perpendicular to the fender line, which is clearly visible in the detailed multibeam bathymetry (Fig. ME2).

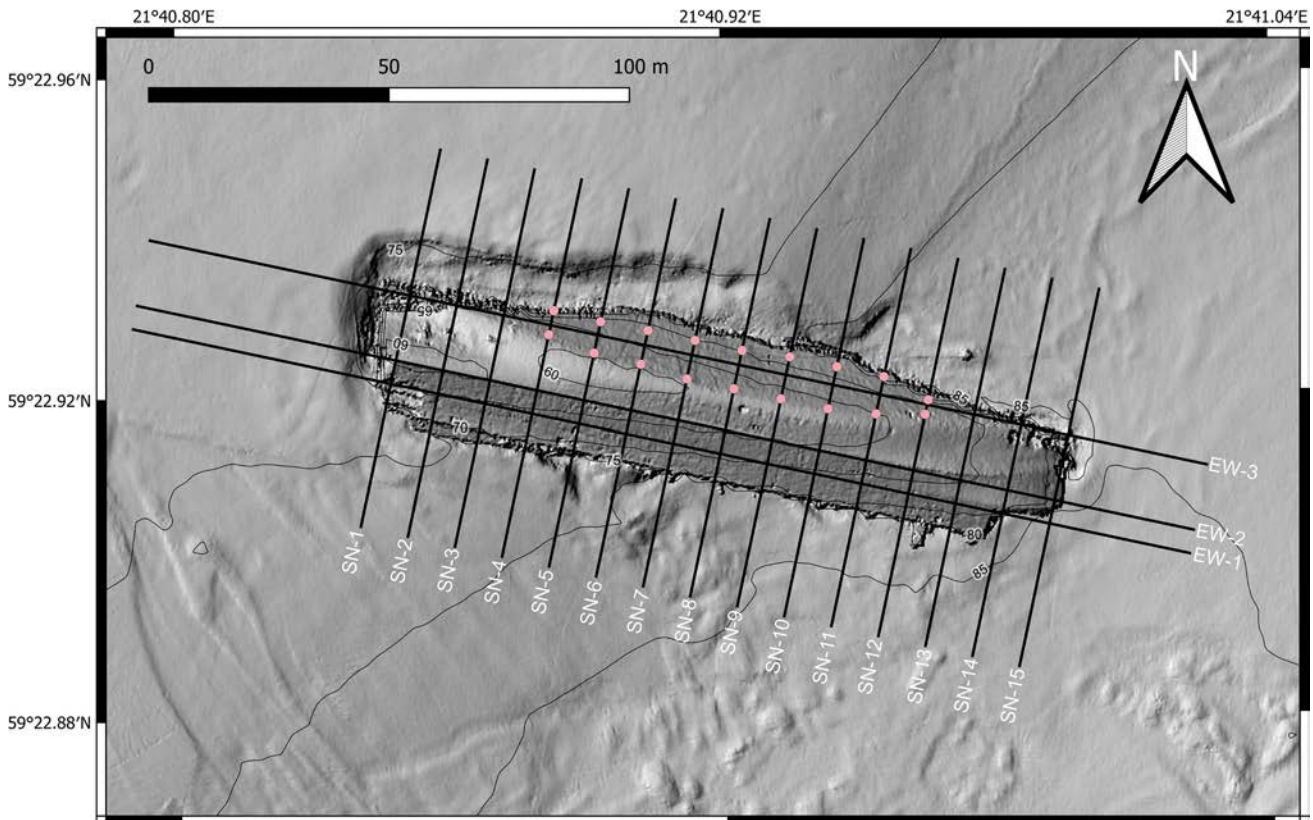


Figure ME1. Location of depth profiles reconstructed using the 0.25×0.25 m grid compiled from the detailed multibeam survey. The sections between the pink dots on profiles SN-4 to SN-12 were found to be located on the flat bottom of the shipwreck and therefore suitable to be used for calculation of the listing. The sections of profiles SN-4 to SN-12 capturing the flat port side were also used to estimate the shipwrecks' listing. Profiles EW-1 to EW-3 were used to calculate MS *Estonia*'s trim (along-ship inclination) relative to sea level.

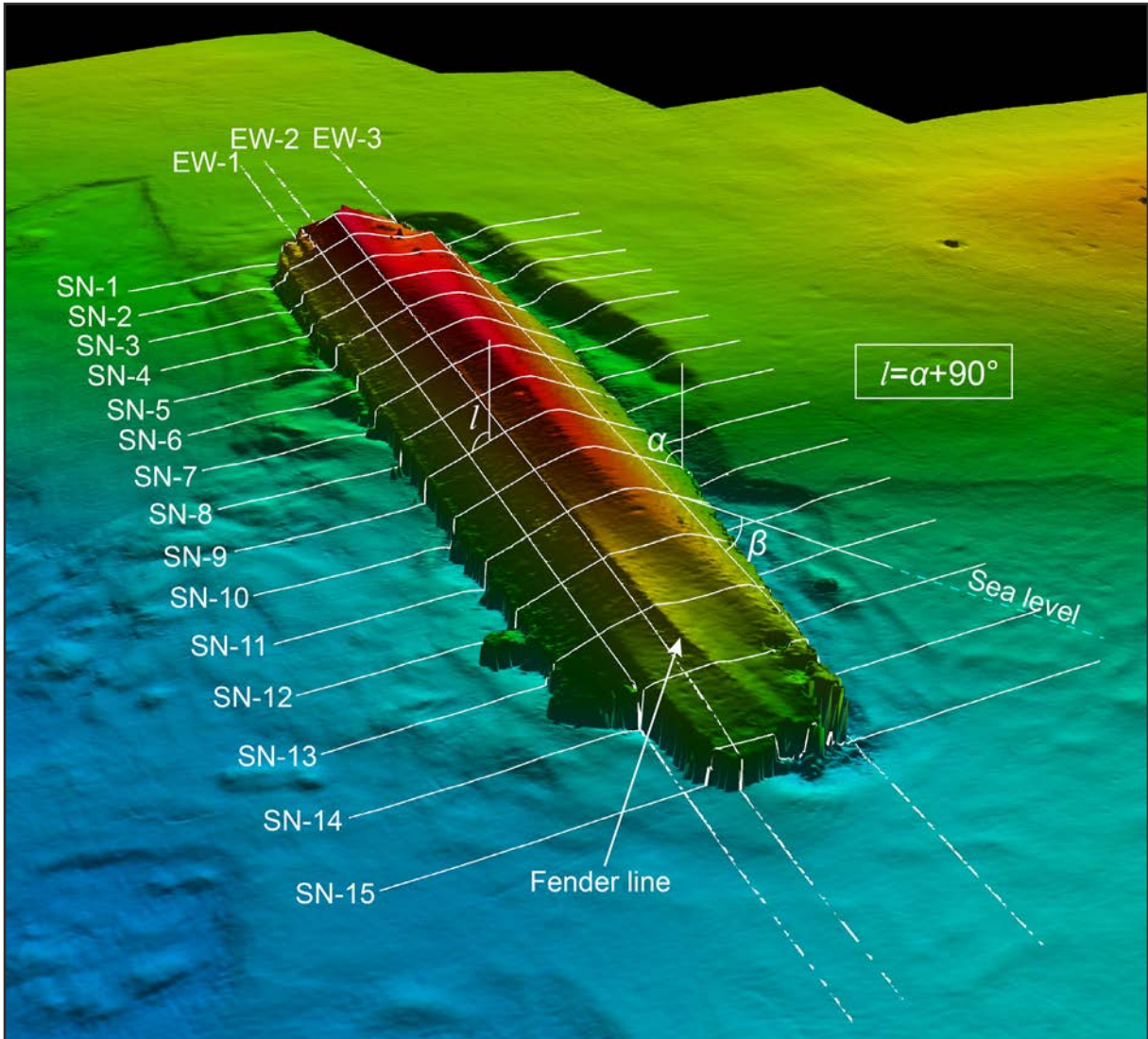


Figure ME2. 3D-view based on the 0.25×0.25 m multibeam grid showing the extracted profiles and how the listing of MS Estonia is calculated as  $\alpha+90^\circ$  and the trim  $\beta$  of the shipwreck along its length relative to sea level. Listing was also estimated based on the flat port side of the shipwreck.

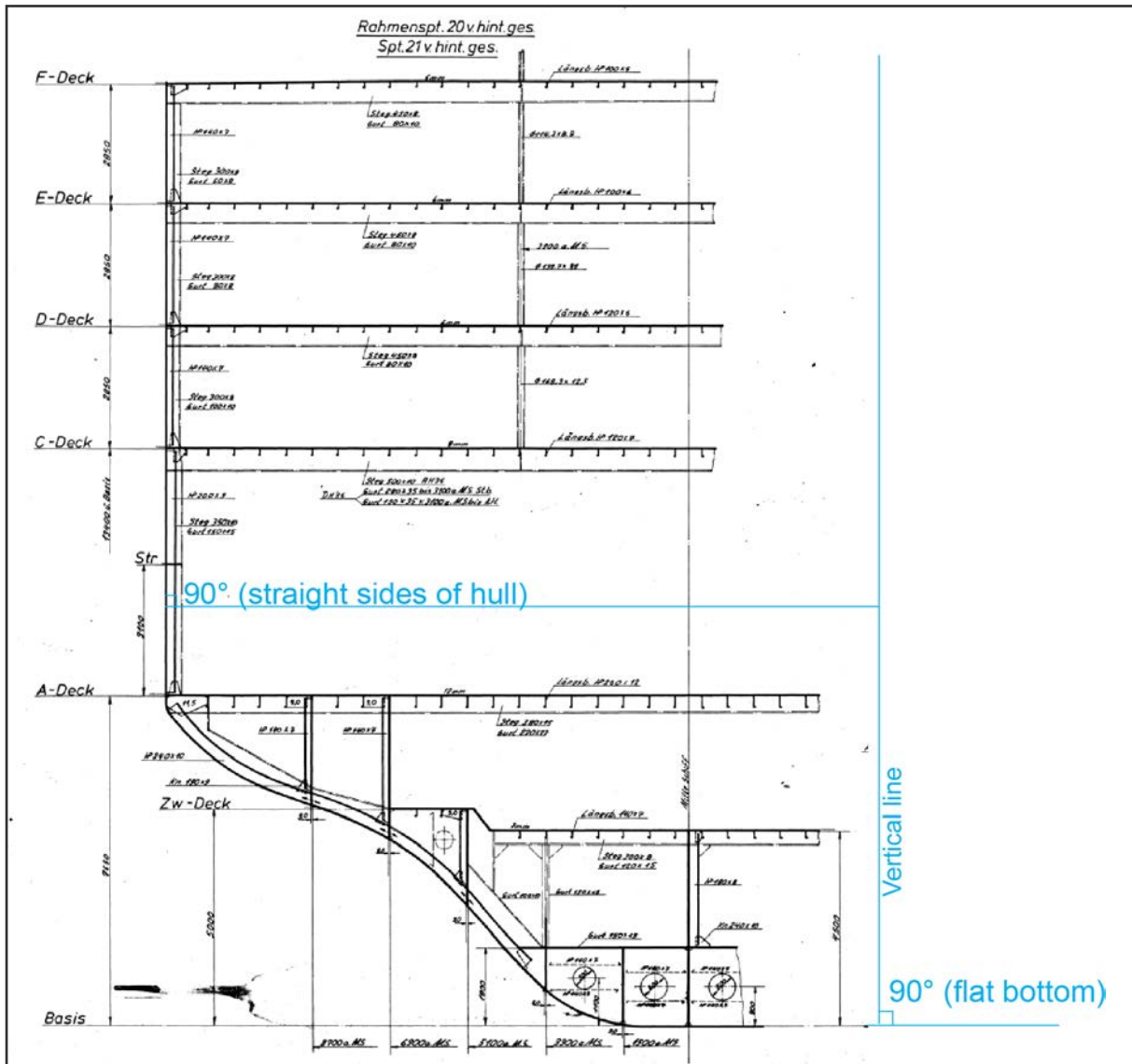


Figure ME3. Part of drawing of MS Estonia by Jos. L. Meyer Papenburg (Ems). The original drawings are from 1980-06-13. The blue lines are inferred to show that the bottom of the ship is flat and the sides are vertical and thus perpendicular to the bottom. This assumption has served as a basis for the measurements in this report of MS Estonia's present listing and whether any hull deformations can be found based on the multibeam bathymetric survey.

**Measured listing based on the flat bottom**

Profiles SN-4 to SN-12 capturing the flat part of the hull's bottom and are therefore suitable for measuring listing (Figs. ME4 and ME5). The flat bottom sections from each of these profiles were identified and marked with dots in Figure M1. A linear regression of all depth values along each flat section was made and the slope  $sr$  of this regression was used to estimate MS Estonia's listing  $l$ , which is equal to the angle  $\alpha$  between the regression line and a vertical line (see Figs. M3 and M4) plus  $90^\circ$  as the ship has tipped over more than  $90^\circ$ :

$$\alpha = \tan^{-1}\left(\frac{1}{sr}\right) \qquad \text{Equation ME1.}$$

$$l = \alpha + 90 \qquad \text{Equation ME2.}$$

Table ME1 presents the calculated listing for each profile and Table ME2 includes the statistics of the regressions of each extracted section. The averaged (n=9) listing is  $133.7^\circ \pm 0.4^\circ$  (as the slope of the regression lines are negative, the calculated listings are negative, but here reported as positive). There is not an apparent systematic difference between the measured listings along the profiles, i.e. the hull does not seem to be twisted based on the measurements of the flat bottom.

#### Measured listing based on the port side

Listing can also be measured from the inclination of the sides of the vessel using the same profiles SN4 to SN-12. This implies that  $l$  is acquired using the slope of the multibeam bathymetry capturing the ship's sides (Fig. ME2) using:

$$l = \tan^{-1}(s_r) + 90 \quad \text{Equation ME3.}$$

The averaged listing based on the flat port side of MS *Estonia* is estimated to  $132.6^\circ \pm 0.4^\circ$ , i.e. approximately one degree less than when measured on the bottom (Table ME1). Furthermore, the estimated listing values based on the flat port side shows a small trend with lower values towards the bow of the shipwreck, while the flat bottom measurements are more constant (Fig. ME5). This may indicate that the side of the shipwreck has become slightly deformed during its impact with the seafloor, or over time. Since the uncertainty of the multibeam is of random character, the observed trends in estimated listing appear to be real, despite being very small.

#### Measured trim

The trim  $\beta$  of MS *Estonia*'s hull on the seafloor is here defined as the angle between the EW profiles and sea level (Fig. ME2). The trim was also calculated using the slope of derived regressions, here for each EW profile between the flat sections of SN-4 and SN-12 (Fig. ME7). The following equation was used:

$$\beta = 90 + \tan^{-1}\left(\frac{1}{s_r}\right) \quad \text{Equation ME4.}$$

The calculated trim are shown in Table ME1 and the average is  $4.5^\circ \pm 0.3$ . We do not find an apparent along-ship deformation through the regression analyses.

Table ME1: Calculated listing of MS *Estonia* based on profiles SN-4 to SN-12 shown in Figures ME4 and ME5 and trim of the hull relative to sea level based on profiles EW-1 to EW-3 shown in Figure ME7. All values are derived through linear regressions (see text). The average listing of all analysed profiles of the flat bottom is  $\sim 133.7^\circ \pm 0.4$ , for the port side  $\sim 132.6^\circ \pm 0.4$  and the average trim relative to sea level is  $\sim 4.5^\circ \pm 0.3$ .

NS Profiles	Listing (°) (based on bottom)	Listing (°) (based on port side)	EW Profiles	Trim (°)
SN-4	133.9	132.9	EW-1	4.3
SN-5	133.9	132.5	EW-2	4.8
SN-6	133.5	133.1	EW-3	4.3
SN-7	134.0	132.6		$\sim 4.5^\circ \pm 0.3$
SN-8	134.0	132.9		
SN-9	132.9	132.5		
SN-10	133.7	132.7		
SN-11	133.7	132.2		
SN-12	133.9	132.0		
	$\sim 133.7^\circ \pm 0.4$	$\sim 132.6^\circ \pm 0.4$		

Table ME2. Statistics of the linear regressions of sections of profiles from the flat bottom of MS Estonia shown in Figures ME4, ME5 and ME6.

<p>Linear Fit - SN-4 Equation <math>Y = -1.0384594 * X - 13.408731</math> Number of data points used = 20 Average X = 49.456869 Average Y = -64.767679 Residual sum of squares = 0.0203342 Regression sum of squares = 46.848097 Coefficient of determination, R-sq'd = 0.9995661 Correlation coefficient, R = 0.9997830 Residual mean square, sigma-hat-sq'd = 0.0011297 P-Value = Less than 0.0001 Standard error of intercept (A) = +/- 0.2523133 Standard error of slope (B) = +/- 0.0050994</p>	<p>Linear Fit - SN-5 Equation <math>Y = -1.0394226 * X - 14.076551</math> Number of data points used = 27 Average X = 48.562300 Average Y = -64.553302 Residual sum of squares = 0.0325383 Regression sum of squares = 115.60842 Coefficient of determination, R-sq'd = 0.9997186 Correlation coefficient, R = 0.9998593 Residual mean square, sigma-hat-sq'd = 0.0013015 P-Value = Less than 0.0001 Standard error of intercept (A) = +/- 0.1695074 Standard error of slope (B) = +/- 0.0034876</p>	<p>Linear Fit - SN-6 Equation <math>Y = -1.0533388 * X - 13.998944</math> Number of data points used = 27 Average X = 48.562300 Average Y = -65.151497 Residual sum of squares = 0.0581615 Regression sum of squares = 118.72477 Coefficient of determination, R-sq'd = 0.9995104 Correlation coefficient, R = 0.9997552 Residual mean square, sigma-hat-sq'd = 0.0023265 P-Value = Less than 0.0001 Standard error of intercept (A) = +/- 0.2266257 Standard error of slope (B) = +/- 0.0046628</p>
<p>Linear Fit - SN-7 Equation <math>Y = -1.0345762 * X - 15.685150</math> Number of data points used = 31 Average X = 48.051118 Average Y = -65.397695 Residual sum of squares = 0.0784940 Regression sum of squares = 173.40754 Coefficient of determination, R-sq'd = 0.9995475 Correlation coefficient, R = 0.9997737 Residual mean square, sigma-hat-sq'd = 0.0027067 P-Value = Less than 0.0001 Standard error of intercept (A) = +/- 0.1966266 Standard error of slope (B) = +/- 0.0040874</p>	<p>Linear Fit - SN-8 Equation <math>Y = -1.0353893 * X - 16.546756</math> Number of data points used = 31 Average X = 48.051118 Average Y = -66.298371 Residual sum of squares = 0.0608659 Regression sum of squares = 173.68021 Coefficient of determination, R-sq'd = 0.9996497 Correlation coefficient, R = 0.9998248 Residual mean square, sigma-hat-sq'd = 0.0020988 P-Value = Less than 0.0001 Standard error of intercept (A) = +/- 0.1731455 Standard error of slope (B) = +/- 0.0035993</p>	<p>Linear Fit - SN-9 Equation <math>Y = -1.0755599 * X - 15.296027</math> Number of data points used = 35 Average X = 48.562300 Average Y = -67.527692 Residual sum of squares = 0.2346259 Regression sum of squares = 269.79181 Coefficient of determination, R-sq'd = 0.9991311 Correlation coefficient, R = 0.9995655 Residual mean square, sigma-hat-sq'd = 0.0071099 P-Value = Less than 0.0001 Standard error of intercept (A) = +/- 0.2685117 Standard error of slope (B) = +/- 0.0055214</p>
<p>Linear Fit - SN-10 Equation <math>Y = -1.0446940 * X - 17.374200</math> Number of data points used = 35 Average X = 48.562300 Average Y = -68.106945 Residual sum of squares = 0.0674911 Regression sum of squares = 254.52927 Coefficient of determination, R-sq'd = 0.9997349 Correlation coefficient, R = 0.9998674 Residual mean square, sigma-hat-sq'd = 0.0020452 P-Value = Less than 0.0001 Standard error of intercept (A) = +/- 0.1440119 Standard error of slope (B) = +/- 0.0029613</p>	<p>Linear Fit - SN-11 Equation <math>Y = -1.0482579 * X - 17.986628</math> Number of data points used = 31 Average X = 49.073482 Average Y = -69.428295 Residual sum of squares = 0.0632319 Regression sum of squares = 178.02430 Coefficient of determination, R-sq'd = 0.9996449 Correlation coefficient, R = 0.9998224 Residual mean square, sigma-hat-sq'd = 0.0021804 P-Value = Less than 0.0001 Standard error of intercept (A) = +/- 0.1802251 Standard error of slope (B) = +/- 0.0036686</p>	<p>Linear Fit - SN-12 Equation <math>Y = -1.0379066 * X - 19.290451</math> Number of data points used = 12 Average X = 48.434505 Average Y = -69.560945 Residual sum of squares = 0.0065375 Regression sum of squares = 10.063381 Coefficient of determination, R-sq'd = 0.9993508 Correlation coefficient, R = 0.9996753 Residual mean square, sigma-hat-sq'd = 0.0006537 P-Value = Less than 0.0001 Standard error of intercept (A) = +/- 0.4052458 Standard error of slope (B) = +/- 0.0083655</p>

<p>Linear Fit - EW-1 (section between SN-04 and SN-12)  Equation <math>Y = -0.0790927 * X - 59.227097</math>  Number of data points used = 333  Average X = 122.52119  Average Y = -68.917624  Residual sum of squares = 3.5250899  Regression sum of squares = 1259.4220  Coefficient of determination, R-sq'd = 0.9972088  Correlation coefficient, R = 0.9986034  Residual mean square, sigma-hat-sq'd = 0.0106498  P-Value = Less than 0.0001  Standard error of intercept (A) = +/- 0.0287413  Standard error of slope (B) = +/- 0.0002300</p>	<p>Linear Fit - EW-2 (section between SN-4 and SN-12)  Equation <math>Y = -0.0833237 * X - 53.921184</math>  Number of data points used = 333  Average X = 122.52119  Average Y = -64.130109  Residual sum of squares = 7.1783122  Regression sum of squares = 1397.7724  Coefficient of determination, R-sq'd = 0.9948907  Correlation coefficient, R = 0.9974421  Residual mean square, sigma-hat-sq'd = 0.0216867  P-Value = Less than 0.0001  Standard error of intercept (A) = +/- 0.0410141  Standard error of slope (B) = +/- 0.0003282</p>	<p>Linear Fit - EW-3 (section between SN-4 and SN-12)  Equation <math>Y = -0.0753374 * X - 57.821785</math>  Number of data points used = 313  Average X = 125.07904  Average Y = -67.244914  Residual sum of squares = 6.1744052  Regression sum of squares = 948.89877  Coefficient of determination, R-sq'd = 0.9935351  Correlation coefficient, R = 0.9967623  Residual mean square, sigma-hat-sq'd = 0.0198534  P-Value = Less than 0.0001  Standard error of intercept (A) = +/- 0.0438321  Standard error of slope (B) = +/- 0.0003446</p>
---	--	--

Table ME3. Statistics of the linear regressions of parts of the profiles extracted from the port side of MS Estonia shown in Figures ME4 and ME5.

<p>Linear Fit - SN-4 (port side)  Equation <math>Y = 0.9286852 * X - 93.841599</math>  Number of data points used = 32  Average X = 30.031949  Average Y = -65.951372  Residual sum of squares = 0.3226939  Regression sum of squares = 153.69960  Coefficient of determination, R-sq'd = 0.9979049  Correlation coefficient, R = 0.9989519  Residual mean square, sigma-hat-sq'd = 0.0107565  P-Value = Less than 0.0001  Standard error of intercept (A) = +/- 0.2340384  Standard error of slope (B) = +/- 0.0077690</p>	<p>Linear Fit - SN-5 (port side)  Equation <math>Y = 0.9168464 * X - 94.486824</math>  Number of data points used = 28  Average X = 30.543131  Average Y = -66.483466  Residual sum of squares = 0.1480381  Regression sum of squares = 100.32819  Coefficient of determination, R-sq'd = 0.9985266  Correlation coefficient, R = 0.9992630  Residual mean square, sigma-hat-sq'd = 0.0056938  P-Value = Less than 0.0001  Standard error of intercept (A) = +/- 0.2114407  Standard error of slope (B) = +/- 0.0069069</p>	<p>Linear Fit - SN-6  Equation <math>Y = 0.9372905 * X - 95.816247</math>  Number of data points used = 28  Average X = 30.543131  Average Y = -67.188460  Residual sum of squares = 0.1283941  Regression sum of squares = 104.85238  Coefficient of determination, R-sq'd = 0.9987770  Correlation coefficient, R = 0.9993883  Residual mean square, sigma-hat-sq'd = 0.0049382  P-Value = Less than 0.0001  Standard error of intercept (A) = +/- 0.1969130  Standard error of slope (B) = +/- 0.0064324</p>
---	---	---

(Continues on the next page)

<p>Linear Fit - SN-7 (port side) Equation <math>Y = 0.9208601 * X - 95.994420</math> Number of data points used = 28 Average X = 30.543131 Average Y = -67.868470 Residual sum of squares = 0.0841199 Regression sum of squares = 101.20854 Coefficient of determination, R-sq'd = 0.9991695 Correlation coefficient, R = 0.9995847 Residual mean square, sigma-hat-sq'd = 0.0032354 P-Value = Less than 0.0001 Standard error of intercept (A) = +/- 0.1593864 Standard error of slope (B) = +/- 0.0052065</p>	<p>Linear Fit - SN-8 (port side) Equation <math>Y = 0.9298034 * X - 97.050287</math> Number of data points used = 28 Average X = 30.543131 Average Y = -68.651181 Residual sum of squares = 0.1435297 Regression sum of squares = 103.18393 Coefficient of determination, R-sq'd = 0.9986109 Correlation coefficient, R = 0.9993052 Residual mean square, sigma-hat-sq'd = 0.0055204 P-Value = Less than 0.0001 Standard error of intercept (A) = +/- 0.2081962 Standard error of slope (B) = +/- 0.0068009</p>	<p>Linear Fit - SN-9 (port side) Equation <math>Y = 0.9151911 * X - 97.528114</math> Number of data points used = 28 Average X = 30.543131 Average Y = -69.575311 Residual sum of squares = 0.0528969 Regression sum of squares = 99.966265 Coefficient of determination, R-sq'd = 0.9994711 Correlation coefficient, R = 0.9997355 Residual mean square, sigma-hat-sq'd = 0.0020345 P-Value = Less than 0.0001 Standard error of intercept (A) = +/- 0.1263912 Standard error of slope (B) = +/- 0.0041287</p>
<p>Linear Fit - SN-10 (port side) Equation <math>Y = 0.9231017 * X - 98.566266</math> Number of data points used = 28 Average X = 30.543131 Average Y = -70.371851 Residual sum of squares = 0.0225468 Regression sum of squares = 101.70187 Coefficient of determination, R-sq'd = 0.9997784 Correlation coefficient, R = 0.9998892 Residual mean square, sigma-hat-sq'd = 0.0008672 P-Value = Less than 0.0001 Standard error of intercept (A) = +/- 0.0825172 Standard error of slope (B) = +/- 0.0026955</p>	<p>Linear Fit - SN-11 (port side) Equation <math>Y = 0.9066594 * X - 98.887307</math> Number of data points used = 28 Average X = 30.543131 Average Y = -71.195090 Residual sum of squares = 0.1564133 Regression sum of squares = 98.111110 Coefficient of determination, R-sq'd = 0.9984083 Correlation coefficient, R = 0.9992038 Residual mean square, sigma-hat-sq'd = 0.0060159 P-Value = Less than 0.0001 Standard error of intercept (A) = +/- 0.2173395 Standard error of slope (B) = +/- 0.0070996</p>	<p>Linear Fit - SN-12 (port side) Equation <math>Y = 0.8989032 * X - 99.439699</math> Number of data points used = 28 Average X = 30.543131 Average Y = -71.984382 Residual sum of squares = 0.1083557 Regression sum of squares = 96.439661 Coefficient of determination, R-sq'd = 0.9988777 Correlation coefficient, R = 0.9994387 Residual mean square, sigma-hat-sq'd = 0.0041675 P-Value = Less than 0.0001 Standard error of intercept (A) = +/- 0.1808955 Standard error of slope (B) = +/- 0.0059091</p>

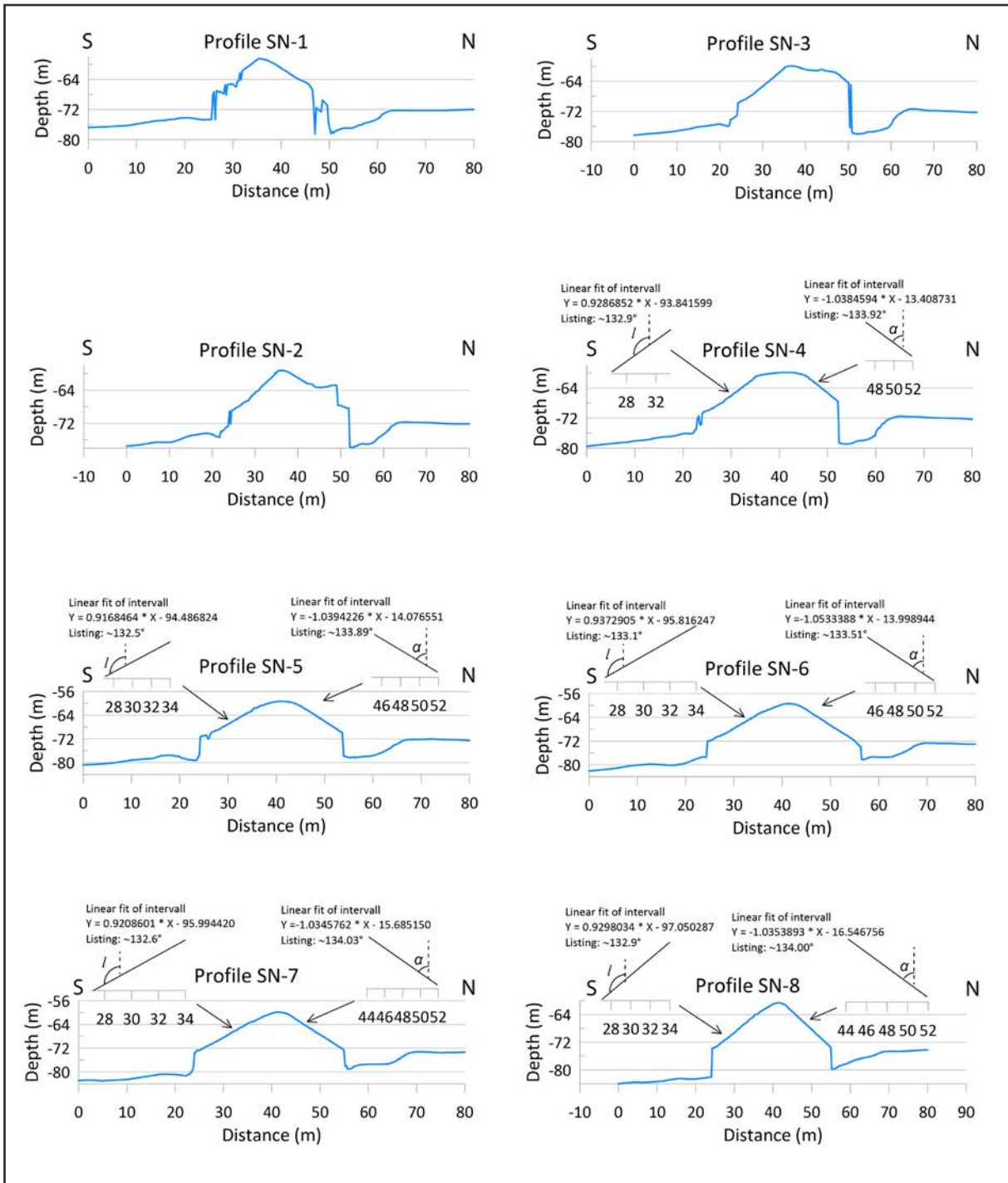


Figure ME4. Depth profiles SN-1 to SN-8 across the hull of MS Estonia from south to north. The depths values along these profiles were extracted from the 0.25x0.25 m grid based on the detailed multibeam survey. The locations of the profiles are shown in Figures ME1 and ME2. Regression lines derived over flat sections of the bottom were used to calculate the present listing  $l$  (see text for explanation of the approach), defined as the shown angle  $\alpha$  plus  $90^\circ$ . In addition, listing was calculated based on the flat port side assumed to be perpendicular to the bottom.

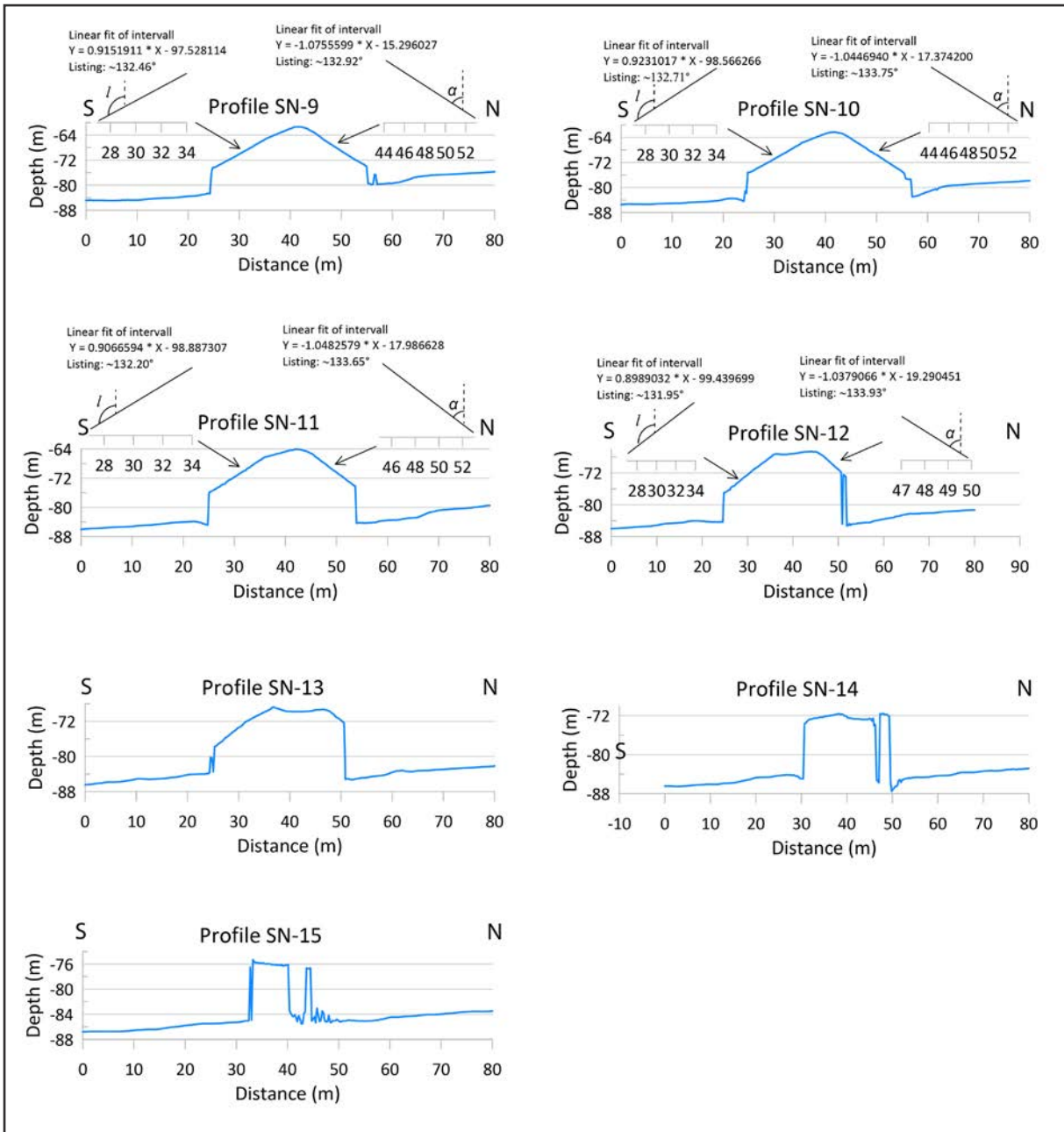


Figure ME5. Depth profiles SN-9 to SN-15. See the caption of Figure M4 for explanation.

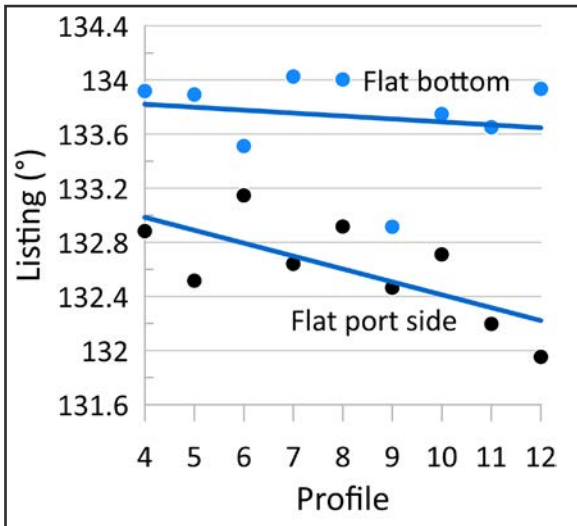


Figure ME6. Comparison between estimated listing along profiles SN-4 to SN-12 based on measurements of the flat bottom (blue dots) and flat port side (black dots).

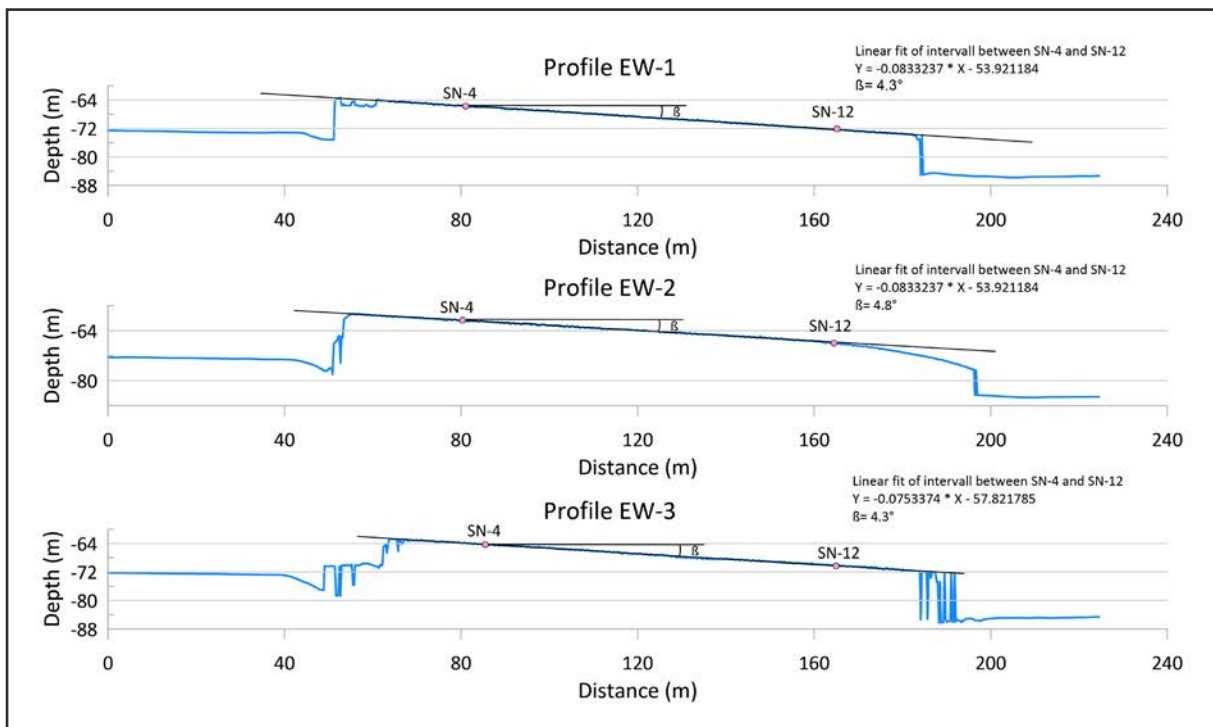


Figure ME7. Depth profiles EW-1 to EW-3 extracted along the hull of MS Estonia. The locations of the profiles are shown in Figures M1 and M2. The trim  $\beta$  is defined as the angle between the hull and sea level. Regression analyses between the crossing profiles SN-4 and SN-12 have been used to calculate  $\beta$  (see text for details).

## Sediment thickness compilation

### Input data and uncertainties

The sediment thickness data are comprised of the digitized Acoustic Basement (AB) in all sub-bottom profiles, identified locations of bedrock at the seafloor in the side-scan and backscatter imagery, CPT probing made by Delft Geotechnics in 1996, sediment cores, and identified bedrock at the seafloor along the northern side of MS *Estonia* using the video acquired with ROV during this survey (Fig. ST1). All these data have been described in this report as well as the methods applied to grid them into a coherent surface. The compiled sediment thickness model provides an indication of the total thickness of unconsolidated sediments resting on top of either bedrock or a till surface (Fig. ST2). The model has several associated uncertainties that must be considered. The applied sound velocity to convert the thickness of the unit above the interpreted AB from two-way travel time to meters was set to  $1600\text{ ms}^{-1}$ . This is one source of uncertainty as the sound velocity will vary, however, not likely with much more than  $\pm 5\%$  in the soft sediment that permits penetration with our sub-bottom profiler. Another source of uncertainty is the gridding itself, which fits a surface through all data points using a minimum curvature spline in tension algorithm (see Methods). This implies a great deal of interpolation between the data points.

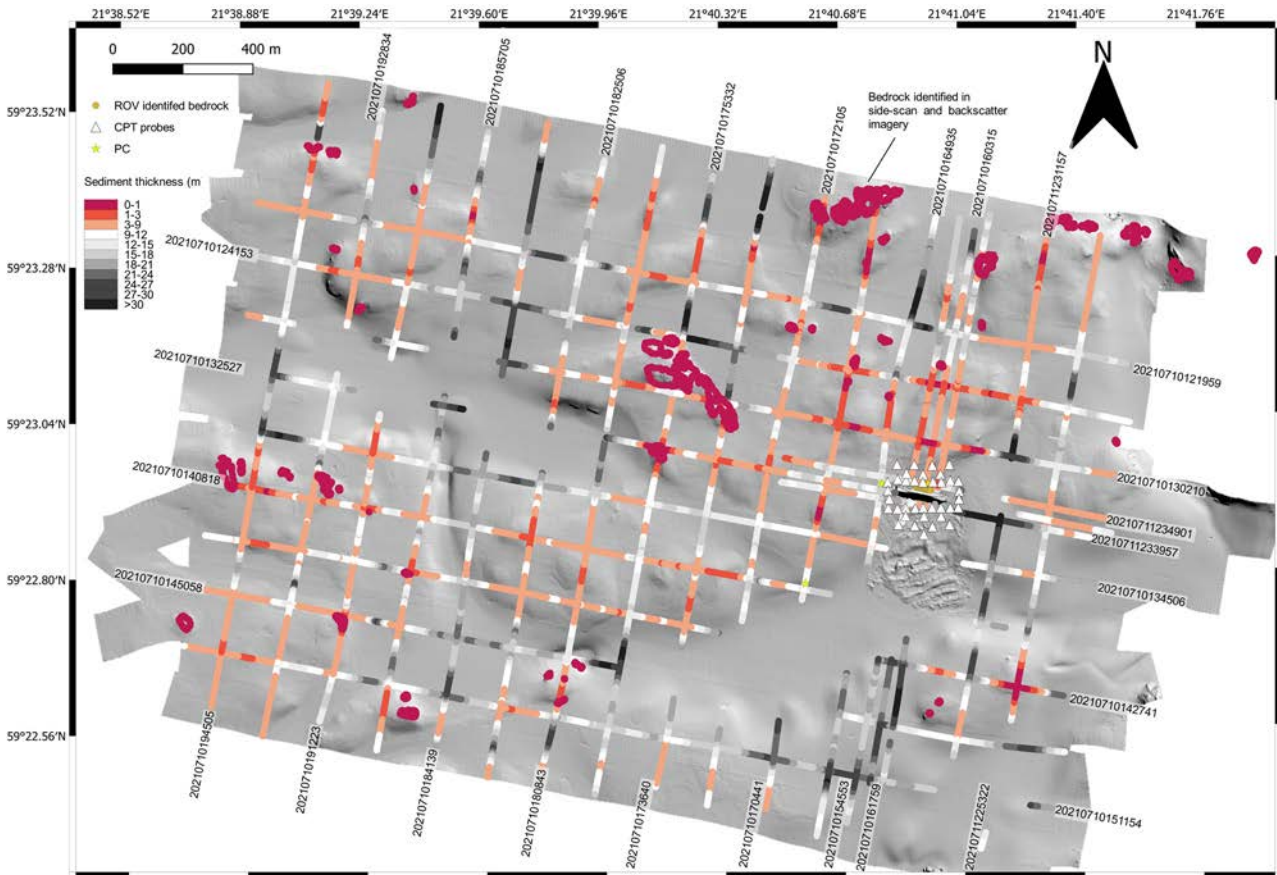


Figure ST1. Sediment thickness data used to compile the gridded sediment thickness model shown in Figure ST2. The sections along the sub-bottom profiles without sediment thickness values marked by colored dots, are where the AB not could be identified, most commonly due to gas blanking. These areas coincide with the deeper basins where the sediment thickness can be assumed to be thick.

There is also an uncertainty associated with identification of the AB, as previously discussed, in particular close to the shipwreck.

### Distribution of sediments

The overview sediment thickness map in Figure ST2 reveals a general pattern with exposed bedrock or thin soft sediment cover on the bathymetric highs and thicker sediment accumulations in the deeper troughs in between. The model suggests that MS *Estonia* rests on bedrock midship, although the model lacks data directly underneath the hull (Fig. ST3). A ridge appears to stretch underneath the shipwreck, which also has been suggested based on previous investigations (see summary by: Rudebeck and Kennedy, 2021). South and southeast of the shipwreck, the sediment accumulations rapidly become greater than 20m, mainly inferred from the previous CPT probes by Delft Geotechnics as the sub-bottom profiles did not permit identification of an AB due to gas blanking. It should be noted that most of the CPT probes in this area southeast of MS *Estonia* yielded a >20m thick sediment cover, while 20m was used in the gridding of the sediment thickness model. This implies that in this area, the model provides a minimum sediment thickness.

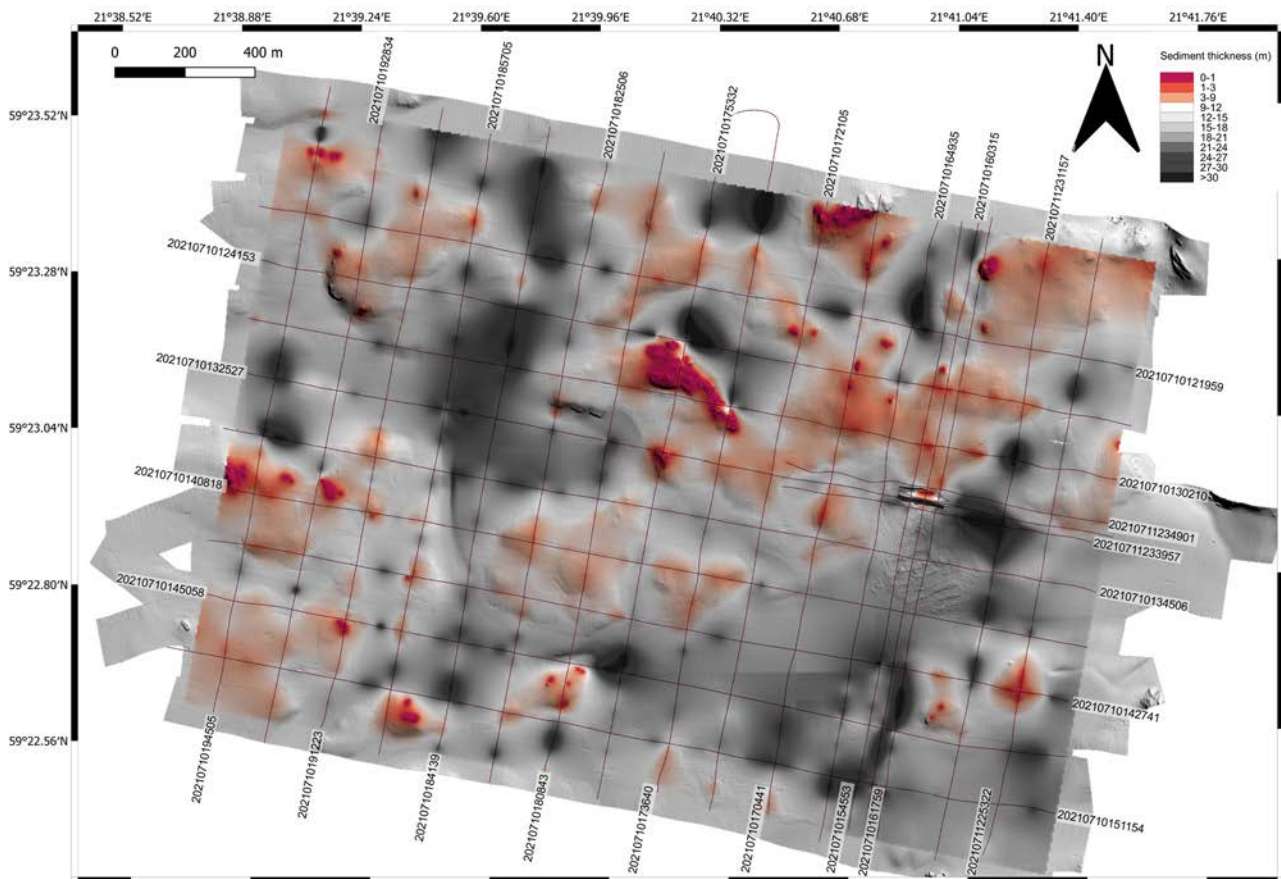


Figure ST2. Sediment thickness map in the survey area. Hill shading from the multibeam bathymetry is applied to provide a depth perception. Exposed bedrock (darker red) is commonly found at the bathymetric highs while the basins in between have the greatest sediment accumulations (darker colors).

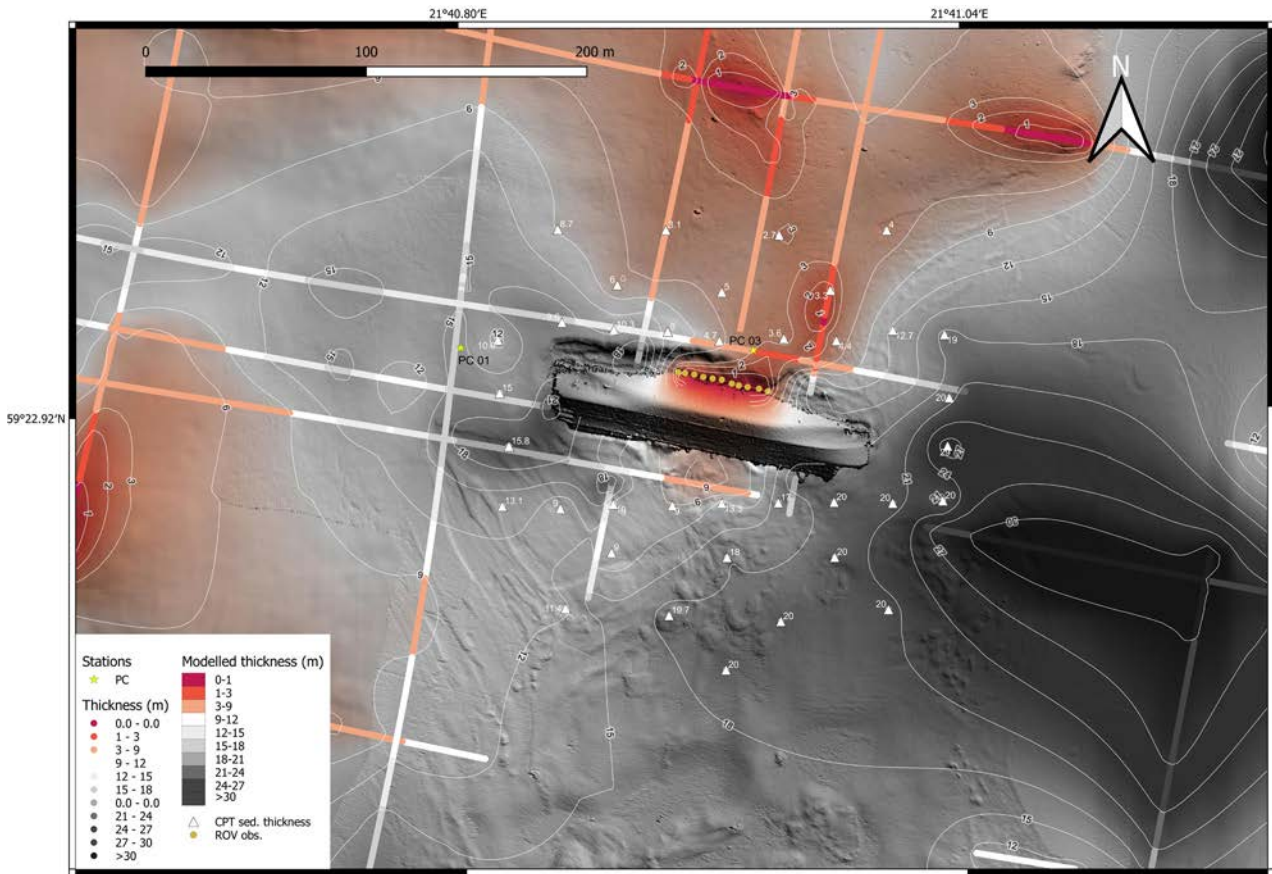


Figure ST3. Sediment thickness in the area of MS Estonia. Isopach contours based on the modelled sediment thickness are shown. They are cropped over MS Estonia, as there are supporting data from below her hull.

## Conclusions

### Seafloor and sub-bottom geology

The geophysical mapping broadly confirms the previously published maps on seafloor deposits by the Naval Research Institute in Finland (Nuorteva, 1995), but provides a more detailed view of exposed bedrock and the boundaries between different sediment types and adds information on seafloor morphology and the occurrence of mass-wasting.

- Mass-wasting on the seafloor is mapped both on the northeastern and southwestern sides of MS *Estonia* as well as south and east of the area where forced penetration strings were placed.
- A section of a 230m long slide scarp west of MS *Estonia* corresponds to the edge of the geotextile placed on the seafloor according to Delft Geotechnic's map (1996-09-19), suggesting that the dumped sand here slid downslope on top of the geotextile.
- Exposed bedrock is identified next to where the two major holes in MS *Estonia*'s hull are found along the northern side, approximately 69m and 89m from the stern respectively. From ocular inspection of its texture and visible parallel jointing, the bedrock appears to be igneous, likely granite or syenite. Denting in the hull is visible where it comes close to exposed bedrock in-between the two major holes.
- A compiled sediment thickness model based on the geophysical mapping, CPT probing by Delft Geotechnics in 1996, sediment cores, and the exposed bedrock identified along the northern side of MS *Estonia* suggests that a ridge of bedrock rises up underneath the hull midship.
- Large (>20m) sediment thicknesses are generally found in the surveyed area in the deeper bathymetric troughs between highs with thinner coverage, where exposed till and bedrock are found.
- South-east of the shipwreck, the sediment thickness is >20m in agreement with previous surveys.
- The sediment thickness model supports previous suggestions that MS *Estonia* is resting on firm seafloor midship but is poorly supported by soft sediments under the bow section.

### MS *Estonia*'s position on the seafloor

The measurements of MS *Estonia* are in this report based on the multibeam bathymetry and assume that the bottom of the hull has a flat part and perpendicular straight sides according to available drawings.

- MS *Estonia* lies on the seafloor with a starboard listing of  $\sim 133.7^\circ \pm 0.4^\circ$  based on the average of measurements made in nine profiles across the flat section of the shipwreck's bottom.
- Measurements of listing based on the flat port side in the nine profiles gives an average of  $\sim 132.6^\circ \pm 0.4^\circ$ , i.e. approximately one degree less than when measured on the flat bottom. There is small trend with lower listing values towards the bow in these profiles.
- Using the flat port side as reference, together with the small one-degree trend with lower listing towards the bow, may indicate a gradual deformation of the hull, where the sides are pressed upward from the pressure of the shipwreck's weight on the seafloor
- MS *Estonia* lies with the straight part of the fender line aligned  $\sim 102^\circ$ , i.e. with the bow towards east-southeast, and has a trim of  $\sim 4.5^\circ \pm 0.3$  relative to sea-level. This trim may cause the observed gradual increase of deformation of the shipwreck port side towards the bow.
- The measured listing in this work can be compared with the estimated listing of  $120^\circ$  during the ROV investigations by Rockwater A/S and Smit Tak. Although it has not been possible to verify the accuracy of the initial listing, it seems likely that the shipwreck has changed position over time.

- A prominent trench is formed in the seafloor sediments along the stern and northern side of MS *Estonia*. This trench is between about 6 and >8m wide, and between 4 and 7m deep. It was likely mainly formed during the impact with the seafloor, but probably changed shape over time as the listing of MS *Estonia* increased.

### Objects on the seafloor

Camera observations were made to identify features visible in the geophysical mapping data.

- Three metal frames, placed north of MS *Estonia* to form a right angle triangle on the seafloor, were identified to have hosted acoustic transponders used during the covering work. A fourth metal frame located close to MS *Estonia* is also identified and may be of the same kind.
- An imprint of the bow visor in the seafloor nearby recovery positions given in previous reports is likely seen in the side-scan imagery and multibeam bathymetry.

### Oceanographic conditions

#### Currents (shipboard and mooring measurements)

- During the water column survey at the MS *Estonia* wreck site, currents were generally weak (typically <0.1 m/s) in the 6.5 to 55 m depth range.
- A mooring was deployed that measured water column currents at one position over five days. Although there are indications of a compass offset in the moored instrument, the data show strong bottom currents between about 70 and 80 m depth, sometimes approaching 1 m/s. The depth interval of these bottom currents coincides with a significant turbidity peak in the hydrological data, indicating resuspension and transport of sediments with the bottom currents.
- Although more data covering longer time periods and further analyses are needed to draw firm conclusions on dominating current regimes, the observed strong bottom currents must be considered when assessing the stability of MS *Estonia* at her location.

#### Hydrological observations

- A halocline is present between about 60 and 80 m depth.
- The boundary between oxic and anoxic conditions in the water column coincided with the halocline, with anoxic conditions prevailing below ~75 m depth during the survey.
- MS *Estonia* was therefore partly in contact with anoxic waters during the survey period. The depth of the halocline (and thus also the depth of the oxycline) can, however, vary significantly over time and oxygen conditions may change rapidly in response to Major Baltic inflows.
- The port aft section of MS *Estonia* is shallowest, partly rising to a depth of about 57 m, implying that this part reaches into the oxic zone. The shipwreck is thus exposed to different conditions with respect to corrosion.

## References

- Abbott, B. (2021). “A Preliminary Assessment of the MS *Estonia* Shipwreck using the MS 1000 Scanning Sonar”. Abbott Underwater Acoustics LCC).
- Andrén, T., Björck, S., Andrén, E., Conley, D., Zillén, L., and Anjar, J. (2011). “The Development of the Baltic Sea Basin During the Last 130 ka,” in *The Baltic Sea Basin*, eds. J. Harff, S. Björck & P. Hoth. (Berlin, Heidelberg: Springer Berlin Heidelberg), 75–97.
- BenDor, E., and Banin, A. (1989). Determination of organic matter content in aridzone soils using a simple “loss-on-ignition” method. *Communications in Soil Science and Plant Analysis* 20, 1675–1695.
- Calder, B.R., and Mayer, L.A. (2003). Automatic processing of high-rate, high-density multi-beam echosounder data. *Geochemistry Geophysics Geosystems* 4, 1–22.
- De Geer, G. (1912). “A geochronology of the last 12 000 years”, in: *The 11th International Geological Congress in Stockholm 1910*. (Stockholm).
- Fonseca, L., and Calder, B.R. (Year). “Geocoder: An Efficient Backscatter Map Constructor”, in: *U.S. Hydrographic Conference (US HYDRO): The Hydrographic Society of America*.
- Holtermann, P.L., Burchard, H., Gräwe, U., Klingbeil, K., and Umlauf, L. (2014). Deep-water dynamics and boundary mixing in a nontidal stratified basin: A modeling study of the Baltic Sea. 119, 1465–1487.
- Hughes, A.L.C., Gyllencreutz, R., Lohne, Ø.S., Mangerud, J., and Svendsen, J.I. (2016). The last Eurasian ice sheets – a chronological database and time-slice reconstruction, DATED-1. *Boreas* 45, 1–45.
- Iso/Ts 17892-6 (2004). “Geotechnical investigations and testing – Laboratory testing of soil.”, in: *ISO/TS 17892-6 10.*
- Lurton, X., Eleftherakis, D., and Augustin, J.-M. (2018). Analysis of seafloor backscatter strength dependence on the survey azimuth using multibeam echosounder data. *Marine Geophysical Research* 39, 183–203.
- Mesdag, C.S. (1997). “Seismic Survey at *Estonia* Site”. (Haarlem, The Netherlands: Netherlands Institute of Applied Geoscience TNO).
- Mitasova, H., Mitas, L., and Harmon, R.S. (2005). Simultaneous spline approximation and topographic analysis for lidar elevation data in open-source GIS. *IEEE Geoscience and Remote Sensing Letters* 2, 375–379.
- Mohrholz, V. (2018). Major Baltic Inflow Statistics – Revised. 5.
- Nuorteva, J. (1995). *M/S Estonia: Merenpohjan Kerrostumat* (Sea Floor Deposits). 1:5000. Merivoimien tutkimustaitos, Helsinki, Finland.

- Qgis Development Team (2018). “QGIS Geographic Information System. Open Source Geospatial Foundation Project”. 3.4.1-Madeira ed.).
- Reissmann, J.H., Burchard, H., Feistel, R., Hagen, E., Lass, H.U., Mohrholz, V., Nausch, G., Umlauf, L., and Wiczorek, G. (2009). Vertical mixing in the Baltic Sea and consequences for eutrophication – A review. *Progress in Oceanography* 82, 47–80.
- Rockwater A/S, and Smit Tak (1994). “Condition survey of ferry “Estonia”: Survey Report”. Rockwater A/S).
- Rudebeck, D., and Kennedy, H. (2021). “Fartyget M/S *Estonia*: Genomgång av getekniskt underlag”. (Linköping, Sverige: Statens geotekniska institut).
- Stranne, C., Mayer, L.A., Weber, T.C., Ruddick, B.R., Jakobsson, M., Jerram, K., Weidner, E., Nilsson, J., and Gårdfeldt, K. (2017). Acoustic Mapping of Thermohaline Staircases in the Arctic Ocean. *Scientific Reports* 7, 15192.
- Tuukritööde OÜ (2021). “Summary of underwater robot survey of passenger ferry *Estonia* 14–15.07.2021”. (Tallin, *Estonia*: Tuukritööde OÜ).
- Weidner, E., Stranne, C., Sundberg, J.H., Weber, T.C., Mayer, L., and Jakobsson, M. (2020). Tracking the spatiotemporal variability of the oxic–anoxic interface in the Baltic Sea with broadband acoustics. *ICES Journal of Marine Science* 77, 2814–2824.
- Yurkovskis, A. (2005). Seasonal benthic nepheloid layer in the Gulf of Riga, Baltic Sea: Sources, structure and geochemical interactions. *Continental Shelf Research* 25, 2182–2195.



**MEDDELANDEN från STOCKHOLMS UNIVERSITETS  
INSTITUTION för GEOLOGISKA VETENSKAPER No 383**

**Rapportserie**

ISBN print: 978-91-89107-20-5

ISBN pdf: 978-91-89107-21-2

No 372. HANSMAN, R.J. Cryptic orogeny : uplift of the Al Hajar mountains at an alleged passive margin. Stockholm 2018.

No 373. KIELMAN, R. Assessing the reliability of detrital zircon in early-earth provenance studies. Stockholm 2018.

No 374. THIESSEN, F.K. The evolution of lunar breccias : U-Pb geochronology of Ca-phosphates and zircon using secondary ion mass spectrometry. Stockholm 2018.

No 375. HIRST, C. Iron in the Lena river basin, NE Russia : insights from microscopy, spectroscopy and isotope analysis. Stockholm 2018.

No 376. BENDER, H. Assembly of the Caledonian Orogenic Wedge, Jämtland, Sweden. Stockholm 2019.

No 377. REGHELLIN, D. Eastern equatorial Pacific bulk sediment properties and paleoceanography since the late Neogene. Stockholm 2019.

No 378. SJÖBERG, S. Microbially mediated manganese oxides enriched in yttrium and rare earth elements in the Ytterby mine, Sweden. Stockholm 2019.

No 379. JANSEN, J. Carbon trace gas dynamics in subarctic lakes. Stockholm 2020.

No 380. TOLLEFSEN, E. Experimental, petrological and geochemical investigations of ikaite ( $\text{CaCO}_3 \cdot 6\text{H}_2\text{O}$ ) formation in marine environments. Stockholm 2020.

No 381. GDANIEC, S.  $^{231}\text{Pa}$ ,  $^{230}\text{Th}$  and  $^{232}\text{Th}$  as tracers of deep water circulation and particle transport. Insights from the Mediterranean Sea and the Arctic Ocean. Stockholm 2020.

No 382. SJÖSTRÖM, J. Mid-Holocene mineral dust deposition in raised bogs in southern Sweden. Processes and links. Stockholm 2021.

Formerly/1990–2021: MEDDELANDEN från STOCKHOLMS UNIVERSITETS  
INSTITUTION för Geologi och Geokemi (ISSN 1101-1599)

**Department of Geological Sciences**

Stockholms universitet SE-106 91 Stockholm [www.geo.su.se](http://www.geo.su.se)

